UCSF
UC San Francisco Electronic Theses and Dissertations

Title
Phenotypes Occuring in Saccharomyces cerevisiae Early after Telomerase Inactivation

Permalink
https://escholarship.org/uc/item/68q699zq

Author
Jay, Kyle Aaron

Publication Date
2015

Peer reviewed|Thesis/dissertation

eScholarship.org Powered by the California Digital Library
University of California

Phenotypes Occuring in Saccharomyces cerevisiae
Early after Telomerase Inactivation

by

Kyle Jay

DISSERTATION

Submitted in partial satisfaction of the requirements for the degree of

DOCTOR OF PHILOSOPHY

in

Biochemistry and Molecular Biology

in the

GRADUATE DIVISION

of the

UNIVERSITY OF CALIFORNIA, SAN FRANCISCO

[redacted]

Acknowledgements

This thesis has been a long time in the making. The process of completing a PhD is not an easy one, and I know that without my support system it would have been a far more ominous mountain to climb. First, I would like to thank my PhD advisor, Elizabeth Blackburn. Your endless encouragement and optimism have been an immeasurable boon, and your words of wisdom have helped me find my way amidst a sea of data. I'd like to thank my thesis committee members: Joachim Li, Dave Toczyski, and Dave Morgan. Thank you lending me your time, insight, and experience. Your constructive criticism and guiding suggestions have helped me to become a better scientist.

Second, I would like to thank my friends: To my comrades-in-arms of my graduate school class, who fought together with me through the first few years of our graduate program until we eventually became so immersed in our research that we saw each other not nearly enough. To my colleagues in the Blackburn lab: Dana, big Jue, Beth, Tracy, Nancy, Toni, Josh, little Jie, Imke, Tet, Francesca, Brad, Shang, and to Tanya, who is no longer with us. Thank you for always letting me pick your brains, for offering advice and friendship, and listening to me complain endlessly when my project wasn't going quite as well as I'd hoped. Special thanks are also due to Dana for teaching me so much about working with yeast and for always helping me find things in the lab, even when I should have known where they were. To Jue, for her sweet, helpful demeanor and our mutual love of yogurt. To Beth, for commiserating with me and for her comic relief, and to Francesca, for brightening up any room she enters. To Tracy, for her

seemingly unending joy to help out a friend, and to Imke, for giving it to me straight when I needed to hear the blunt truth. Thank you to Tet, for helping me with my molecular biology woes, and to Brad, Shang, and Tanya for their wisdom, advice, and entertainment. And of course, to Nancy and Toni, who are not only great friends and confidants, but without whom this lab would cease to function. I'd also like to thank my collaborators Hao Li and Zhengwei Xie for helping me get a somewhat stuck project off the ground. To my friends and teachers from dance, who lifted my spirits when they needed lifting, and reminding me that no matter how bad things may seem, you can always let it go and dance it out. And last, but not least, to my best friend of over a decade, Si-Han, I thank you for your encouragement and tough love. You helped me get myself on the right track.

Lastly, I'd like to thank my parents, without whom I would not be here for more reasons than one. Their unconditional support has bolstered and sometimes even surprised me. They have worked so hard so that I could have the best opportunities, paid my absolutely ridiculous college tuition, and given me all the love and support a child could hope for, and have deeply shaped the person I am today.

Acknowledgements (Published Material)

Chapter 2 has been previously published as “Early telomerase inactivation accelerates aging independently of telomere length.” Xie Z, Jay KA, Smith DL, Zhang Y, Liu Z, Zheng J, Tian R, Li H, Blackburn EH. Cell, published February 26th, 2015. I performed the experiments in Figures 2-3, 2-5, 2-6, 2-7D, 2-9E, 2-9F, 2-11E, 2-11F, 2-12, 2-13A, 2-13B, and designed the model proposed in Figure 2-16 in collaboration with the other authors. The remaining chapters and appendices were written entirely by me.

Phenotypes Occuring in *Saccharomyces cerevisiae*

Early after Telomerase Inactivation

Abstract

Telomeres are DNA and protein complexes that cap the ends of linear chromosomes. These caps serve two primary functions: to buffer against the loss of terminal DNA sequences resulting from the end replication problem and to conceal chromosome ends from the cellular DNA damage response (DDR) and inappropriate repair events. Telomeres are maintained by telomerase, a multi-component ribonucleoprotein complex with reverse transcriptase activity. *Saccharyomyces cerevisiae* cells constitutively express telomerase, allowing nearly unlimited growth of the bulk population. However, when telomerase activity is removed from *Saccharyomyces cerevisiae* cells, telomeres shorten over time and cells can continue to divide for approximately 60-80 cell divisions before chromosome ends lose their protective cap and initiate a permanent cell cycle arrest known as senescence. It had previously been believed that these cells lacking telomerase activity grow indistinguishably from wild-type cells until telomeres begin to reach a critically short length. However, I will show that even Early after Telomerase Inactivation (ETI), cells lacking telomerase activity display numerous detrimental phenotypes. ETI cells displayed altered cell cycle kinetics and a dependence on certain DDR components for full viability. ETI cells also displayed an acceleration of mother cell aging, a process by which yeast mother cells cease to produce daughters after a certain number of divisions and which has not previously been shown to interact with telomere maintenance pathways. These phenotypes occurred independently of telomere length

and were rescued by elevated nucleotide pools resulting from deletion of Sml1, an inhibitor of ribonucleotide reductase. This suggests that ETI cells struggle to resolve telomeric DNA replication stress. ETI cells were also sensitive to downregulation of TOR kinases, which have diverse roles in metabolic and structural regulation of the cell. These findings suggest that telomerase is required for more than the counteraction of the slow erosion of telomere ends. Telomerase functions extend to the relief of telomeric DNA replication stress, maintenance of normal healthy lifespan, and interactions with other diverse cellular pathways.

Table of Contents

Title Page i

Acknowledgements iii

Abstract vi

Table of Contents viii

List of Tables ix

List of Figures x

Chapter 1. Introduction 1

Chapter 2. Early Telomerase Inactivation Accelerates Aging Independently of Telomere Length 20

Chapter 3. Early Telomerase Inactivated Cells Depend on a Functional DNA Damage Response for Full Viability 77

Chapter 4. Early Telomerase Inactivated Cells are Sensitive to Rapamycin and TOR Downregulation 110

Materials and Methods 127

Appendix 1 138

Appendix 2 145

Library Release Form 148

List of Tables

Table 2-1. Microarray Data in Telomerase Deleted Yeast Time Courses from Nautiyal et al 2002 ..... n/a

Table 2-2. Top Ten Published Gene Expression Profiles with the Highest Correlation with the ETI Profile 74

Table 2-3. Top Five Non-redundant GO Categories Contributing to Overall Correlation of Gene Expression Between ETI and Diamide Treatment (GSM971 1.5mM Diamide, 5min) 75

Table 2-4. Genes Involved in Response to Oxidative Stress that are Upregulated in ETI Cells (>1.5 fold) 76

Table A1-1. Strains Used in this Thesis 138

List of Figures

Figure 2-1. ETI Mother Cells Show a Non-progressive Cell Cycle Length Phenotype and Reduced Lifespan that is Rescued by SML1 Deletion 58

Figure 2-2. ETI Induces a Transient G2/M Pause in Bulk Population Time-course Experiments 59

Figure 2-3. Escape from the G2/M Cell Cycle Extension in ETI Cells is Not Dependent on DNA Damage Adaptation pathways 60

Figure 2-4. Initial Cell Cycle Length was not Predictive of Next Cell Cycle Length 61

Figure 2-5. *SML1* Deletion Rescues Mother Cell Lifespan of ETI Cells Independently of Telomere Length 62

Figure 2-6. *SML1* Deletion does not Alter the Kinetics of Telomere Shortening or Onset of Senescence Caused by *est2D530A* 63

Figure 2-7. The Cellular Response to ETI is Distinct from the Response to Classic DNA Damage or to LTI Senescence 64

Figure 2-8. ETI Mother Cells Age with Terminal Cellular and Mitochondrial Morphologies Distinct from LTI Senescence but Similar to those of Normal Mother Cell Aging 65

Figure 2-9. *TEL*1 Deletion Exacerbates ETI Cell Cycle and Lifespan Phenotypes but not Senescence or Telomere Shortening Rates 66

Figure 2-10. Mother Cell Lifespans of Selected DDR Mutants 67

Figure 2-11. *MRC1* Mutation Exacerbates ETI Cell Cycle and Lifespan Phenotypes but not Senescence or Telomere Shortening Rates 68

Figure 2-12. Bulk Population Epistasis Analysis of Tel1 and Mrc1 Mutants on G2/M Cell Cycle Extension 69

Figure 2-13. Genotype Dependence of Telomere Fusions and Transient DNA Damage Response Episodes in Mother Cells 70

Figure 2-14. Multiple Factors Showing No Evidence of a Causative Role in the ETI Mother Cell Aging Phenotypes 71

Figure 2-15. Cell Cycle Length and Mitochondrial Staining Measured During Early Divisions are Predictive of Lifespan Across Various Genotypes 72

Figure 2-16. Proposed Model 73

Figure 3-1. ETI Cells Do Not Display Growth Defects in the Absence of Mec1 and Tel1 PIKK Kinases 96

Figure 3-2. ETI Mutants Show a Dependence on the DNA Damage Response that can be Alleviated by Sml1 Deletion 97

Figure 3-3. Semi-Quantitative Serial Dilutions Show ETI *mrc1*^{AQ}*rad9*Δ Synthetic Phenotype and Rescue via Sml1 Deletion 98

Figure 3-4. ETI *mrc1*^{AQ}*rad9*Δ Synthetic Phenotype is Specific for Mrc1 Activity 99

Figure 3-5. Hypomorphic Telomerase Does Not Show Synthetic Phenotype with *mrc1*^{AQ}*rad9*Δ Mutation 100

Figure 3-6. RNR1 Overexpression Can Also Rescue ETI *mrc1^{AQ}rad9*Δ Synthetic Phenotype 101

Figure 3-7. ETI Strains are Not Sensitive to HU Treatment 102

Figure 3-8. ETI Strains are Not Sensitive to Dun1 Deletion 103

Figure 3-9. Introduction of a Hyper-stabilized Sml1 Allele had No Significant Effect on ETI Mutants 104

Figure 3-10. Overexpression of Sml1 had No Effect on Colony Growth Phenotypes of ETI Mutants 105

Figure 3-11. Recombination is Not Required for ETI *mrc1^{AQ}rad9*Δ Synthetic Phenotype Nor its Rescue via Sml1 Deletion 106

Figure 3-12. ETI *mrc1^{AQ}rad9*Δ Synthetic Phenotype and *sm1*Δ Rescue Cannot be Explained by Changing Telomere Lengths or Accelerated Senescence 107

Figure 3-13. ETI Strains Reach Senescence after Three to Four passages on Solid Media 108

Figure 3-14. Rescue via Sml1 Deletion may be Partially due to Reduction in Deprotected Telomeres in Strains Lacking a Functional DNA Damage Response 109

Figure 4-1. ETI Cells are Sensitive to Rapamycin Treatment 120

Figure 4-2. ETI Sensitivity to Rapamycin Treatment is Progressive 121

Figure 4-3. ETI Cells are Sensitive to Genetic Repression of TOR1 122

Figure 4-4. ETI Cells are Sensitive to Genetic Repression of TOR2 123

Figure 4-5. ETI Mutations Negate Resistance to Rapamycin Provided by TOR1/2 Overexpression 124

Figure 4-6. Strains Become Inviable When Kog1, Avo3, or Lst8 are Placed Under Galactose Promoter Control 125

Figure 4-7. Deletion of Sml1 had No Effect on ETI Rapamycin Sensitivity .. 126

Figure A2-1. Comparative Telomere Lengths in *tlc1*Δ and *est2D530A* mutant strains 146

Figure A2-2. Comparative Telomere Lengths in *tlc1*Δ and *est2D530A* mutant strains 147

Chapter 1: Introduction

Telomeres

Unlike simple prokaryotes, whose genetic information is stored in circular chromosomes, the chromosomes of eukaryotes are linear. However, the evolution of linear chromosomes has introduced some interesting problems. First, due to the mechanism of DNA replication, it is not possible to fully replicate the ends of a linear chromosome. As a result, a small amount of DNA is lost from the end of a linear chromosome each time it is replicated (Soudet et al., 2014). Over time, this can result in the loss of vital sequences and result in cell death. Second, the cell must be able to distinguish the natural ends of its own chromosomes from naked DNA ends that result from a DNA double-strand break (DSB) so that the cellular DNA Damage Response (DDR) and repair pathways do not attempt to fuse these exposed ends together. This could result in dicentric chromosomes, chromosome missegregation or breakage, and a global genomic instability (O'Sullivan and Karlseder, 2010). The telomere is the solution to these two problems.

Telomeres are DNA-protein complexes located at the ends of linear chromosomes. In most eukaryotes they consist of terminal repetitive sequences and their bound protective proteins. In the budding yeast *Saccharomyces cerevisiae*, telomeric DNA consists of approximately 300bp of double-stranded TG1-3 repeats (Lydall, 2003) as

well as a short single stranded overhang of the G-rich strand (Henderson and Blackburn, 1989). These repetitive sequences act as a buffer to be lost in place of more vital sequences when chromosome ends cannot be fully replicated. These telomeric DNA sequences and bound proteins act as a protective cap that conceals the chromosome end from DNA repair and DSB processing activities and aid in maintaining genomic stability.

The telomeric binding proteins associate with different sections of the terminal repeats and have various roles in the protection of telomeres and the regulation of their length. The full length of the double-stranded telomeric repeats is bound by the protein Rap1 (Longtine et al., 1989), which also has many roles in transcriptional regulation (Shore, 1994). The c-terminal end of Rap1 binds to the proteins Rif1 and Rif2, which are "counted" as part of a negative feedback mechanism to limit telomere length (Marcand et al., 1997). The heterodimeric protein Ku binds to the distal double-stranded telomere repeats and is important for telomere length regulation and protecting the chromosome end from degradation (Fisher and Zakian, 2005). The single-stranded overhang of telomeres is bound by the protein Cdc1, which has separate roles in telomere end protection and replication (Pennock et al., 2001). Cdc13 and Ku are both required to maintain normal telomere length due to their roles in recruiting the enzyme telomerase (Evans and Lundblad, 2000; Grandin et al., 2000; Stellwagen et al., 2003).

Telomerase

In certain eukaryotic cells, the length of the telomere puts an upper limit on the number of potential divisions a cell can undergo. However, in *Saccharomyces cerevisiae* telomere length is maintained at a steady level, allowing nearly unlimited growth at the bulk population level. This is accomplished via the expression of a telomere-lengthening enzyme known as telomerase (Greider and Blackburn, 1985, 1987), a multi-component ribonucleoprotein complex.

The two primary components of telomerase are the reverse transcriptase subunit, in yeast called Est2 (Lingner et al., 1997a), and the bound template-containing RNA, TLC1 (Singer and Gottschling, 1994). The template region within the TLC1 RNA hybridizes to the single stranded 3' G-rich overhang of the telomere and enables the Est2 reverse transcriptase to catalyze the addition of dNTPs to the chromosome end (Lingner et al., 1997a). The complex also contains two proteins, Est1 and Est 3, which are essential for in vivo telomerase function but dispensable for in vitro telomerase activity (Lingner et al., 1997b). The budding yeast telomerase RNA is large and complex and acts as a scaffold for the assembly of the telomerase holoenzyme. It not only contains the template region, which determines the sequence of telomeric repeats synthesized by telomerase, but it also contains binding sites for the Est2 protein as well as that for several other accessory proteins (Theimer and Feigon, 2006). These accessory proteins include Est1, Ku, and Sm, which have roles in regulating telomerase activity and telomere length.

The focus of this thesis research was to discover potential alternative functions of telomerase outside countering the slow erosion of telomere length during cell cycling. This was accomplished by searching for phenotypes in cells early after telomerase inactivation, but far before cellular senescence.

Senescence and Early Telomerase Inactivation

The telomerase enzyme can be inactivated in a number of ways. In this thesis, telomerase activity was eliminated either by deletion of the RNA template (*tlc1*Δ), deletion of the catalytic reverse transcriptase subunit (*est2*Δ) or by replacing the reverse transcriptase subunit with a catalytically-dead allele (*est2D530A*) (Lingner et al., 1997a). This catalytically dead allele is mutated at an invariant aspartate residue, which is one of three aspartate residues required for phosphoryl transfer in reverse transcriptases (Counter et al., 1997). The two deletion mutations result in disassembly of the telomerase complex, whereas the catalytically-dead point mutant results in an intact telomerase complex that is unable to extend the 3' G-rich telomeric overhang as it lacks DNA polymerization activity. All three mutants cause telomeres to shorten at the same rate, though the *est2D530A* mutant produces telomeres that are slightly shorter when maintained as a heterozygous diploid or with a covering plasmid, compared to the *tlc1*Δ and *est2*Δ mutations (Appendix 2). When budding yeast are deprived of telomerase activity, telomeres begin shortening by approximately 5bp per cell cycle (Soudet et al., 2014). In otherwise WT cells, after 60-80 cell cycles in the absence of telomerase activity, *L*ate after *T*elomerase *I*nactivation (LTI), the telomeres become too short to maintain the complex of bound proteins that constitute the chromosome end cap. The

loss of this protective capping function (telomere deprotection) results in the recognition of the exposed chromosome end by the DDR and results in a permanent cell cycle arrest known as senescence (Lundblad and Szostak, 1989). Some cells can escape this permanent G2/M cell cycle arrest by extending their telomeres through alternative methods involving recombination (Lundblad and Blackburn, 1993). However, these cells, known as "survivors," will not be addressed here.

The eventual senescence that occurs in LTI cells and the genetic dependencies of this process have been well studied (Abdallah et al., 2009; d' Adda di Fagagna et al., 2003; Enomoto et al., 2002; Lundblad and Blackburn, 1993; Lundblad and Szostak, 1989). It was previously believed that cells lacking telomerase would grow without any detrimental consequences until their telomeres reached the critically short length at which end protection was lost. However, the work described here will show that even shortly after telomerase loss, while these cells appear to be growing similarly to the wild-type (WT), certain discernable phenotypes arise. The main focus of this project has been to analyze these phenotypes, which arise *E*arly after *T*elomerase *I*nactivation (ETI).

Yeast DNA Damage Response

In LTI cells, when telomeres have reached a critically short length, telomere deprotection shares many properties with classic DNA damage (d' Adda di Fagagna et al., 2003; Dewar and Lydall, 2012; Nautiyal et al., 2002). In addition, many DDR proteins bind telomeres and have functions in telomere maintenance (Jain and Cooper,

2010). DNA damage signaling in budding yeast is primarily initiated by two upstream phosphatidylinositol 3-kinase (PI3K)-related kinases, Mec1 and Tel1 (Melo and Toczyski, 2002). In addition to their functions in the DDR, Mec1 and Tel1 have a slight and major role, respectively, in telomere length regulation, with cells lacking both senescing as if they did not have active telomerase (Chan et al., 2001).

The Mec1 and Tel1 proteins are functionally redundant to some degree, but are also able to respond to different distinct types of DNA damage. For example, Mec1 is required to sense the single stranded DNA which arises in response to replication stress and stalled DNA replication forks (Friedel et al., 2009). Deletion of Mec1 is lethal, but can be suppressed by deletion of Sml1, which results in elevated dNTP pools and facilitates DNA replication (Andreson et al., 2010; Chabes et al., 1999). Tel1 is thought to be more important for the detection, processing, and repair of DNA double-strand breaks (Usui et al., 2001) and has been shown to be protective against telomeric end-to-end fusions (Chan and Blackburn, 2003).

Downstream of Mec1/Tel1 in the yeast DDR are two semi-redundant adaptor proteins, Mrc1 and Rad9. Mrc1 is required for the DNA replication stress response and travels as a component of the DNA replication fork (Alcasabas et al., 2001; Bando et al., 2009). In addition, Mrc1 becomes activated in response to telomere erosion and has been shown to protect uncapped telomeres from exonuclease activity (Grandin et al., 2005; Tsolou and Lydall, 2007). Rad9 is also important for the response to DNA damage, and cells lacking Rad9 are especially sensitive to DSB-inducing chemicals and ultraviolet/ionizing

radiation (Dolling et al., 2000; Al-Moghrabi et al., 2001). In response to DNA damage, one or both of these adapter proteins will become phosphorylated and mediate signaling to downstream kinases and target proteins (Alcasabas et al., 2001; Vialard et al., 1998). Through this signaling cascade, a multitude of actions can be taken in response to the recognition of DNA damage, which will eventually result in the resolution of the genetic insult in question and the maintenance of genomic stability. Here I will present phenotypes suggesting that, unlike WT cells, ETI cells are dependent on a functional DNA damage response for full viability, even in the absence of introduced DNA damage.

TOR

In addition to the DNA Damage PIKK Kinases Mec1 and Tel, a third type of PIKK kinase exists in *Saccharomyces cerevisiae*: TOR. The TOR proteins get their name from the drug that inhibits them: *T*arget *O*f *R*apamycin. The drug rapamycin has become quite well known for its function as an immunosuppressant, potential anti-cancer drug, and for its ability to extend lifespan in a variety of organisms (Harrison et al., 2009; Medvedik et al., 2007). Budding yeast contain both two TOR proteins, TOR1 and TOR2, and two TOR complexes, TORC1 and TORC2, only the former of which is sensitive to rapamycin (Inoki et al., 2005). TORC1 has a general role in cell metabolism, growth, and starvation responses, while TORC2 has a role in maintaining actin organization and cell wall integrity (Kupiec and Weisman, 2012). In addition, inhibition of TORC1 by rapamycin in yeast has been shown to render cells more sensitive to DNA damage (Shen et al., 2007) and to reduce telomere length by reducing the level of Ku (Ungar et

al., 2011), a protein that binds to telomeres and regulates telomere length. In this thesis, I will show that ETI cells also display sensitivity to rapamycin and TOR downregulation.

Yeast Mother Cell Aging

Yeast cells are also capable of another form of aging completely distinct from telomere-shortening related senescence. This form of aging is due to the asymmetric cell divisions that occur in budding yeast and occurs even in WT cells. Dividing budding yeast cells ("mother cells") produce a small bud, which eventually grows into a new cell ("daughter cell"). A single WT mother cell can produce approximately 25-30 daughter cells before it itself ceases to divide and each daughter cell, for the majority of the mother's lifespan, is rejuvenated and can itself undergo the full number of cell cycles as a mother before it too will cease divisions (Egilmez and Jazwinski, 1989; Kennedy et al., 1994).

One hypothesis is that this division limit is due to the asymmetric sequestration of harmful elements, such as extrachromosomal ribosomal DNA circles, acentric chromosome fragments, or damaged mitochondria or proteins, into the mother cell during cytokinesis (Aguilaniu et al., 2003; Kaeberlein, 2010; Murray and Szostak, 1983; Veatch et al., 2009). Alternatively, it could be due to the accumulation of DNA damage in older mothers or due to the reduced capacity to repair spontaneous damage (Lesur and Campbell, 2004). It was also found that mother cell lifespan could be extended by caloric restriction or via inhibition of the TOR complex via treatment with rapamycin (Jiang et al., 2000; Medvedik et al., 2007). However, despite the identification of multiple

genes that regulate mother cells lifespans (Bishop and Guarente, 2007; Johnson et al., 1999; Kaeberlein, 2010), the mechanisms causing mother cell aging of even WT yeast remain poorly understood. Here I will show that, despite no previously known interaction between WT mother cell aging and telomere shortness-induced senescence (Austriaco and Guarente, 1997; D'Mello and Jazwinski, 1991; Lesur and Campbell, 2004), absence of telomerase function causes an acceleration of mother cell aging.

Replication Stress in the Telomere

Telomeres are increasingly recognized as genomic regions prone to replication stress and impaired DNA replication fork movement in baker's yeast (Chang et al., 2009), fission yeast (Miller et al., 2006) and mammals (Drosopoulos et al., 2012; Meena et al., 2015; Sfeir et al., 2009; Zimmermann et al., 2014). In addition, many of these studies have found that telomere binding proteins (Buonomo et al., 2009; Lue et al., 2014; Miller et al., 2006; Sfeir et al., 2009; Zimmermann et al., 2014), or telomerase activity (Chang et al., 2009; Meena et al., 2015) is required to suppress or survive this replication stress. This is consistent with the discovery of several interactions between telomerase or telomere components and the lagging strand DNA replication machinery (Chen and Lingner, 2013; Lue et al., 2014; Ray et al., 2002), suggesting that proper replication of the telomere requires the coordinated action of many telomere-associated factors. In addition to being highly repetitive and tightly bound by protein, telomeric DNA sequences are also very G-rich and single stranded telomeric DNA forms highly stable G-quadruplex structures that inhibit DNA replication in mammalian systems (Vannier et

al., 2012). Overall, telomeres present a difficult landscape for the DNA replication machinery.

In this thesis I will present evidence for, and propose, a model by which several of the phenotypes observed in ETI cells are due to an inability to resolve DNA replication stress in the telomere. Accordingly, several of these phenotypes are exacerbated by mutation of DNA damage components, which would be expected to stabilize or repair broken forks. Furthermore, elevation of dNTP pools in the cell, known to facilitate DNA replication (Reichard, 1988), reverses many of these ETI phenotypes to near wild-type levels. Therefore, it has become apparent that an active telomerase enzyme is a requirement for proper telomere replication independent of bulk telomere length, and that this requirement can be alleviated by facilitating DNA replication.

References

Abdallah, P., Luciano, P., Runge, K.W., Lisby, M., Géli, V., Gilson, E., and Teixeira, M.T. (2009). A two-step model for senescence triggered by a single critically short telomere. Nat. Cell Biol *11*, 988–993.

D' Adda di Fagagna, F., Reaper, P.M., Clay-Farrace, L., Fiegler, H., Carr, P., Von Zglinicki, T., Saretzki, G., Carter, N.P., and Jackson, S.P. (2003). A DNA damage checkpoint response in telomere-initiated senescence. Nature *426*, 194–198.

Aguilaniu, H., Gustafsson, L., Rigoulet, M., and Nyström, T. (2003). Asymmetric inheritance of oxidatively damaged proteins during cytokinesis. Science *299*, 1751–1753.

Alcasabas, A.A., Osborn, A.J., Bachant, J., Hu, F., Werler, P.J.H., Bousset, K., Furuya, K., Diffley, J.F.X., Carr, A.M., and Elledge, S.J. (2001). Mrc1 transduces signals of DNA replication stress to activate Rad53. Nat Cell Biol *3*, 958–965.

Andreson, B.L., Gupta, A., Georgieva, B.P., and Rothstein, R. (2010). The ribonucleotide reductase inhibitor, Sml1, is sequentially phosphorylated, ubiquitylated and degraded in response to DNA damage. Nucleic Acids Res. *38*, 6490–6501.

Austriaco, N.R., and Guarente, L.P. (1997). Changes of telomere length cause reciprocal changes in the lifespan of mother cells in Saccharomyces cerevisiae. Proc. Natl. Acad. Sci. U.S.A. *94*, 9768–9772.

Bando, M., Katou, Y., Komata, M., Tanaka, H., Itoh, T., Sutani, T., and Shirahige, K. (2009). Csm3, Tof1, and Mrc1 form a heterotrimeric mediator complex that associates with DNA replication forks. J. Biol. Chem. *284*, 34355–34365.

Bishop, N.A., and Guarente, L. (2007). Genetic links between diet and lifespan: shared mechanisms from yeast to humans. Nat. Rev. Genet. *8*, 835–844.

Buonomo, S.B.C., Wu, Y., Ferguson, D., and de Lange, T. (2009). Mammalian Rif1 contributes to replication stress survival and homology-directed repair. J. Cell Biol *187*, 385–398.

Chabes, A., Domkin, V., and Thelander, L. (1999). Yeast Sml1, a protein inhibitor of ribonucleotide reductase. J. Biol. Chem. *274*, 36679–36683.

Chan, S.W.-L., and Blackburn, E.H. (2003). Telomerase and ATM/Tel1p protect telomeres from nonhomologous end joining. Mol. Cell *11*, 1379–1387.

Chan, S.W., Chang, J., Prescott, J., and Blackburn, E.H. (2001). Altering telomere structure allows telomerase to act in yeast lacking ATM kinases. Curr. Biol. *11*, 1240–1250.

Chang, M., Luke, B., Kraft, C., Li, Z., Peter, M., Lingner, J., and Rothstein, R. (2009). Telomerase is essential to alleviate pif1-induced replication stress at telomeres. Genetics *183*, 779–791.

Chen, L.-Y., and Lingner, J. (2013). CST for the grand finale of telomere replication. Nucleus *4*, 277–282.

Counter, C.M., Meyerson, M., Eaton, E.N., and Weinberg, R.A. (1997). The catalytic subunit of yeast telomerase. Proc. Natl. Acad. Sci. U.S.A. *94*, 9202–9207.

Dewar, J.M., and Lydall, D. (2012). Similarities and differences between “uncapped” telomeres and DNA double-strand breaks. Chromosoma *121*, 117–130.

D’Mello, N.P., and Jazwinski, S.M. (1991). Telomere length constancy during aging of Saccharomyces cerevisiae. J. Bacteriol. *173*, 6709–6713.

Dolling, J.A., Boreham, D.R., Bahen, M.E., and Mitchel, R.E. (2000). Role of RAD9-dependent cell-cycle checkpoints in the adaptive response to ionizing radiation in yeast, Saccharomyces cerevisiae. Int. J. Radiat. Biol. *76*, 1273–1279.

Drosopoulos, W.C., Kosiyatrakul, S.T., Yan, Z., Calderano, S.G., and Schildkraut, C.L. (2012). Human telomeres replicate using chromosome-specific, rather than universal, replication programs. J. Cell Biol. *197*, 253–266.

Egilmez, N.K., and Jazwinski, S.M. (1989). Evidence for the involvement of a cytoplasmic factor in the aging of the yeast Saccharomyces cerevisiae. J. Bacteriol. *171*, 37–42.

Enomoto, S., Glowczewski, L., and Berman, J. (2002). MEC3, MEC1, and DDC2 are essential components of a telomere checkpoint pathway required for cell cycle arrest during senescence in Saccharomyces cerevisiae. Mol. Biol. Cell *13*, 2626–2638.

Evans, S.K., and Lundblad, V. (2000). Positive and negative regulation of telomerase access to the telomere. J. Cell. Sci. *113 Pt 19*, 3357–3364.

Fisher, T.S., and Zakian, V.A. (2005). Ku: a multifunctional protein involved in telomere maintenance. DNA Repair (Amst.) *4*, 1215–1226.

Friedel, A.M., Pike, B.L., and Gasser, S.M. (2009). ATR/Mec1: coordinating fork stability and repair. Curr. Opin. Cell Biol. *21*, 237–244.

Grandin, N., Damon, C., and Charbonneau, M. (2000). Cdc13 cooperates with the yeast Ku proteins and Stn1 to regulate telomerase recruitment. Mol. Cell. Biol. *20*, 8397–8408.

Grandin, N., Bailly, A., and Charbonneau, M. (2005). Activation of Mrc1, a mediator of the replication checkpoint, by telomere erosion. Biol. Cell *97*, 799–814.

Greider, C.W., and Blackburn, E.H. (1985). Identification of a specific telomere terminal transferase activity in Tetrahymena extracts. Cell *43*, 405–413.

Greider, C.W., and Blackburn, E.H. (1987). The telomere terminal transferase of Tetrahymena is a ribonucleoprotein enzyme with two kinds of primer specificity. Cell *51*, 887–898.

Harrison, D.E., Strong, R., Sharp, Z.D., Nelson, J.F., Astle, C.M., Flurkey, K., Nadon, N.L., Wilkinson, J.E., Frenkel, K., Carter, C.S., et al. (2009). Rapamycin fed late in life extends lifespan in genetically heterogeneous mice. Nature *460*, 392–395.

Henderson, E.R., and Blackburn, E.H. (1989). An overhanging 3’ terminus is a conserved feature of telomeres. Mol. Cell. Biol. *9*, 345–348.

Inoki, K., Ouyang, H., Li, Y., and Guan, K.-L. (2005). Signaling by target of rapamycin proteins in cell growth control. Microbiol. Mol. Biol. Rev. *69*, 79–100.

Jain, D., and Cooper, J.P. (2010). Telomeric strategies: means to an end. Annu. Rev. Genet. *44*, 243–269.

Jiang, J.C., Jaruga, E., Repnevskaya, M.V., and Jazwinski, S.M. (2000). An intervention resembling caloric restriction prolongs life span and retards aging in yeast. FASEB J. *14*, 2135–2137.

Johnson, F.B., Sinclair, D.A., and Guarente, L. (1999). Molecular Biology of Aging. Cell *96*, 291–302.

Kaeberlein, M. (2010). Lessons on longevity from budding yeast. Nature *464*, 513–519.

Kennedy, B.K., Austriaco, N.R., and Guarente, L. (1994). Daughter cells of Saccharomyces cerevisiae from old mothers display a reduced life span. J. Cell Biol. *127*, 1985–1993.

Kupiec, M., and Weisman, R. (2012). TOR links starvation responses to telomere length maintenance. Cell Cycle *11*, 2268–2271.

Lesur, I., and Campbell, J.L. (2004). The transcriptome of prematurely aging yeast cells is similar to that of telomerase-deficient cells. Mol. Biol. Cell *15*, 1297–1312.

Lingner, J., Hughes, T.R., Shevchenko, A., Mann, M., Lundblad, V., and Cech, T.R. (1997a). Reverse transcriptase motifs in the catalytic subunit of telomerase. Science *276*, 561–567.

Lingner, J., Cech, T.R., Hughes, T.R., and Lundblad, V. (1997b). Three Ever Shorter Telomere (EST) genes are dispensable for in vitro yeast telomerase activity. Proc. Natl. Acad. Sci. U.S.A. *94*, 11190–11195.

Longtine, M.S., Wilson, N.M., Petracek, M.E., and Berman, J. (1989). A yeast telomere binding activity binds to two related telomere sequence motifs and is indistinguishable from RAP1. Curr. Genet. *16*, 225–239.

Lue, N.F., Chan, J., Wright, W.E., and Hurwitz, J. (2014). The CDC13-STN1-TEN1 complex stimulates Pol α activity by promoting RNA priming and primase-to-polymerase switch. Nat Commun *5*, 5762.

Lundblad, V., and Blackburn, E.H. (1993). An alternative pathway for yeast telomere maintenance rescues est1- senescence. Cell *73*, 347–360.

Lundblad, V., and Szostak, J.W. (1989). A mutant with a defect in telomere elongation leads to senescence in yeast. Cell *57*, 633–643.

Lydall, D. (2003). Hiding at the ends of yeast chromosomes: telomeres, nucleases and checkpoint pathways. J. Cell. Sci. *116*, 4057–4065.

Marcand, S., Wotton, D., Gilson, E., and Shore, D. (1997). Rap1p and telomere length regulation in yeast. Ciba Found. Symp. *211*, 76–93; discussion 93–103.

Medvedik, O., Lamming, D.W., Kim, K.D., and Sinclair, D.A. (2007). MSN2 and MSN4 link calorie restriction and TOR to sirtuin-mediated lifespan extension in Saccharomyces cerevisiae. PLoS Biol. *5*, e261.

Meena, J.K., Cerutti, A., Beichler, C., Morita, Y., Bruhn, C., Kumar, M., Kraus, J.M., Speicher, M.R., Wang, Z.-Q., Kestler, H.A., et al. (2015). Telomerase abrogates aneuploidy-induced telomere replication stress, senescence and cell depletion. EMBO J. *34*, 1371–1384.

Melo, J., and Toczyski, D. (2002). A unified view of the DNA-damage checkpoint. Curr. Opin. Cell Biol *14*, 237–245.

Miller, K.M., Rog, O., and Cooper, J.P. (2006). Semi-conservative DNA replication through telomeres requires Taz1. Nature *440*, 824–828.

Al-Moghrabi, N.M., Al-Sharif, I.S., and Aboussekhra, A. (2001). The Saccharomyces cerevisiae RAD9 cell cycle checkpoint gene is required for optimal repair of UV-induced pyrimidine dimers in both G(1) and G(2)/M phases of the cell cycle. Nucleic Acids Res. *29*, 2020–2025.

Murray, A.W., and Szostak, J.W. (1983). Pedigree analysis of plasmid segregation in yeast. Cell *34*, 961–970.

Nautiyal, S., DeRisi, J.L., and Blackburn, E.H. (2002). The genome-wide expression response to telomerase deletion in Saccharomyces cerevisiae. Proc. Natl. Acad. Sci. U.S.A. *99*, 9316–9321.

O'Sullivan, R.J., and Karlseder, J. (2010). Telomeres: protecting chromosomes against genome instability. Nat. Rev. Mol. Cell Biol *11*, 171–181.

Pennock, E., Buckley, K., and Lundblad, V. (2001). Cdc13 delivers separate complexes to the telomere for end protection and replication. Cell *104*, 387–396.

Ray, S., Karamysheva, Z., Wang, L., Shippen, D.E., and Price, C.M. (2002). Interactions between telomerase and primase physically link the telomere and chromosome replication machinery. Mol. Cell. Biol. *22*, 5859–5868.

Reichard, P. (1988). Interactions between deoxyribonucleotide and DNA synthesis. Annu. Rev. Biochem. *57*, 349–374.

Sfeir, A., Kosiyatrakul, S.T., Hockemeyer, D., MacRae, S.L., Karlseder, J., Schildkraut, C.L., and de Lange, T. (2009). Mammalian Telomeres Resemble Fragile Sites and Require TRF1 for Efficient Replication. Cell *138*, 90–103.

Shen, C., Lancaster, C.S., Shi, B., Guo, H., Thimmaiah, P., and Bjornsti, M.-A. (2007). TOR signaling is a determinant of cell survival in response to DNA damage. Mol. Cell. Biol. *27*, 7007–7017.

Shore, D. (1994). RAP1: a protean regulator in yeast. Trends Genet. *10*, 408–412.

Singer, M.S., and Gottschling, D.E. (1994). TLC1: template RNA component of Saccharomyces cerevisiae telomerase. Science *266*, 404–409.

Soudet, J., Jolivet, P., and Teixeira, M.T. (2014). Elucidation of the DNA end-replication problem in Saccharomyces cerevisiae. Mol. Cell *53*, 954–964.

Stellwagen, A.E., Haimberger, Z.W., Veatch, J.R., and Gottschling, D.E. (2003). Ku interacts with telomerase RNA to promote telomere addition at native and broken chromosome ends. Genes Dev. *17*, 2384–2395.

Theimer, C.A., and Feigon, J. (2006). Structure and function of telomerase RNA. Curr. Opin. Struct. Biol. *16*, 307–318.

Tsolou, A., and Lydall, D. (2007). Mrc1 protects uncapped budding yeast telomeres from exonuclease EXO1. DNA Repair (Amst.) *6*, 1607–1617.

Ungar, L., Harari, Y., Toren, A., and Kupiec, M. (2011). Tor complex 1 controls telomere length by affecting the level of Ku. Curr. Biol. *21*, 2115–2120.

Usui, T., Ogawa, H., and Petrini, J.H. (2001). A DNA damage response pathway controlled by Tel1 and the Mre11 complex. Mol. Cell *7*, 1255–1266.

Vannier, J.-B., Pavicic-Kaltenbrunner, V., Petalcorin, M.I.R., Ding, H., and Boulton, S.J. (2012). RTEL1 dismantles T loops and counteracts telomeric G4-DNA to maintain telomere integrity. Cell *149*, 795–806.

Veatch, J.R., McMurray, M.A., Nelson, Z.W., and Gottschling, D.E. (2009). Mitochondrial dysfunction leads to nuclear genome instability via an iron-sulfur cluster defect. Cell *137*, 1247–1258.

Vialard, J.E., Gilbert, C.S., Green, C.M., and Lowndes, N.F. (1998). The budding yeast Rad9 checkpoint protein is subjected to Mec1/Tel1-dependent hyperphosphorylation and interacts with Rad53 after DNA damage. EMBO J. *17*, 5679–5688.

Zimmermann, M., Kibe, T., Kabir, S., and de Lange, T. (2014). TRF1 negotiates TTAGGG repeat-associated replication problems by recruiting the BLM helicase and the TPP1/POT1 repressor of ATR signaling. Genes Dev. *28*, 2477–2491.

Chapter 2: Early Telomerase Inactivation Accelerates Aging Independently of Telomere Length

Zhengwei Xie[1,2,3*], Kyle A. Jay[2*], Dana L. Smith[2], Yi Zhang[1,2,3], Zairan Liu[1,2,3], Jiashun Zheng[2,3], Ruilin Tian[1], Hao Li,[2,3] and Elizabeth Blackburn[2]

[1]Center for Quantitative Biology, School of Physics and The Peking-Tsinghua Center for Life Sciences, Peking University, Beijing 100871, China

[2]Department of Biochemistry and Biophysics, University of California, San Francisco, CA 94158, USA

[3]California Institute for Quantitative Biosciences, University of California, San Francisco, CA 94158, USA

[*] These authors contributed equally to this work.

The work presented in this chapter was published in the Feb 26, 2015 edition of Cell. I have included minor additions here, including Figures 2-3 and 2-12.

Author Contribution

K.A.J. performed strain constructions (30,000 series), sample genotyping, bulk population colony growth studies, adaptation and epistasis bulk cell cycle assays, telomere length (southern blot) experiments, and PCR-based telomere deprotection assays. K.A.J and E.H.B conceived the plans, interpreted and analyzed the data, and wrote the paper in collaboration with the other authors.

Abstract

Telomerase is required for long-term telomere maintenance and protection. Using single budding yeast mother cell analyses we found that, even *E*arly after *T*elomerase *I*nactivation (ETI), yeast mother cells show transient DNA Damage Response (DDR) episodes, stochastically altered cell cycle dynamics, and accelerated mother cell aging. The acceleration of ETI mother cell aging was not explainable by increased reactive oxygen species (ROS), Sir protein perturbation, or deprotected telomeres. The combined ETI phenotypes, which occurred well before the population senescence caused late after telomerase inactivation (LTI), were morphologically distinct from LTI senescence, were genetically uncoupled from telomere length, and were rescued by genetically elevating dNTP pools via Sml1 deletion. Our combined genetic and single-cell analyses show that even well before critical telomere shortening, telomerase is continuously required to respond to previously unrecognized transient DNA replication stress in mother cells, and a lack of telomerase accelerates otherwise normal aging.

Introduction

Telomeres, protective DNA-protein complexes at the ends of eukaryotic chromosomes, buffer against the loss of sequence during DNA replication and distinguish normal chromosome ends from potentially dangerous double-strand breaks. Telomeres are composed of sequence-specific DNA binding proteins bound to highly repetitive DNA sequences and are increasingly recognized as genomic regions prone to replication stress (Miller et al., 2006; Sfeir et al., 2009; Drosopoulos et al., 2012). Without the telomeric DNA-elongating enzyme telomerase, progressive telomere shortening

eventually causes the collapse of the protective DNA-protein complex (deprotection), but this occurs only after many cell divisions, *L*ate after *T*elomerase *I*nactivation (LTI). In LTI cells, telomere deprotection shares many properties with classic DNA damage (Nautiyal et al., 2002; Fagagna et al., 2003) and induces a DNA Damage Response (DDR) and a permanent G2/M cell cycle arrest (senescence).

Previously, responses to telomerase deletion have generally been reported only after a significant delay (in *S. cerevisiae*, after ~50-80 divisions). Thus, it was thought that cells sense altered telomere properties that signal senescence only when telomeres become critically short and deprotected. Hence, responses and phenotypes of cells *E*arly after *T*elomerase *I*nactivation (ETI) have not been extensively investigated. However, it was previously shown that, in ETI cells, very short telomeres appear at low frequencies that fuse to an induced double-strand break (DSB) (~10^{-4} to 10^{-3}). These rare fusions became molecularly detectable when telomerase was inactivated by either deletion of the telomerase RNA template *TLC1* (*tlc1Δ*) or by replacing the reverse transcriptase subunit, *EST2*, with the mutant *est2-D530A*, which assembles a telomerase ribonucleoprotein enzyme complex lacking telomeric DNA polymerization activity (Chan and Blackburn, 2003; Lingner et al., 1997). These fusogenic telomeres arose in ETI cells well before any signs of bulk population senescence and even if the telomeres had been pre-lengthened. Therefore, even the short-term absence of telomerase activity causes cells to experience a low but detectable genomic instability.

In a process distinct from the permanent bulk population cell-cycle arrest resulting from critically short telomeres in senescent LTI cells, an individual wild type (WT) yeast mother cell will cease divisions after it has produced approximately 25 daughter cells. As of yet, there has been very little evidence suggesting interaction between the pathways that regulate these two kinds of aging, hereafter referred to as “LTI senescence” and “mother cell aging/lifespan”, respectively. Despite the identification of multiple genes that regulate mother cells lifespans (Bishop and Guarente, 2007; Johnson et al., 1999; Kaeberlein, 2010), the mechanisms causing mother cell aging of even WT yeast remain poorly understood.

Here we report experiments employing single cell methodologies supporting a model in which budding yeast mother cells lacking telomerase activity are less able to resolve replication stress inherent to telomeres. These cells show induction of a signaling pathway indicative of transient DNA replication stress, altered cell cycle dynamics even in young mother cells, and accelerated aging (reduced lifespan), independently of telomere length. Our results demonstrate that this occurs well before the onset of LTI senescence and that the accelerated aging of ETI mother cells resembles the normal mother cell aging process.

Results

Mother Cells Lacking Active Telomerase Show Increased Heterogeneity of Cell Cycle Durations and Reduced Lifespans

We analyzed the properties of individual haploid ETI mother cells, well before any signs of cellular LTI senescence, freshly isolated from sporulation of heterozygous telomerase-competent diploids. Following genotyping, cells were taken from logarithmically growing cell cultures (~ 25-30 generations after telomerase loss), in which the overwhelming majority of cells were robustly-growing newborn or very young mother cells. These cells were placed in a microfluidic device, and the budding cycles and lifespans of individual mother cells were continuously monitored for two days by repeated microscopic imaging (Xie et al., 2012; Zhang et al., 2012).

First, even the youngest ETI mother cells (*tlc1*Δ or *est2D530A*) immediately showed higher frequencies of stochastically longer, and more heterogeneous cell cycle durations than WT (Figure 2-1A, 2-1B, 2-1C; note especially between times 0 to 5 hours as marked on Y axes). As the durations of the last two budding cycles were highly heterogeneous in both WT and ETI mothers, they were discarded from all cell cycle duration analyses discussed here. This cell cycle heterogeneity was consistent with observations of bulk ETI population budding kinetics, as manifested by cells lingering in the large-budded state (G2/M), the resolution of which did not require DNA damage adaptation pathways, and enrichment for cells with short spindles and unsegregated chromosomes (Figure 2-2A, 2-2B, 2-2C, 2-3). Secondly, we analyzed the mother cell aging of individual ETI cells and found that the lack of telomerase activity reduced ETI

mother cell lifespan. Mean budding lifespan for *tlc1*Δ was 12.6 (7 replicates), and 7.6 generations for *est2D530A* (3 replicates), compared to 22.1 for WT mother cells (Figure 2-1A, 2-1B, 2-1C, 2-1E). Furthermore, the catalytically-inactive telomerase *est2D530A* point mutant showed even longer cell cycle durations than *tlc1*Δ ETI mother cells, and the lifespan reduction was even more severe. Hence, lack of telomerase enzymatic activity, rather than the absence of an assembled telomerase ribonucleoprotein complex, causes increased cell cycle heterogeneity and faster mother cell aging.

Heterogeneous Cell Cycles do not Progressively Worsen with Shortening Telomeres

If the extended, heterogeneous cell cycle lengths of ETI mother cells were due solely to telomere shortening, we would have expected the phenotype to worsen progressively with each successive cell division. However, this was not the case. First, as individual mother cells progressed from being very young to old, ETI mother cells did not show any significant progressive increase in mean duration or heterogeneity of mother cell cycle lengths relative to WT (Figure 2-1G). Second, during the individual ETI mother cell lineages, a young mother cell whose initial cell cycle was long had no greater probability of having subsequent longer cell cycles or a shorter lifespan than one with an initial short cell cycle (Figure 2-4), supporting a stochastic and episodic, rather than progressive, nature of the occurrence of longer cell cycles. These highly stochastic episodes of cell cycle heterogeneity and lack of any progressive worsening of this phenotype as ETI mother cells aged, are not the predicted result of progressive telomere shortening.

SML1 Deletion Rescues Mother Cell Lifespan of ETI Cells Independently of Telomere Length

Because we observed an extended G2/M phase in bulk population analyses (Figure 2-2), which is often the result of DDR activation, we determined if mutations affecting the DDR affected the above ETI phenotypes. Responses to various forms of DNA damage, including that sensed at critically short telomeres in LTI senescence, involve a cascade of phosphorylation events, with early upstream steps occurring at the source of DNA damage through PIKK family member kinases Mec1 (*ATR*) and/or Tel1 (*ATM*). Strains lacking only Mec1 are inviable, but this *mec1Δ* lethality can be rescued by deletion of *SML1* (Zhao et al., 1998). Sml1 inhibits ribonucleotide reductase (RNR), which catalyzes the rate limiting step in dNTP production (Reichard, 1988). Deletion of Sml1 increases RNR activity and elevates dNTP pools, obviating the need for certain DDR components under healthy growing conditions, and can be protective against some forms of DNA damage (Andreson et al., 2010; Jossen and Bermejo, 2013). Strikingly, deletion of *SML1* in ETI *tlc1Δ* strains efficiently rescued the ETI-induced heterogeneity of budding cycle durations (Figure 2-1D) as well as the shortening of mother cell lifespan (Figure 2-1F). However, *SML1* deletion alone produced no change in the rates of bulk telomere shortening in ETI cells, nor in the subsequent onset of LTI senescence (Figure 2-5, 2-6). We also confirmed that the deletion of *SML1* alone caused no significant effect on mother cell lifespans and telomere length compared to WT (Figure 2-1F, 2-7B). Hence, the dramatic rescue of ETI cell cycle heterogeneity and accelerated

mother cell aging by *SML1* deletion cannot be explained by increased telomere length or by slower rates of telomere shortening.

ETI Mother Cells Age with Terminal Cellular and Mitochondrial Morphologies Distinct from LTI Senescence but Similar to those of Normal Mother Cell Aging

We tested further whether budding cessation due to mother cell aging in ETI or WT cells was distinguishable from the G2/M arrest caused by LTI senescence by examining cell and mitochondrial morphology at the end of the lifespans (terminal morphology). Typical WT mother cell aging produces terminal cells that are mostly small-budded with minimal or no mitochondrial fluorescence signal from a mitochondrially-localized GFP (mtGFP) (Figure 2-8Ai) and a smaller population of elongated cells with brighter mitochondrial fluorescence (Figure 2-8Aii). In contrast, cells terminally arrested due to LTI senescence accumulate with a swollen, large-budded ("dumbbell") morphology and with mitochondrial fluorescence that gradually forms very bright dots (Figure 2-8Aiii) (Nautiyal et al., 2002). We created and analyzed two populations of *tlc1*Δ*sml1*Δ cells. The first population was isolated as soon as possible after genotyping (ETI) and was enriched for mother cells that would reach their aging limit prior to LTI senescence. The second population was passaged for approximately 10 additional generations prior to microfluidics analysis, thus enriching for cells that would undergo LTI senescence (critically short telomeres) before the mother cells reached their aging limit (Figure 2-8B). Terminally aged ETI *tlc1*Δ and ETI *tlc1*Δ*sml1*Δ mother cells accumulated mostly in two dominant terminal morphologies, which resembled the two dominant WT terminal morphology phenotypes (Xie et al., 2012), and only very rarely in the dumbbell

morphology (Figure 2-8A, 2-8C). In contrast, in terminal LTI *tlc1*Δ*sml1*Δ mother cells, terminal dumbbell morphologies became the major type observed, indicating that a large proportion of the population had entered LTI senescence (Figure 2-8Aiii, 2-8C). These results support terminal cellular and mitochondrial morphology as an accurate distinction between LTI senescence and normal mother cell aging, and provide further evidence that ETI mother cells cease divisions as a result of mother cell aging rather than LTI senescence.

Mutation of Specific DDR Components Exacerbates ETI Cell Cycle and Lifespan Phenotypes

We investigated other proteins previously implicated in yeast telomere maintenance and in the DDR for effects on mother cell aging. Maintenance of yeast telomeres at normal length requires DDR kinases Mec1 and Tel1 (Sabourin and Zakian, 2008; Takata et al., 2004) and the replication stress-specific DDR adaptor protein Mrc1 (Grandin et al., 2005). First, we found that cell cycle heterogeneity and mother cell lifespan were similar in WT, *tel1*Δ, and *mec1*Δ*sml1*Δ strains (Figure 2-1A, 2-9A, 2-9C, 2-7C, 2-10A). Because *tel1*Δ in haploid cells reduces telomerase action on telomeres, telomeres decline to a short length that is then stably maintained (Greenwell et al., 1995; Lustig and Petes, 1986). The *tel1*Δ cells used here were isolated immediately after sporulation of heterozygous parent diploids and analyzed when telomeres were still shortening from near-WT lengths. Therefore, having telomeres that are shortening but eventually stably maintained is not alone sufficient to alter cell cycle duration and lifespan.

Next, we examined how mutations of Mec1 and Tel1 affect the ETI phenotypes. Because *sml1*Δ, as shown above, efficiently rescues the accelerated aging of ETI mother cells, it is difficult to determine if Mec1 has a role in this process, due to the necessity of deleting *SML1* for viability in *mec1*Δ strains. However, ETI *tlc1*Δ*tel1*Δ double mutant mother cells had even greater cell cycle heterogeneity and shorter budding lifespan (mean 9.8 generations, 2 replicates) than control ETI *tlc1*Δ single mutant mother cells (Figure 2-1B, 2-9B, 2-9D). As shown previously, freshly isolated ETI haploid cells that are also mutated for Tel1 or Mec1 (*tlc1Δmec1Δsml1Δ* or *tlc1Δtel1Δ*) have a rate of initial telomere-shortening and progression to LTI population senescence similar to *tlc1Δ* single mutants (Chan and Blackburn, 2003) (Figure 2-9E, 2-9F). Hence, the exacerbation of the ETI cell cycle heterogeneity and lifespan reduction phenotypes caused by lack of Tel1 is not explained by faster telomere shortening or accelerated population senescence.

Because *sml1*Δ rescues the cell cycle and lifespan phenotypes of *tlc1*Δ mother cells, and is known to facilitate DNA replication by increasing nucleotide levels (Chabes et al., 2003), we suspected that ETI cells may be more vulnerable to telomeric DNA replication stress. Therefore, we mutated the DDR adaptor protein Mrc1, which is required specifically for the DNA replication stress checkpoint (Alcasabas et al., 2001; Osborn and Elledge, 2003) and has a minor role in telomere length maintenance (Tsolou and Lydall, 2007). Mutation of 17 potential PIKK family kinase consensus phosphorylation sites on Mrc1 (*mrc1*^{AQ}) allows full cell viability but disables the DNA replication stress response (Osborn and Elledge, 2003). Despite the lack of any mother cell lifespan or

cell cycle effect of *mrc1^{AQ}* alone (Figure 2-11A, 2-11C), *tlc1*Δ*mrc1^{AQ}* double mutant ETI mother cells showed even greater cell cycle length heterogeneity than the *tlc1*Δ single mutant ETI cells (Figure 2-11B). Consistent results were also seen in the G2/M durations in bulk populations (Figure 2-2D) and mean lifespan was markedly reduced to 8.8 generations (2 replicates), compared with 12.6 generations for the control *tlc1*Δ ETI strains (Figure 2-1B, 2-11D). These effects were not explainable by reduced telomere length or accelerated senescence, as the *mrc1^{AQ}* mutant allele produced stable telomeres only slightly shorter than WT and had no effect on the kinetics of telomere shortening or bulk population senescence (Figure 2-11E, 2-11F). We also tested the epistasis relationship of *tel1*Δ and *mrc1^{AQ}* in the ETI context. ETI triple mutant *tlc1*Δ*tel1*Δ*mrc1^{AQ}* cells showed the same lifespan shortening as the double ETI mutants (Figure 2-10B) This was also consistent with bulk population assays, which showed no exacerbation of the G2/M cell cycle extension in triple mutant ETI *tlc1*Δ*tel1*Δ*mrc1^{AQ}* cells relative to ETI double mutants (Figure 2-12). We conclude that *Tel1* and *Mrc1* checkpoint functions act in the same pathway and that lack of either one acts synthetically with the ETI mother cell phenotypes.

In the DDR cascade, downstream of Tel1 or Mec1, the DDR adaptor protein Rad9 can act semi-redundantly with the adaptor protein Mrc1. Mrc1 is specifically involved in the replication stress response while Rad9 is mostly important for responding to DNA breaks and other DNA damage. In contrast to *tlc1*Δ*mrc1^{AQ}* ETI cells, *tlc1*Δ*rad9*Δ ETI mother cell cycle durations and lifespans were not significantly different from *tlc1*Δ ETI cells, consistent with bulk population analyses (Figure 2-2, and data not shown). The

ETI *tlc1*Δ *rad9*Δ mother cells had a mean lifespan of 16.5 generations (2 replicates), while the control *tlc1*Δ strain had a mean lifespan of 13.7 generations (Figure 2-10C). Thus, *rad9*Δ did not significantly affect the accelerated aging phenotypes of ETI mother cells. These results confirmed the specificity of the Mrc1 checkpoint function in the ETI mother cell phenotypes and indicate the involvement of a DNA replication stress response, rather than a response to other forms of DNA damage, which requires Rad9. In summary, disrupting the DDR via *tel1*Δ or *mrc1*^{AQ} mutations, but not by *mec1*Δ*sml1*Δ or *rad9*Δ, strongly exacerbated the cell cycle abnormalities and acceleration of mother cell aging in ETI cells, independently of telomere length and without accelerating LTI senescence.

ETI Mother Cell Phenotypes are Not Caused by Deprotected Telomeres

Previous results showed that short, fusogenic telomeres occur spontaneously at very low frequencies in ETI cells (Chan and Blackburn, 2003). These fusogenic telomeres derive from rare individual deprotected telomeres and can be detected by PCR assays upon their fusion to an induced DNA double-stranded break. We tested whether the amount of such fusogenic telomeres correlated with the severity of our ETI mother cell phenotypes using the same system (Chan and Blackburn, 2003) for semi-quantitative PCR analyses. In agreement with the published work, we found that single mutant ETI (*tlc1*Δ) and *tel1*Δ strains each showed detectable but low amounts of fusions resulting from a deprotected telomere fusing to an induced DSB and that *tlc1*Δ*tel1*Δ strains showed a synergistic increase (Figure 2-13A, 2-13B). However, in *tlc1*Δ*mrc1*^{AQ} ETI cells (Figure 2-13A), the *mrc1*^{AQ} mutation produced no further significant increase over a

*tlc1*Δ single mutant. Furthermore, *sml1*Δ did not reduce (and possibly increased) the number of fusogenic telomeres detected (Figure 2-13A, 2-13B). This complete non-concordance in these various ETI genotypes with the novel phenotypes we have observed here in ETI mother cells argues strongly against deprotected telomeres as a cause for the exacerbated cell cycle heterogeneity and accelerated mother cell aging.

Further evidence that ETI phenotypes are not caused by deprotected telomeres, which induce a robust DDR (d' Adda di Fagagna et al., 2003; Nautiyal et al., 2002), came from comparing the genetic dependencies of ETI cell phenotypes versus DNA damage sensitivity. As previously reported, *mec1*Δ*sml1*Δ and *rad9*Δ mutations made cells highly sensitive to treatment with various classic DNA damaging agents (HU, UV, phleomycin or MMS) (Figure 2-7D). This is in dramatic contrast to the experiments described above, in which *mec1*Δ*sml1*Δ and *rad9*Δ did not exacerbate the ETI phenotypes. Hence, the genotype dependencies of ETI mother cell phenotypes are quite distinct from the dependencies of responses to classic DNA damaging agents.

Altered Recombination Levels are Not Responsible for ETI Mother Cell Phenotypes

Recombination is another process that has been implicated in maintaining yeast telomeres and occurs when telomeres lose protection, such as in LTI cells (McEachern and Blackburn, 1996; Basenko et al., 2011). Following the onset of LTI senescence, Rad52-dependent recombination at telomeres allows a small fraction (~10^{-4}) of senescing LTI yeast cells to survive and continue dividing (Lundblad and Blackburn,

1993). Also, DNA replication stress can be relieved by mechanisms involving recombination. We therefore asked if recombination plays any role in the ETI accelerated mother cell cycle kinetics and aging response. Deletion of *RAD52* alone causes no changes in telomere length maintenance and telomeres in *tlc1*Δ*rad52*Δ strains shorten no faster than with *tlc1*Δ alone (Lundblad and Blackburn, 1993). However, *rad52*Δ alone caused increased mother cell cycle duration heterogeneity (data not shown) and an acceleration of mother cell budding aging (Park et al., 1999). Notably, these *rad52*Δ phenotypes were not substantially rescued by *SML1* deletion (mean lifespan, *rad52*Δ: 9.4, n=130 versus *rad52*Δ*sml1*Δ: 13.2, n=70) (Figure 2-14A and data not shown). Furthermore, the mean lifespan of ETI *tlc1*Δ*rad52*Δ*sml1*Δ mother cells was even lower than *rad52*Δ*sml1*Δ: 8.2 versus 13.2 (Figure 2-14A). Hence, lack of Rad52 function appears to act additively to the effect of *TLC1* deletion. This epistasis relationship indicates that absence of telomerase activity and of Rad52 each causes acceleration of mother cell aging, but by two distinct mechanisms.

ETI Phenotypes are Not Caused By Relocalization of Sir Proteins

Another pathway previously implicated in yeast mother cell aging involves changes in Sir protein concentration and localization. For example, Sir2 overexpression has been shown to increase mother cell lifespan (Kaeberlein et al., 1999). However, several lines of evidence argue that Sir2 sequestration in ETI cells does not explain their accelerated aging. First, all our ETI strains mated normally, implying that the mating type loci were still silenced and arguing against a large relocalization of Sir proteins. Second, localized puncta of Sir3-GFP, indicative of telomere-bound Sir complex proteins (Martin et al.,

1999) were not significantly different between ETI and WT mother cells (Figure 2-14B). Third, although a single induced unrepairable DNA break has been reported to cause Rad9-dependent delocalization of Sir2 from telomeres (Martin et al., 1999; Mills et al., 1999), as described above, *rad9*Δ neither exacerbated nor significantly rescued the accelerated aging in ETI mother cells. Together, these findings indicate that altered sequestration of the Sir complex is not the mechanism causing the accelerated aging of ETI cells.

Lifespan Reduction of ETI Mother Cells is Not Caused by Increased Reactive Oxygen Species (ROS)

We re-examined the previously described transcriptional profile datasets (Nautiyal et al., 2002; Table 2-1, passage 1) of ETI *tlc1*Δ cells. In an unbiased approach, we compared the large available number of yeast gene expression profiles, measured under different environmental conditions and genetic backgrounds (Edgar et al., 2002), to that of ETI cells (Tables 2-2, 2-3, 2-4). The top hit (Pearson correlation = 0.495, *p*-value < 1e-254) was treatment with diamide, a thiol-oxidizing agent that causes oxidative stress. Because intracellular ROS have long been theorized to play a role in aging and ROS levels can be elevated as a result of DNA damage (Rowe et al., 2008; Salmon et al., 2004), we tested if oxidative stress caused the ETI mother cell phenotypes.

We assessed oxidative stress in ETI cells by quantifying ROS levels in our strains. If the accelerated aging of ETI cells is caused by higher intracellular ROS levels, it would be predicted that ETI *tlc1*Δ mother cells would have higher ROS than WT and that ETI

*tlc1*Δ *sml1*Δ cells would have lower ROS levels than ETI single *tlc1*Δ mutants. However, ETI cells did not have significantly higher levels of ROS than WT (Figure 2-14C). Furthermore, *sml1*Δ and *tlc1*Δ*sml1*Δ strains showed even higher levels of ROS, the opposite effect from that predicted if ETI causes faster aging of cells via higher intracellular ROS level. We also tested the effects of anti-oxidants by treatment with N-Acetyl-L-Cysteine (NAC). However, NAC equally and only modestly lengthened mother cell lifespans of both ETI and WT mother cells (Figure 2-14D). Hence, we conclude that even though the transcriptional profile changes in ETI cells include features of an oxidative stress response, increased ROS levels and oxidative stress are not a primary cause of accelerated mother cell aging elicited by ETI.

ETI Cells Show Transient RNR3 Upregulation during Mother Cell Divisions

Given the connections between DNA damage and cell cycle regulation, we turned to a more detailed analysis to establish if DDR signaling was induced in ETI mother cells. Notably, phosphorylation of DDR components such as Rad53 and Mrc1 is only detectable in LTI cells and not in ETI cells (Grandin et al., 2005) (Figure 2-7A). Therefore, we employed a more sensitive single cell monitoring method to detect evidence for DDR signaling. We examined DDR activation during mother cell aging using a GFP-tagged allele of *RNR3,* a gene that is strongly induced as a downstream component of the DDR. We monitored GFP intensity during mother cell lifespan assays and quantified RNR3-GFP peaks (at least 1.3 fold above background) using strains containing *RNR3-GFP* and all relevant combinations of *tlc1*Δ, *sml1*Δ, *mrc1*^{AQ}, and *tel1*Δ mutations. Peaks were classified as occurring before the last two cell divisions or

during/after the last two divisions, referred to here as “still-dividing” and “terminal” peaks respectively (Figure 2-13C, 2-13E). Terminal peaks were scored as peaks per mother cell, and still-dividing peaks were scored as peaks per cell cycle as mother cells underwent a different average number of cycles depending on genotype (Figure 2-13D, 2-13F). In WT mother cells (2 replicates), a transient RNR3-GFP peak appeared at a low frequency during the cell cycles of still-dividing mother cells (0.0062, 95% confidence limits 0.0031 - 0.0111; n=11 events in 1,766 cell cycles) and terminal peaks occurred in 25.0% of mother cells (24/96 cells, 95% confidence limits 0.1736 - 0.3456). In contrast, in *tlc1*Δ ETI mother cell lineages (3 replicates), RNR3-GFP peaks occurred at significantly greater frequency in still-dividing mother cells (0.0177, 95% confidence limits 0.0123 - 0.0252; n=30 events out of 1,696 cell cycles, p-value < 0.0025 compared with WT), and in 27.7% of terminal mother cells (44/159 cells, 95% confidence limits 0.213 - 0.351). Hence, in still-dividing mother cells, ETI elicits an increased number of transient episodes of DDR signaling.

Notably, relative to *tlc1*Δ single mutants, RNR3-GFP peaks in *tlc1*Δ*sml1*Δ ETI mother cells (3 replicates) were significantly diminished in frequency in the still-dividing mother cells (0.0104, 95% confidence limits 0.0071 - 0.0152; n=27 events in 2,587 cell cycles, *p*-value < 0.05 compared with *tlc1*Δ), and terminal peaks occurred in only 13.1% of mother cells (22/168 cells, 95% confidence limits 0.087 - 0.191, *p*-value < 0.01 compared with *tlc1*Δ). This result is explainable as *sml1*Δ raises nucleotide pools, making replication fork stalling less likely to occur (Andreson et al., 2010; Jossen and

Bermejo, 2013), hence reducing the possibility of eliciting a DNA replication stress response.

ETI *tlc1*Δ*tel1*Δ mother cells (2 replicates) showed fewer RNR3 peaks than WT (or *tlc1*Δ ETI) in still-dividing cells (0.006, 95% confidence limits 0.0034 - 0.0124; n=10 events in 1,505 cell cycles, *p*-value < 0.006 compared with *tlc1*Δ) and peaks occurred in 12.0% of terminal mother cells (15/125 cells, 95% confidence limits 0.0730 - 0.1897, *p*-value < 0.009 compared with *tlc1*Δ). This finding indicates that abrogating Tel1 greatly exacerbated the ETI mother cell aging phenotypes (Figure 2-9B, 2-9D), while reducing RNR3 induction events. We propose that the optimal response to the replication stress in *tlc1*Δ ETI cells requires Tel1 checkpoint function to activate DDR signaling, monitored here as downstream RNR3 induction.

Interestingly, the *tlc1*Δ*mrc1*^{AQ} ETI mother cells showed significantly more RNR3 peaks than WT cells in both still-dividing (0.0193, 95% confidence limits 0.0127 - 0.0289; n=23 events in 1,192 cell cycles) and terminal mothers (32.4 %, 35/108 cells, 95% confidence limits 0.243 - 0.417), and also trends to more RNR3 peaks than *tlc1*Δ (3 replicates). Because the *mrc1*^{AQ} mutation exacerbates the ETI cell cycle duration and lifespan reduction phenotypes, this finding indicates that telomeric replication stress requires Mrc1 checkpoint function in order to elicit an appropriate response in the absence of telomerase, but not for induction of the RNR3 reporter.

As the Rad9 adaptor protein is semi-redundant with Mrc1 in the DDR cascade, we investigated whether Rad9 is required for induction of RNR3 in the absence of Mrc1 checkpoint function. However, when combined with the *tlc1*Δ mutation, the *mrc1*^{AQ} *rad9*Δ double mutation induced rapid lethality of the bulk ETI cell population, precluding mother cell analyses. Remarkably, this loss of viability in *tlc1*Δ*mrc1*^{AQ}*rad9*Δ cells was also completely rescued by *sml1*Δ (see Chapter 3). We conclude that if ETI mother cells lack either Tel1 or Mrc1 checkpoint function, the response to, or repair of, telomeric DNA replication stress-induced damage is compromised.

The Degree of Heterogeneity of Cell Cycle Durations and Mitochondrial Changes in Young ETI Mother Cells each Quantitatively Predict Lifespan

Strikingly, for each mother cell genotype described above, the frequency and degree of lengthened cell cycles in young mother cells predicted the degree of reduction in mean lifespan (Figure 2-15A, 2-15B). Furthermore, for both WT and ETI mother cells, the extent of the mitochondrial fluorescence quantified at a given early time point in the budding lineage (4 hours) predicted the lifespan of that particular mother cell (Figure 2-15C, 2-15D). The finding that these relationships held across multiple genotypes suggests that responses that occur in even the youngest mother cells are caused by the same problem that eventually regulates the lifespan of the cell.

Discussion

Here we have shown that lack of active telomerase affects yeast mother cells much earlier than expected, well before any effect on cells that can be attributed to critical telomere shortness. Notably, early telomerase inactivation in yeast mother cells caused increased heterogeneity of the cell cycle and accelerated aging. These phenotypes were rescued by increasing nucleotide pool levels and were sensitive to inactivation of specific DDR components. By several criteria, the ETI mother cell aging phenotype is consistent with an acceleration of normal mother cell aging processes and not senescence caused by loss of telomere protective function. These criteria included terminal cell and mitochondrial morphologies characteristic of aging WT mother cells and distinct from those in senescent cells.

Previously, it was thought that telomeres had to become critically short in order to elicit a cellular DDR. In contrast, our results suggest that independent of critical telomere shortness, ETI cells initiate signaling that accelerates an otherwise normal mother cell aging pathway. In the ETI setting, across multiple genotypes, the premature onset of mother cell aging is anticipated by the frequency and severity of stochastically slower cell cycling events occurring in even young mother cells. In addition, we have shown that it is a lack of telomerase activity, rather than the lack of an assembled telomerase complex, that is the proximate cause of the response. Therefore, the action of telomerase on telomeres appears to be the most likely molecular property whose alteration causes these effects in ETI cells.

Our combined findings provide evidence for the model shown in Figure 2-16. In this model, during mother cell divisions in ETI cells, lack of telomerase activity may eliminate a potential bypass mechanism for replication stress in the telomere. This causes transient episodes of a much milder DDR than the robust and sustained DDR elicited by critically short telomeres (Nautiyal et al., 2002; d' Adda di Fagagna et al., 2003). We propose that deletion of Sml1, via its known phenotype of increasing dNTP levels, alleviates this replication stress at an upstream level, preventing DNA damage signaling. This explains why Sml1 deletion suppressed both the transient DDR signaling and the accelerated aging in ETI mother cells. We propose that such replication stress arises often in telomeres and is sensed by Tel1, which is required to cause the observed transient rises in RNR3 levels in ETI cells. This response promotes either repair or tolerance of the replication stress that allows ETI cells to bypass it and enter the next cell cycle. In ETI cells lacking the checkpoint functions of Tel1 or Mrc1 (*tlc1*Δ*tel1*Δ or *tlc1*Δ *mrc1*^{AQ}), cells cannot activate the appropriate response to this replication stress, thus exacerbating the ETI phenotypes. Without Mrc1 checkpoint function, compensation by the semi-redundant adaptor Rad9 occurs to some degree, but the telomeric replication stress is not fully resolved and further damage can ensue. However, in the absence of telomerase, even a fully functional DDR is not sufficient to fully alleviate telomeric replication stress and prevent accelerated mother cell aging.

We determined that neither ROS, recombination, deprotected (fusogenic) telomeres, redistribution of SIR protein complexes, nor a DDR similar to that in response to classic

DNA damaging agents, can account for the accelerated mother cell aging of ETI cells. Deletion of *SML1* rescued the cell cycle, lifespan, and DDR (RNR3) induction phenotypes in dividing ETI mother cells and is known to suppress replication fork stalling (Andreson et al., 2010; Jossen and Bermejo, 2013). The majority of mutant phenotypes known to be suppressed by *sml1*Δ are related to DNA replication, including replication fork progression. This suggests that suppression by *sml1*Δ is very specific, and occurs through elevated nucleotide pools, via the release of inhibition of the RNR complex. Furthermore, the transcriptional profile of ETI *tlc1*Δ cells indicates that they upregulate *RNR2*, *3*, and *4* gene expression (Nautiyal et al., 2002) (Table 2-1). Taken together with previous findings, our results suggest that the higher nucleotide pools in *sml1*Δ cells prevent telomeric replication stress from occurring, thus suppressing the ETI phenotype by preventing any need for DDR activation or telomerase intervention.

Telomerase is predicted to be recruited to backtracked replication forks resulting from stalling, which has been proposed to occur at measurable frequencies in telomeric DNA (Miller et al., 2006; Drosopoulos et al., 2012). Such backtracked forks will expose single-stranded leading strand $TG_{(1-3)}$ repeat sequence DNA, which is the substrate for telomerase elongation. Also, telomerase could aid in the repair of a broken telomeric fork generated when a stalled replisome collapses (Chang et al., 2009). The resulting shortened telomere is a known preferred telomerase substrate (Miller et al., 2006). Other known interactions between DNA polymerase and telomerase actively engaged on telomeres may normally be required to optimize fork movement or fork restarting in telomeres. For example, the telomere-binding Cdc13-Stn1-Ten1 complex interacts via

its Cdc13 subunit with a subunit of the telomerase complex (Est1) and also interacts (via Stn1) with a subunit of DNA polymerase alpha (Grossi et al., 2004).

The causal mechanism underlying mother cell aging remains unknown even for WT yeast despite extensive identification of genetic and environmental modifiers of this process. Our findings indicate that telomerase functionality is required throughout the divisions of yeast mother cells in a more continuous mode than previously thought. The novel findings reported here indicate that telomerase activity is required to alleviate normal telomeric replication stress and allow mother cell aging to occur with wild type kinetics. In addition, mutations known to inhibit telomerase activity or telomere maintenance have been implicated in the premature onset of diseases of aging and reduced lifespan in humans and mice (Codd et al., 2013) (Armanios and Blackburn, 2012) and replication stress has been shown to induce aging in mouse cells (Flach et al., 2014). Therefore, this early requirement for active telomerase in preventing premature mother cell aging in yeast suggests a new possibility: that loss of telomerase activity may have telomere length independent consequences that accelerate aging and cause aging related diseases in other eukaryotes.

Acknowledgements

This work was supported by NIH grant GM26259 to EHB and NIH grants (GM070808 & AG043080) and a Packard Fellowship in Science and Engineering to HL, and by the NIH Center for Systems and Synthetic Biology (P50 GM081879).

References

D' Adda di Fagagna, F., Reaper, P.M., Clay-Farrace, L., Fiegler, H., Carr, P., Von Zglinicki, T., Saretzki, G., Carter, N.P., and Jackson, S.P. (2003). A DNA damage checkpoint response in telomere-initiated senescence. Nature *426*, 194–198.

Alcasabas, A.A., Osborn, A.J., Bachant, J., Hu, F., Werler, P.J.H., Bousset, K., Furuya, K., Diffley, J.F.X., Carr, A.M., and Elledge, S.J. (2001). Mrc1 transduces signals of DNA replication stress to activate Rad53. Nat Cell Biol *3*, 958–965.

Andreson, B.L., Gupta, A., Georgieva, B.P., and Rothstein, R. (2010). The ribonucleotide reductase inhibitor, Sml1, is sequentially phosphorylated, ubiquitylated and degraded in response to DNA damage. Nucleic Acids Res *38*, 6490–6501.

Armanios, M., and Blackburn, E.H. (2012). The telomere syndromes. Nat. Rev. Genet. *13*, 693–704.

Basenko, E., Topcu, Z., and McEachern, M.J. (2011). Recombination Can either Help Maintain Very Short Telomeres or Generate Longer Telomeres in Yeast Cells with Weak Telomerase Activity. Eukaryotic Cell *10*, 1131–1142.

Chabes, A., Georgieva, B., Domkin, V., Zhao, X., Rothstein, R., and Thelander, L. (2003). Survival of DNA damage in yeast directly depends on increased dNTP levels allowed by relaxed feedback inhibition of ribonucleotide reductase. Cell *112*, 391–401.

Chan, S.W.-L., and Blackburn, E.H. (2003). Telomerase and ATM/Tel1p Protect Telomeres from Nonhomologous End Joining. Molecular Cell *11*, 1379–1387.

Codd, V., Nelson, C.P., Albrecht, E., Mangino, M., Deelen, J., Buxton, J.L., Hottenga, J.J., Fischer, K., Esko, T., Surakka, I., et al. (2013). Identification of seven loci affecting mean telomere length and their association with disease. Nat Genet *45*, 422–427.

Drosopoulos, W.C., Kosiyatrakul, S.T., Yan, Z., Calderano, S.G., and Schildkraut, C.L. (2012). Human telomeres replicate using chromosome-specific, rather than universal, replication programs. J. Cell Biol. *197*, 253–266.

Edgar, R., Domrachev, M., and Lash, A.E. (2002). Gene Expression Omnibus: NCBI gene expression and hybridization array data repository. Nucl. Acids Res. *30*, 207–210.

Grandin, N., Bailly, A., and Charbonneau, M. (2005). Activation of Mrc1, a mediator of the replication checkpoint, by telomere erosion. Biology of the Cell *97*, 799–814.

Greenwell, P.W., Kronmal, S.L., Porter, S.E., Gassenhuber, J., Obermaier, B., and Petes, T.D. (1995). TEL1, a gene involved in controlling telomere length in S. cerevisiae, is homologous to the human ataxia telangiectasia gene. Cell *82*, 823–829.

Grossi, S., Puglisi, A., Dmitriev, P.V., Lopes, M., and Shore, D. (2004). Pol12, the B subunit of DNA polymerase α, functions in both telomere capping and length regulation. Genes Dev. *18*, 992–1006.

Jossen, R., and Bermejo, R. (2013). The DNA damage checkpoint response to replication stress: A Game of Forks. Front Genet *4*, 26.

Kaeberlein, M., McVey, M., and Guarente, L. (1999). The SIR2/3/4 complex and SIR2 alone promote longevity in Saccharomyces cerevisiae by two different mechanisms. Genes Dev *13*, 2570–2580.

Lundblad, V., and Blackburn, E.H. (1993). An alternative pathway for yeast telomere maintenance rescues est1- senescence. Cell *73*, 347–360.

Lustig, A.J., and Petes, T.D. (1986). Identification of yeast mutants with altered telomere structure. Proc. Natl. Acad. Sci. U.S.A. *83*, 1398–1402.

Martin, S.G., Laroche, T., Suka, N., Grunstein, M., and Gasser, S.M. (1999). Relocalization of telomeric Ku and SIR proteins in response to DNA strand breaks in yeast. Cell *97*, 621–633.

McEachern, M.J., and Blackburn, E.H. (1996). Cap-prevented recombination between terminal telomeric repeat arrays (telomere CPR) maintains telomeres in Kluyveromyces lactis lacking telomerase. Genes Dev. *10*, 1822–1834.

Miller, K.M., Rog, O., and Cooper, J.P. (2006). Semi-conservative DNA replication through telomeres requires Taz1. Nature *440*, 824–828.

Mills, K.D., Sinclair, D.A., and Guarente, L. (1999). MEC1-Dependent Redistribution of the Sir3 Silencing Protein from Telomeres to DNA Double-Strand Breaks. Cell *97*, 609–620.

Nautiyal, S., DeRisi, J.L., and Blackburn, E.H. (2002). The genome-wide expression response to telomerase deletion in Saccharomyces cerevisiae. Proc. Natl. Acad. Sci. U.S.A. *99*, 9316–9321.

Osborn, A.J., and Elledge, S.J. (2003). Mrc1 is a replication fork component whose phosphorylation in response to DNA replication stress activates Rad53. Genes Dev. *17*, 1755–1767.

Park, P.U., Defossez, P.-A., and Guarente, L. (1999). Effects of Mutations in DNA Repair Genes on Formation of Ribosomal DNA Circles and Life Span inSaccharomyces cerevisiae. Mol. Cell. Biol. *19*, 3848–3856.

Reichard, P. (1988). Interactions Between Deoxyribonucleotide and DNA Synthesis. Annual Review of Biochemistry *57*, 349–374.

Rowe, L.A., Degtyareva, N., and Doetsch, P.W. (2008). DNA damage-induced reactive oxygen species (ROS) stress response in Saccharomyces cerevisiae. Free Radic. Biol. Med. *45*, 1167–1177.

Sabourin, M., and Zakian, V.A. (2008). ATM-like kinases and regulation of telomerase: lessons from yeast and mammals. Trends in Cell Biology *18*, 337–346.

Salmon, T.B., Evert, B.A., Song, B., and Doetsch, P.W. (2004). Biological consequences of oxidative stress-induced DNA damage in Saccharomyces cerevisiae. Nucleic Acids Res. *32*, 3712–3723.

Takata, H., Kanoh, Y., Gunge, N., Shirahige, K., and Matsuura, A. (2004). Reciprocal Association of the Budding Yeast ATM-Related Proteins Tel1 and Mec1 with Telomeres In Vivo. Molecular Cell *14*, 515–522.

Toczyski, D.P., Galgoczy, D.J., and Hartwell, L.H. (1997). CDC5 and CKII control adaptation to the yeast DNA damage checkpoint. Cell *90*, 1097–1106.

Tsolou, A., and Lydall, D. (2007). Mrc1 protects uncapped budding yeast telomeres from exonuclease EXO1. DNA Repair (Amst) *6*, 1607–1617.

Xie, Z., Zhang, Y., Zou, K., Brandman, O., Luo, C., Ouyang, Q., and Li, H. (2012). Molecular phenotyping of aging in single yeast cells using a novel microfluidic device. Aging Cell *11*, 599–606.

Zhang, Y., Luo, C., Zou, K., Xie, Z., Brandman, O., Ouyang, Q., and Li, H. (2012). Single Cell Analysis of Yeast Replicative Aging Using a New Generation of Microfluidic Device. PLoS ONE *7*, e48275.

Zhao, X., Muller, E.G., and Rothstein, R. (1998). A suppressor of two essential checkpoint genes identifies a novel protein that negatively affects dNTP pools. Mol. Cell *2*, 329–340.

Figure Legends

Figure 2-1. ETI Mother Cells Show a Non-progressive Cell Cycle Length Phenotype and Reduced Lifespan that is Rescued by SML1 Deletion

Mother cell budding profiles for (A) WT, (B) *tlc1*Δ, (C) *est2D530A*, (D) *tlc1*Δ*sml1*Δ, showing cell cycle durations and heterogeneity (see exponential color scale, cell cycles with durations 1.4 hours or less were colored in purple). The x-axis displays individual mother cells shown as vertical bars with budding events indicated as horizontal white divisions. Mean lifespan for each genotype is presented in the upper left corner of the plot. (E) ETI mother cells showed reduced replicative lifespans compared to WT cells (number of cells (n): *tlc1*Δ, 354; *est2D530A*, 117; WT, 234. *p*-value for difference between *tlc1*Δ and WT < 1e-37). (F) Deletion of Sml1 restores lifespan of ETI mother cells to WT levels (n: *tlc1*Δ*sml1*Δ, 77; *sml1*Δ, 39). (G) The heterogeneity of cell cycle

lengths in ETI cells did not progressively worsen relative to WT as mother cells aged. Fold increase in cell cycle variability from 1st and 2nd to 3rd and 4th last cell cycles compared for each genotype (shown below each set). The variance of 1st and 2nd cell cycles of *tlc1*Δ and *est2D530A* is significantly greater than that of WT (F-test *p*-value < 1e-16 and 1e-13 respectively).

Figure 2-2. ETI Induces a Transient G2/M Pause in Bulk Population Time-course Experiments

Bulk population time-course experiments to measure cell cycle progression, spindle length and chromosome segregation in synchronized yeast cultures of WT or ETI (*tlc1*Δ) cells. (A) Fraction of cells at the indicated budding stages following alpha-factor release. (B) Fraction of cells with indicated spindle length, visualized through expression of GFP-tubulin following release from alpha-factor. (C) Fraction of cells carrying an unsegregated GFP-marked chromosome IV. All cells were analyzed either 30 or 40 (as indicated) generations after loss of TLC1 or replacement of *EST2* with the catalytically-dead allele, *est2D530A*. (D) G2/M pause of ETI cells is increased with *mrc1*^{AQ} and *tel1*Δ but not *mec1*Δ*sml1*Δ. Cell cycle progression and spindle length were measured in synchronized cells following release from alpha-factor. Left and Middle panel: Budding kinetics, indicated by percentage of large-budded cells, in indicated genotypes. Right panel: Comparing fraction *mrc1*^{AQ} or *rad9*Δ cells (with or without *ETI)* that have short spindles, indicative of G2/M cell cycle phase. Spindles were visualized through expression of GFP-tubulin.

Figure 2-3. Escape from the G2/M Cell Cycle Extension in ETI Cells is Not Dependent on DNA Damage Adaptation pathways

WT and ETI cells were analyzed as in Figure 2 with or without the addition of the *cdc5ad* mutation, which makes cells unable to adapt to DNA Damage (Toczyski et al., 1997). The percentage of cells with large-budded morphologies was quantified to determine the number of cells in the G2/M cell cycle phase. As shown previously, ETI *tlc1*Δ cells displayed an extension of G2/M. However, this extension was not altered in the absence of the capacity to adapt to DNA damage (ETI *tlc1*Δ*cdc5ad*).

Figure 2-4. Initial Cell Cycle Length was not Predictive of Next Cell Cycle Length

ETI cells with initially longer cell cycle durations (blue lines) and those with initially short ones (red lines) did not show a bias towards longer or shorter cell cycles as the cells aged. This result showed that the initial cell cycle itself was not predictive of the quality of future divisions, and indicates that at each successive cell division the probability of a longer cell cycle occurring is mostly “reset” throughout much of the mother aging process.

Figure 2-5. *SML1* Deletion Rescues Mother Cell Lifespan of ETI Cells Independently of Telomere Length

(A) *SML1* deletion had no significant effect on the rate of bulk population senescence in ETI cells passaged on solid media to induce LTI-senescence. (B) Southern blot analysis of telomeric DNA restriction fragment lengths of cells taken from serial streaks shown in (A), using $TG_{(1\text{-}3)}$ repeat telomeric probe. ETI (*tlc1*Δ) and ETI *sml1*Δ (*tlc1*Δ*sml1*Δ)

displayed similar rates of telomere shortening and the lower end of the telomere length distributions were similar.

Figure 2-6. *SML1* Deletion does not Alter the Kinetics of Telomere Shortening or Onset of Senescence Caused by *est2D530A*

The experiment was performed and analyzed as in Figure 2-5. (A) The *est2D530A* and *est2D530Asml1*Δ mutants displayed similar rates of population senescence when passaged by serial streaks on solid media. (B) Southern blot analysis of telomeric DNA restriction fragment lengths using a $TG_{(1-3)}$ repeat probe to measure telomere length. Cells were taken from passages 1 through 3.

Figure 2-7. The Cellular Response to ETI is Distinct from the Response to Classic DNA Damage or to LTI Senescence

(A) Mrc1 is phosphorylated after prolonged loss of telomerase (LTI) but not in early passages (ETI). Phosphorylation state of Mrc1-myc13 in *tlc1*Δ mutant monitored by western blot of protein extracts made after indicated number of passages without telomerase and probed with 9E10 anti-myc antibody. The first passage represents roughly 30 generations without telomerase and each successive passage represents approximately 20 more generations. Positive control for Mrc1 phosphorylation is WT MRC1 strain extract from cells treated with 200mM hydroxyurea for 2 hours. (B) and (C) Mother cell lifespan and cell cycle durations of the *sml1Δ* and *mec1Δ sml1Δ* mutants are similar to WT. (D) Genotype dependence of cellular viability responses to other forms of DNA damage. $4x10^6$ cells from log phase cultures were serially diluted 5-fold and

spotted onto YPD plates with or without DNA damaging agents (1.0mM HU, 0.01% MMS, 1µg/mL phleomycin, or plates were treated with 120J/m^2 UV irradiation) as indicated.

Figure 2-8. ETI Mother Cells Age with Terminal Cellular and Mitochondrial Morphologies Distinct from LTI Senescence but Similar to those of Normal Mother Cell Aging

(A) Three possible terminal death morphologies were observed in WT, ETI, and/or LTI (see text for definition) mother cells: small budded (type i), elongated (type ii), and a G2/M large-budded ("dumbbell" shape) (type iii). Mitochondrial volume was measured using mitochondrially localized GFP (mtGFP). (B) ETI and LTI populations of *tlc1*Δ*sml1*Δ cells were prepared to distinguish cell death from normal mother cell aging and LTI senescence. *tlc1*Δ*sml1*Δ LTI strains senesced and showed reduced lifespan as expected. (C) ETI cells terminally arrest in a manner similar to WT mother cells and distinct from LTI senescence. Most of the cells in ETI *tlc1*Δ and ETI *tlc1*Δ*sml1*Δ show type i or type ii death morphologies (>95%), similar to terminal WT mother cells. In LTI cells, a major fraction (~70%) displayed type iii morphology (*p*-value < 1e-4 compared to ETI *tlc1*Δ*sml1*Δ by Fisher's exact test) indicative of senescence induced by critically short telomeres.

Figure 2-9. *TEL*1 Deletion Exacerbates ETI Cell Cycle and Lifespan Phenotypes but not Senescence or Telomere Shortening Rates

Mother cell budding profiles for *tel1*Δ (A) and *tlc1*Δ*tel1*Δ (B). (C) *tel1*Δ (n=38) strain lifespan does not differ from WT. (D) *tlc1*Δ*tel1*Δ (n=83) mutation worsens the lifespan reduction caused by ETI mutations in mother cells (*p*-value < 1e-4, compared with *tlc1*Δ alone). (E) ETI and ETI *tel1*Δ mutants displayed similar rates of senescence when passaged on solid media. (F) Southern blot analysis of telomeric DNA restriction fragment lengths of cells taken from plates after serial streaks shown in (E).

Figure 2-10. Mother Cell Lifespans of Selected DDR Mutants

(A) *mec1*Δ*sml1*Δ (n=33) lifespan is not different from WT. (B) Tel1 and Mrc1 epistasis. ETI *tlc1*Δ*tel1*Δ*mrc1^{AQ}* (n=103) lifespan was similar to ETI *tlc1*Δ*tel1*Δ (n=83) lifespan (mean, 11.5 and 9.8 respectively), indicating that Tel1 and Mrc1 function in the same pathway regulating mother cell aging. (C) ETI acceleration of mother cell aging lifespan is exacerbated by *mrc1^{AQ}* and *tel1*Δ but not by *rad9*Δ. ETI *tlc1*Δ*rad9*Δ (n = 81) lifespan was no worse than ETI *tlc1*Δ (n = 78) lifespan (mean, 16.5 and 13.7 respectively) and showed a minor improvement.

Figure 2-11. *MRC1* Mutation Exacerbates ETI Cell Cycle and Lifespan Phenotypes but not Senescence or Telomere Shortening Rates

Mother cell budding profiles for *mrc1^{AQ}*(A) and *tlc1*Δ *mrc1^{AQ}* (B). (C) *mrc1^{AQ}* (n=40) strain lifespan does not differ from WT. (D) *tlc1*Δ*mrc1^{AQ}* (n=90) mutation worsens the lifespan reduction caused by ETI mutations in mother cells (*p*-value < 2e-7, compared

with *tlc1*Δ). (E) ETI and ETI *mrc1*^{AQ} mutants displayed similar rates of senescence when passaged on solid media. (F) Southern blot analysis of telomeric DNA restriction fragment lengths of cells taken from plates after serial streaks shown in (E).

Figure 2-12. Bulk Population Epistasis Analysis of Tel1 and Mrc1 Mutants on G2/M Cell Cycle Extension

Cells were analyzed as in Figure 2. The percentage of cells with large-budded morphologies was quantified to determine the number of cells in the G2/M cell cycle phase. ETI *tlc*Δ*mrc1*^{AQ}*tel1*Δ mutants showed no greater accumulation of cells in G2/M than was seen in the ETI *tlc*Δ*mrc1*^{AQ} or ETI *tlc*Δ*tel1*Δ double mutants, suggesting that the Tel1- and Mrc1-mediated effects occur via the same pathway.

Figure 2-13. Genotype Dependence of Telomere Fusions and Transient DNA Damage Response Episodes in Mother Cells

(A) Semi-quantitative PCR of DNA species resulting from the fusion of a deprotected telomere with an induced double-strand break in genetic backgrounds containing *ETI* and *mrc1*^{AQ} mutant combinations. (B) Same as in (A), but with genetic backgrounds containing *ETI* and *tel1*Δ mutations. (C) Two representative profiles of RNR3-GFP peaks occurring in still-dividing individual mother cells. Cell divisions (green diamonds) and RNR3-GFP reporter levels (blue circles) were plotted throughout an individual mother cell's lifespan. Spline fitting is shown as red lines. (D) Frequencies of RNR3-GFP induction peaks in still-dividing cells such as those shown in (C). *p*-values < 0.01 (*) and *p*-values < 0.001 (**) by Fisher's exact test are indicated. (E) Two representative

mother cell profiles shown, as in (C), with cells displaying terminal RNR3-GFP induction peaks. (F) Frequencies of RNR3-GFP induction peaks in terminal mother cells, such as those shown in (E).

Figure 2-14. Multiple Factors Showing No Evidence of a Causative Role in the ETI Mother Cell Aging Phenotypes

(A) The effect of recombination on aging is separable from ETI mother cell lifespans in the absence of Rad52. Cells from logarithmically growing haploid cultures of strains with the ETI and/or *rad52Δsml1Δ* genotypes indicated were analyzed as in Figure 2-1. The *rad52*Δ*sml1*Δ mutation alone also reduced mother cell lifespan, and reduction in combination with ETI was additive (n=65 for *tlc1*Δ*rad52*Δ*sml1*Δ. Rank Sum *p*-value ≤ 1.8e-8 when comparing the two strains *rad52*Δ*sml1*Δ and *tlc1*Δ*rad52*Δ*sml1*Δ). (B) Amount of Sir3-GFP puncta representing telomere-bound Sir3 is similar in WT and ETI cells. (C) ROS levels are not elevated in ETI cells or reduced by *sml1*Δ. ETI *tlc1*Δ mother cells have similar ROS level as the WT control strain, shown by staining the cells with 2',7'-dichlorfluorescein-diacetate (DCFH-DA). ETI *tlc1*Δ*sml1*Δ mother cells have even higher levels of ROS. (D) Antioxidant NAC enhances lifespan in a non-specific manner. Lifespan curves of WT and ETI mother cells that aged in the presence of antioxidant (20mM NAC in YPD). Each curve was merged from two independent replicates.

Figure 2-15. Cell Cycle Length and Mitochondrial Staining Measured During Early Divisions are Predictive of Lifespan Across Various Genotypes

(A) Scatter plot for various genotypes showing the log percentage of long-duration cell cycles versus mother cell lifespan (cyan dots) and linear fitting (red line, r = -0.86, p-value ≤ 7e-5). Long-duration cell cycles were defined as durations falling above the tightly clustered Gaussian distribution of most cell cycles. (B) Scatter plot for various genotypes showing the mean duration of mother cell budding cycle intervals versus lifespan (cyan dots) and linear fitting (red line, r = -0.78, p-value ≤ 5e-3). The cell cycle durations analyzed are for all cycles, excluding the first cycle analyzed in the microfluidics analyses, because some cells will be part-way through a budding cycle when they are first monitored, and the terminal two cycles, which even in WT strains have extremely heterogeneous, long durations. (C) and (D) The intensity of the mito-marker was predictive of lifespan when measured early in ETI *tlc1*Δ mother cells (4 hour time point after chip loading), and in WT mother cells.

Figure 2-16. Proposed Model

Top left panel: Proposed signaling interactions that regulate aging in response to telomeric DNA stress. Deleterious effects shown in red. Top right panel: In ETI cells lacking Sml1 (*tlc1*Δ*sml1*Δ*),* telomerase cannot alleviate replication stress. However, due to elevated dNTP levels, replication stress is prevented and aging is not accelerated. Eliminated or reduced signaling is shown in grey. Bottom left panel: In ETI cells lacking Tel1 (*tlc1*Δ*tel1*Δ), as well as lacking telomerase rescue, the DDR response is unavailable to alleviate replication stress, as indicated by the elimination of RNR3

signaling, and ETI-accelerated aging is exacerbated. Bottom right panel: in ETI cells lacking Mrc1 function (*tlc1*Δ*mrc1*^{AQ}), telomerase rescue is unavailable and the DDR response to telomeric replication stress is partially hindered. Rad9 is able to partially compensate and induce RNR3 induction, but other downstream DDR targets cannot be induced, thus exacerbating the ETI-accelerated aging.

Table Legends

Table 2-1. (See separate Excel file) Microarray Data in Telomerase Deleted Yeast Time Courses from Nautiyal et al 2002

In Nautiyal et al 2002, the data in this Table were described, but this full dataset was referenced as available upon request and was not published as part of Nautiyal et al. For ease of future retrieval, this same full microarray dataset is now presented (separately due to its large size). Table 2-1, Table S2 in the original publication, includes two independent repeats of the same experiment: repeat 1 experiment data columns are labeled SN1021_13 and repeat 2 experiment data columns are labeled SN1021_14.

Table 2-2. Top Ten Published Gene Expression Profiles with the Highest Correlation with the ETI Profile

Table 2-3. Top Five Non-redundant GO Categories Contributing to Overall Correlation of Gene Expression Between ETI and Diamide Treatment (GSM971 1.5mM Diamide, 5min)

Table 2-4. Genes Involved in Response to Oxidative Stress that are Upregulated in ETI Cells (>1.5 fold)*

*Genes annotated as "response to oxidative stress" with > 1.5 fold increase. Data shown is from the Experiment repeat 1 dataset, Passage 1, in Table 2-1.

Figure 2-1

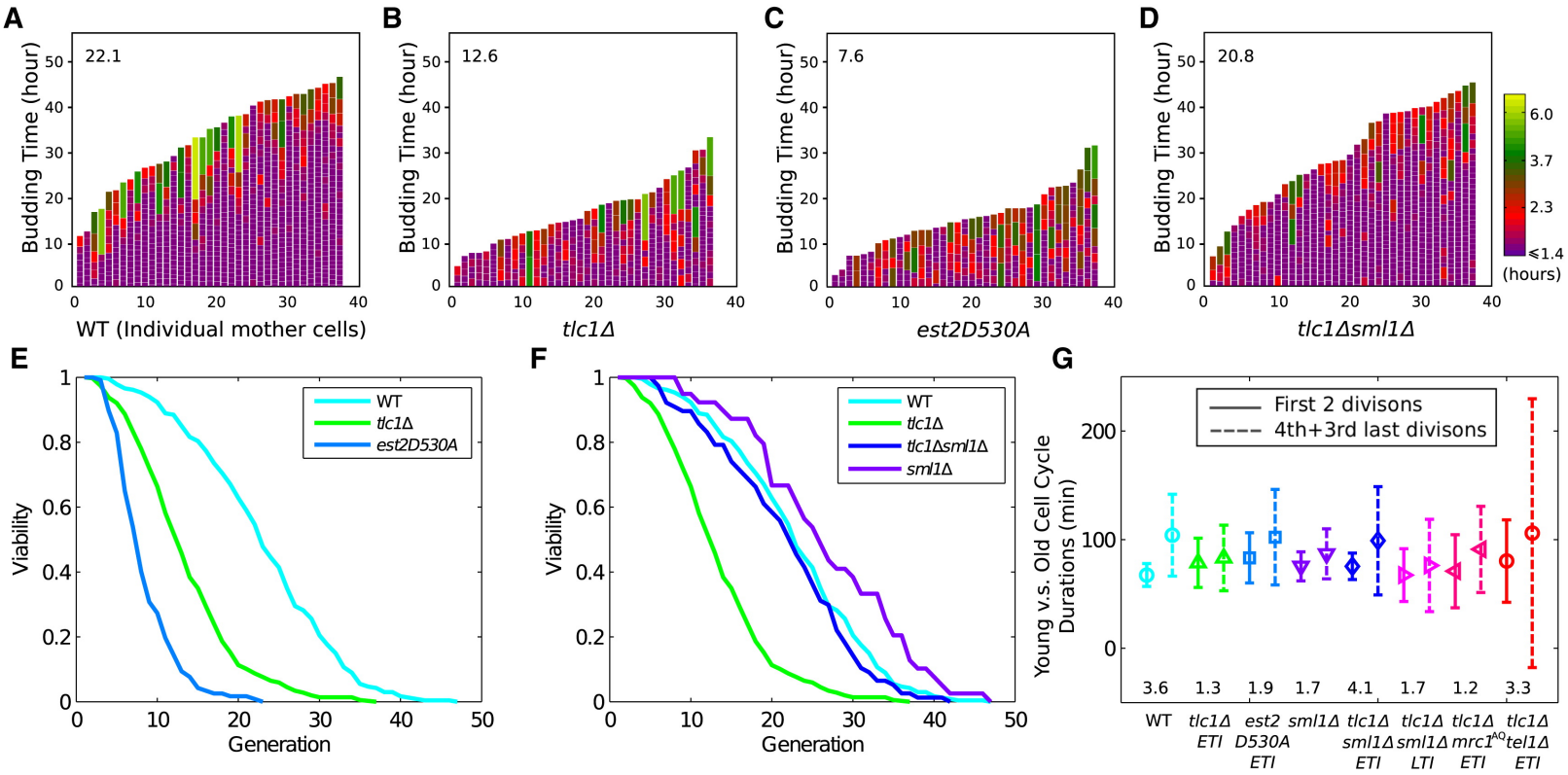
A
B
C
D
22.1
12.6
7.6
20.8
Budding Time (hour)
WT (Individual mother cells)
tlc1Δ
est2D530A
tlc1Δsml1Δ
6.0
3.7
2.3
⩽1.4
(hours)
E
F
G
Viability
Generation
WT
tlc1Δ
est2D530A
tlc1Δsml1Δ
sml1Δ
Young v.s. Old Cell Cycle Durations (min)
First 2 divisons
4th+3rd last divisons
3.6
1.3
1.9
1.7
4.1
1.7
1.2
3.3
WT
tlc1Δ ETI
est2 D530A ETI
sml1Δ
tlc1Δ sml1Δ ETI
tlc1Δ sml1Δ LTI
tlc1Δ mrc1AQ ETI
tlc1Δ tel1Δ ETI

Figure 2-2

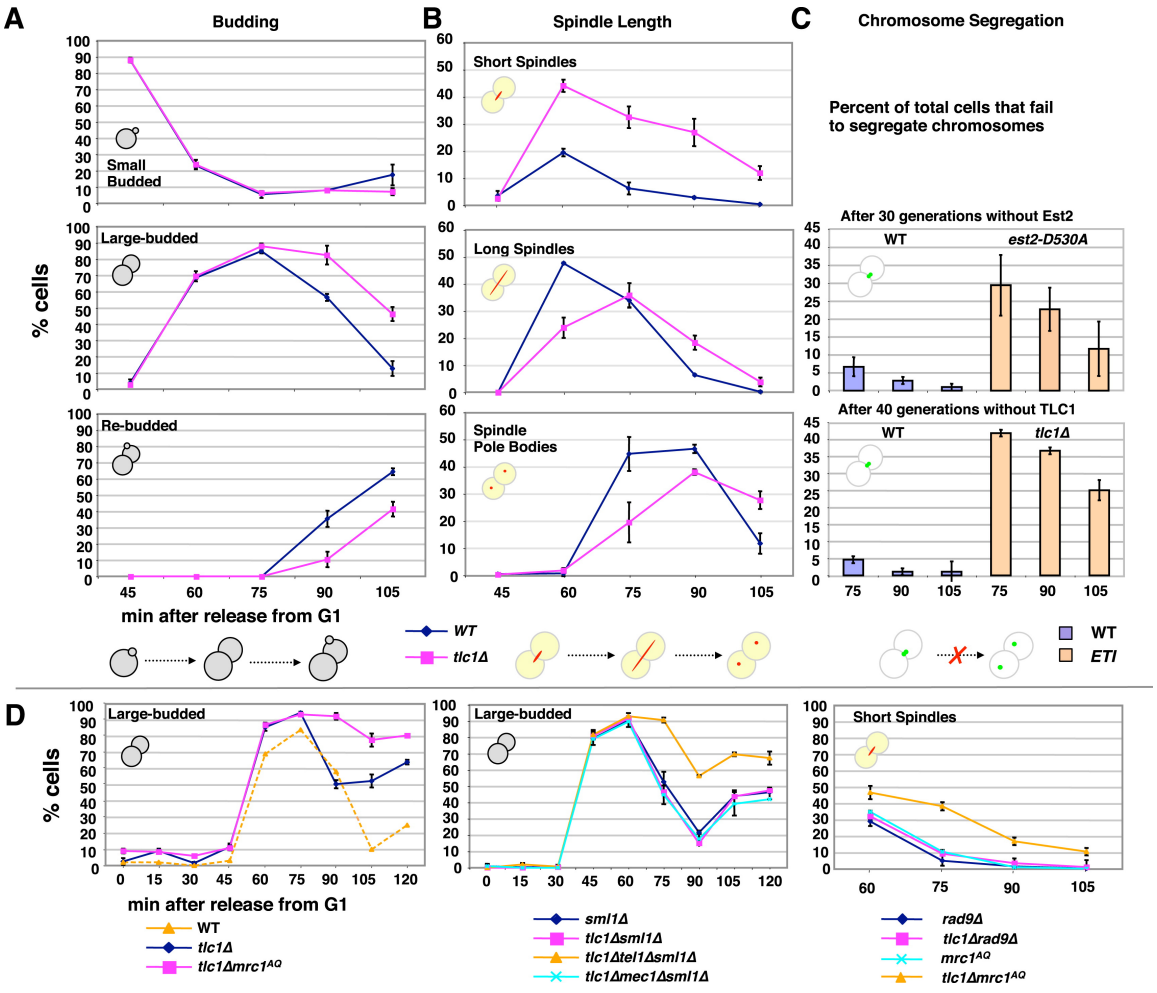
A
Budding
% cells
Small Budded
Large-budded
Re-budded
min after release from G1
WT
tlc1Δ
B
Spindle Length
Short Spindles
Long Spindles
Spindle Pole Bodies
C
Chromosome Segregation
Percent of total cells that fail to segregate chromosomes
After 30 generations without Est2
WT
est2-D530A
After 40 generations without TLC1
WT
tlc1Δ
WT
ETI
D
Large-budded
% cells
min after release from G1
WT
tlc1Δ
tlc1Δmrc1AQ
Large-budded
sml1Δ
tlc1Δsml1Δ
tlc1Δtel1Δsml1Δ
tlc1Δmec1Δsml1Δ
Short Spindles
rad9Δ
tlc1Δrad9Δ
mrc1AQ
tlc1Δmrc1AQ

Figure 2-3

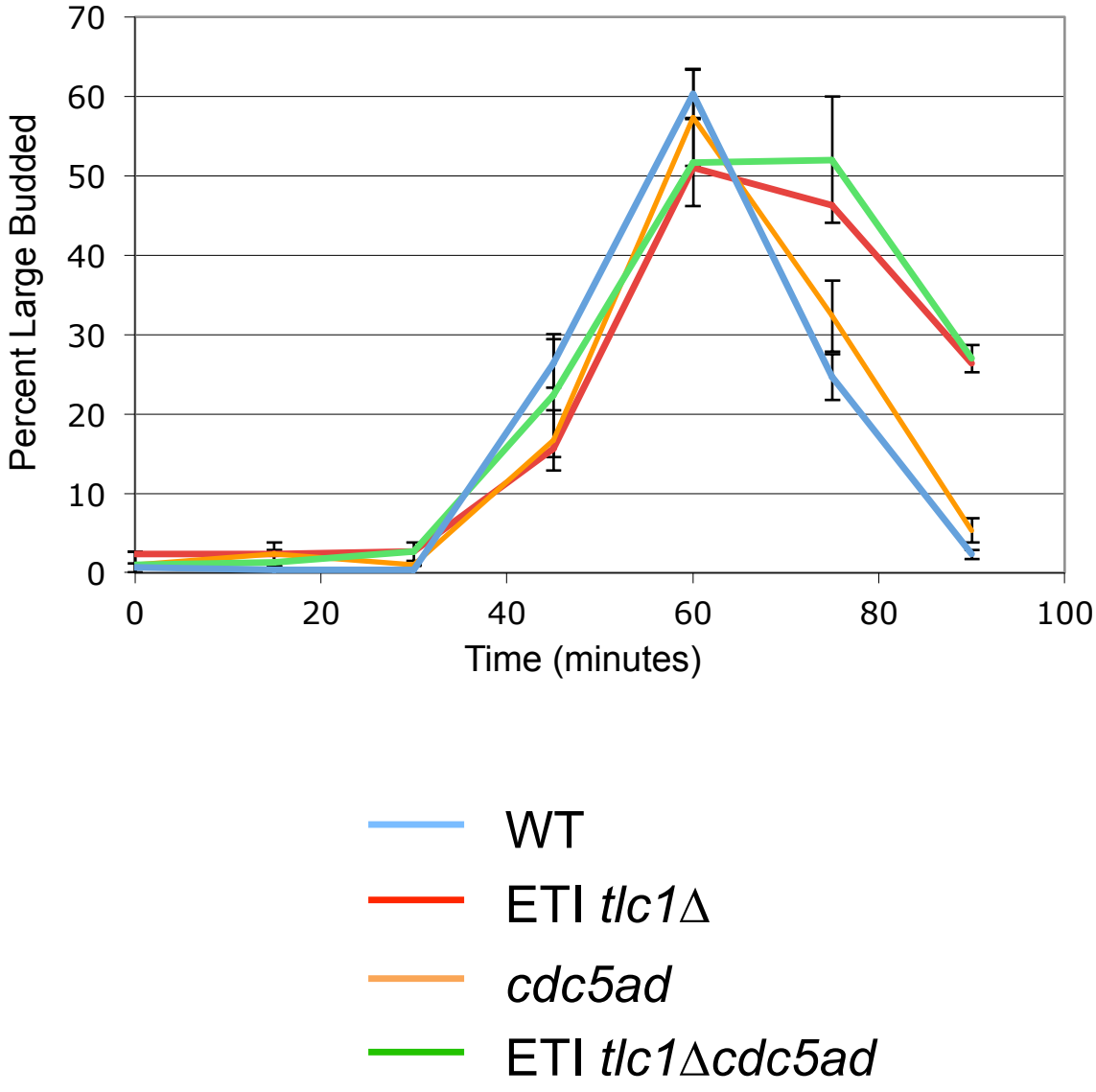
70
60
50
40
30
20
10
0
Percent Large Budded
0
20
40
60
80
100
Time (minutes)
WT
ETI tlc1Δ
cdc5ad
ETI tlc1Δcdc5ad

Figure 2-4

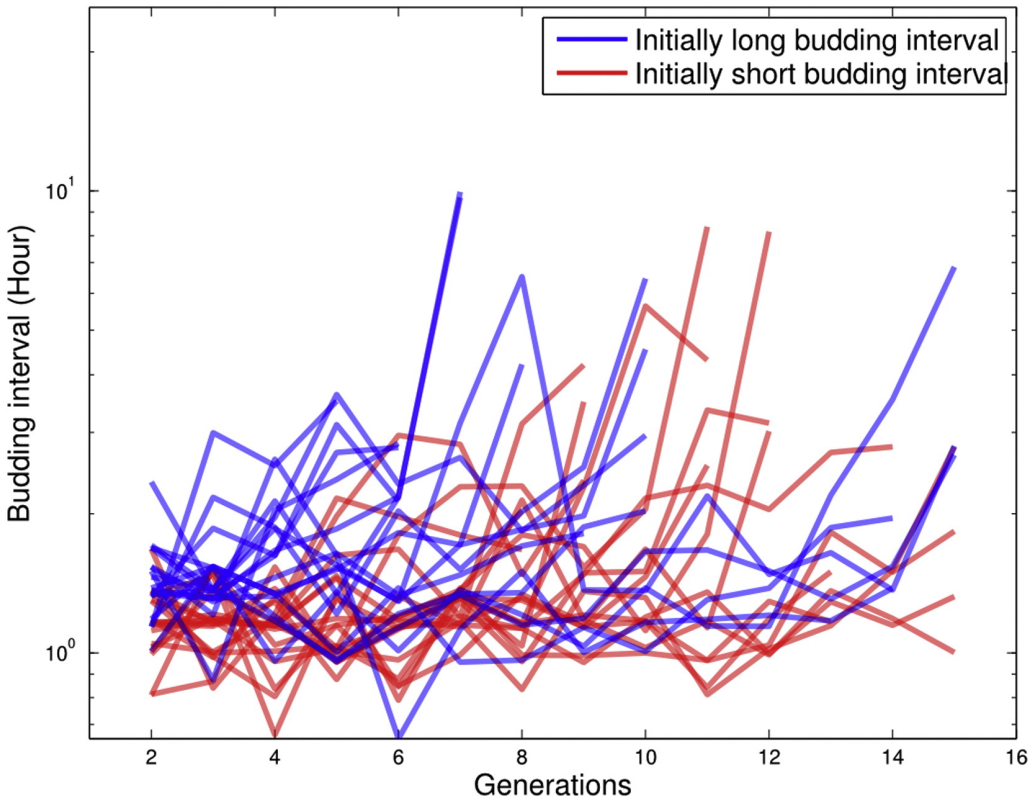
Initially long budding interval
Initially short budding interval
Budding interval (Hour)
10^1
10^0
2
4
6
8
10
12
14
16
Generations

Figure 2-5

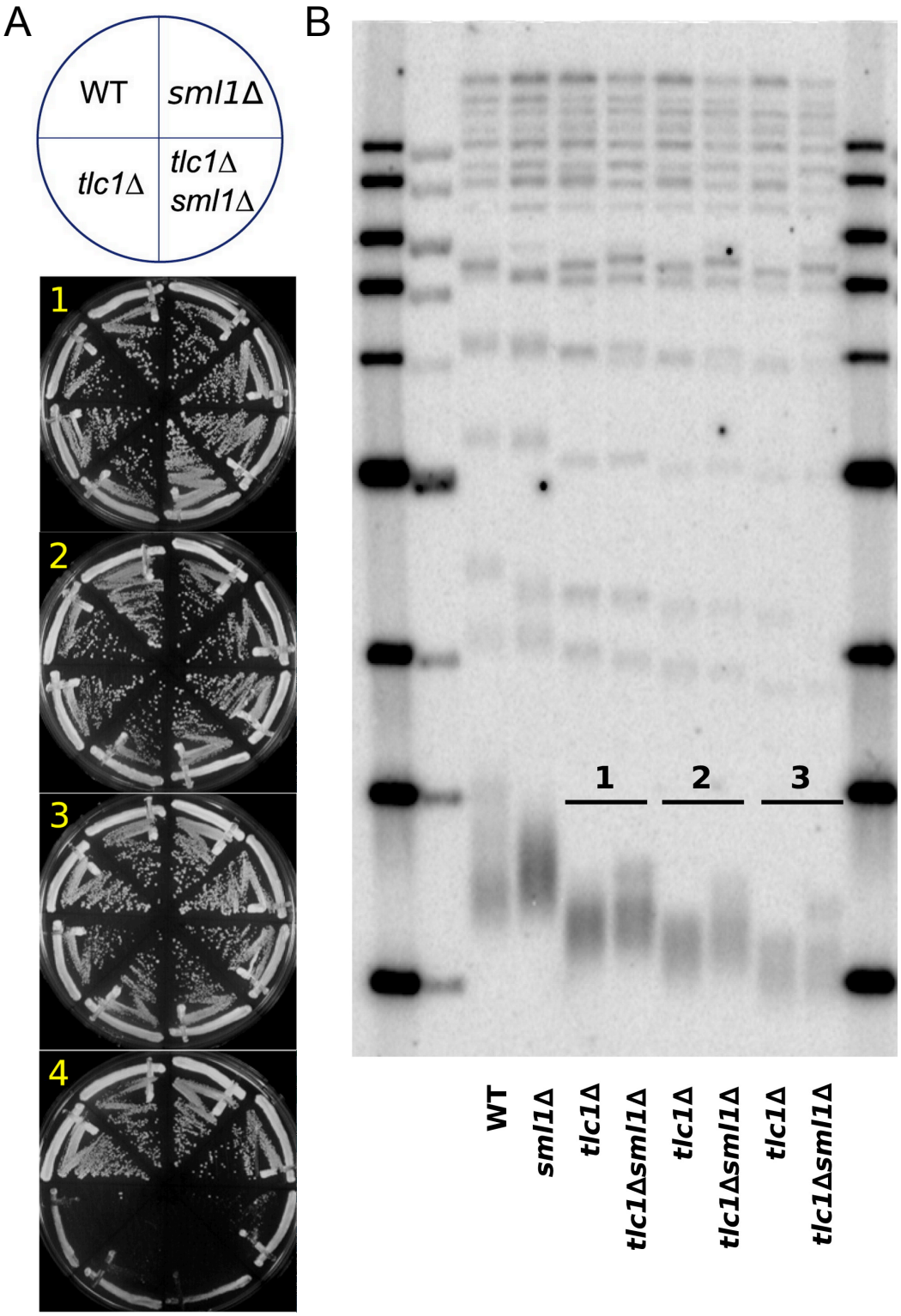
A
WT
sml1Δ
tlc1Δ
tlc1Δ sml1Δ
1
2
3
4
B
1
2
3
WT
sml1Δ
tlc1Δ
tlc1Δsml1Δ
tlc1Δ
tlc1Δsml1Δ
tlc1Δ
tlc1Δsml1Δ

Figure 2-6

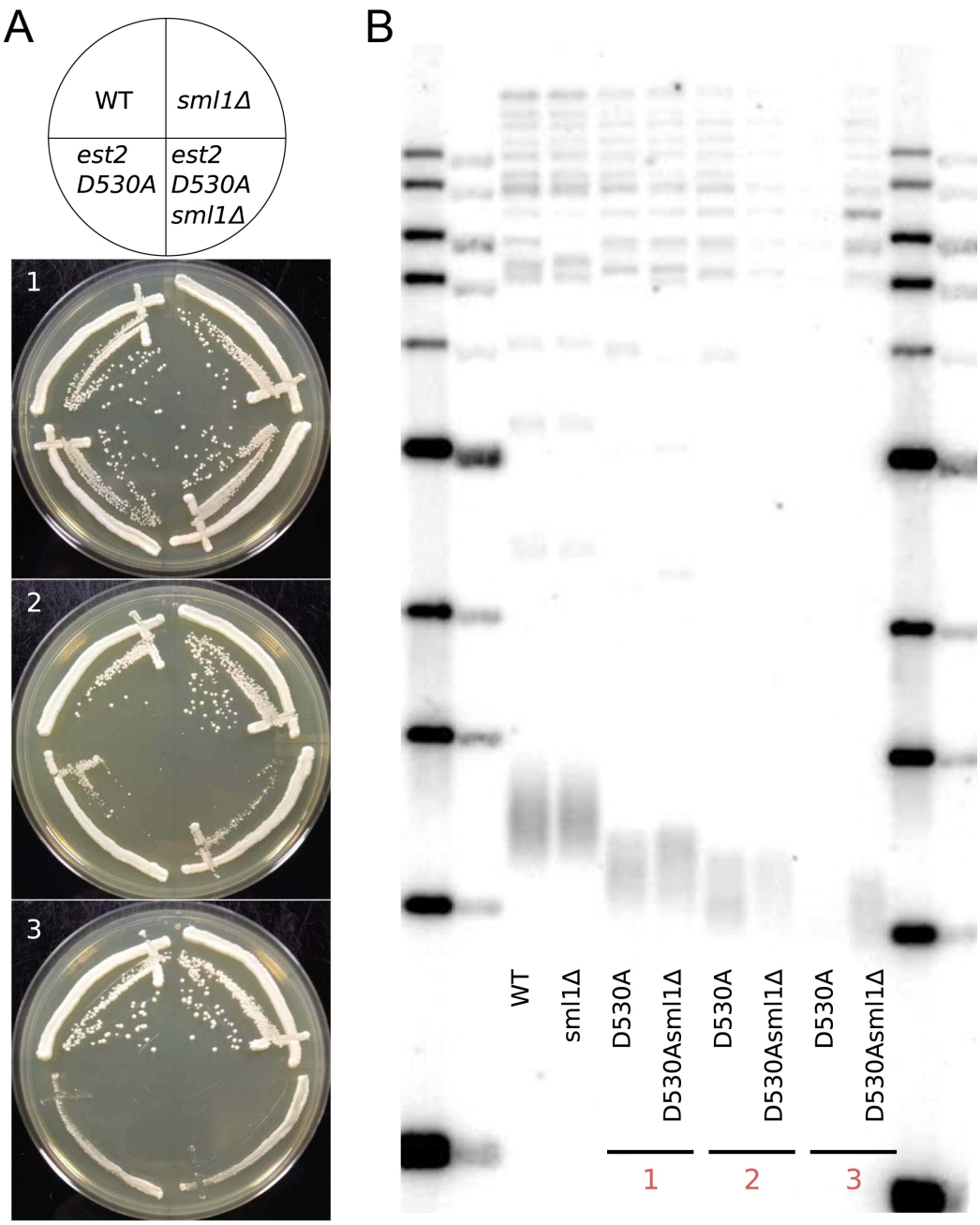
A
WT
sml1Δ
est2 D530A
est2 D530A sml1Δ
1
2
3
B
WT
sml1Δ
D530A
D530Asml1Δ
D530A
D530Asml1Δ
D530A
D530Asml1Δ
1
2
3

Figure 2-7

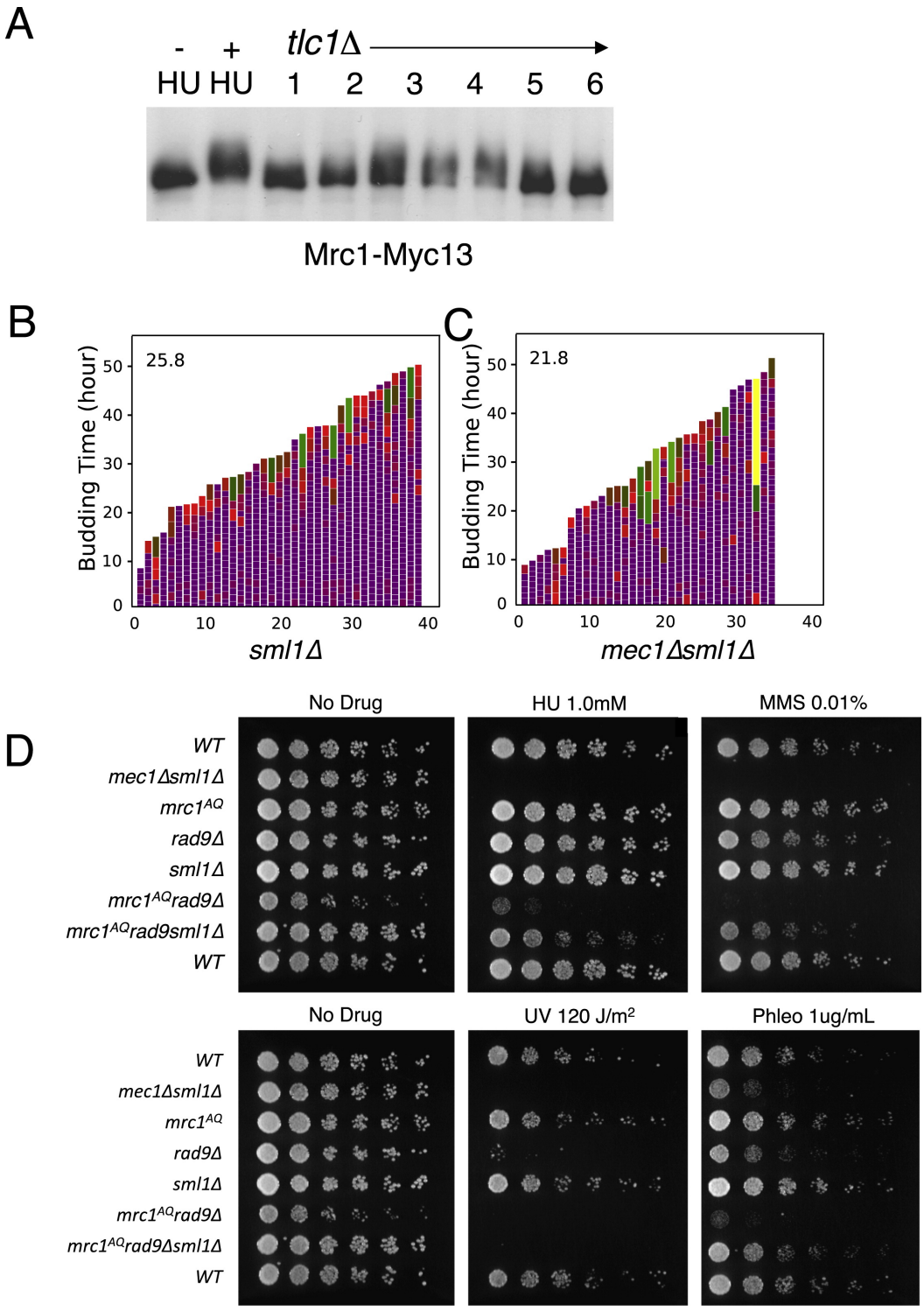
A
- HU
+ HU
tlc1Δ
1
2
3
4
5
6
Mrc1-Myc13
B
25.8
Budding Time (hour)
sml1Δ
C
21.8
Budding Time (hour)
mec1Δsml1Δ
D
No Drug
HU 1.0mM
MMS 0.01%
WT
mec1Δsml1Δ
mrc1AQ
rad9Δ
sml1Δ
mrc1AQrad9Δ
mrc1AQrad9sml1Δ
WT
No Drug
UV 120 J/m2
Phleo 1ug/mL
WT
mec1Δsml1Δ
mrc1AQ
rad9Δ
sml1Δ
mrc1AQrad9Δ
mrc1AQrad9Δsml1Δ
WT

Figure 2-8

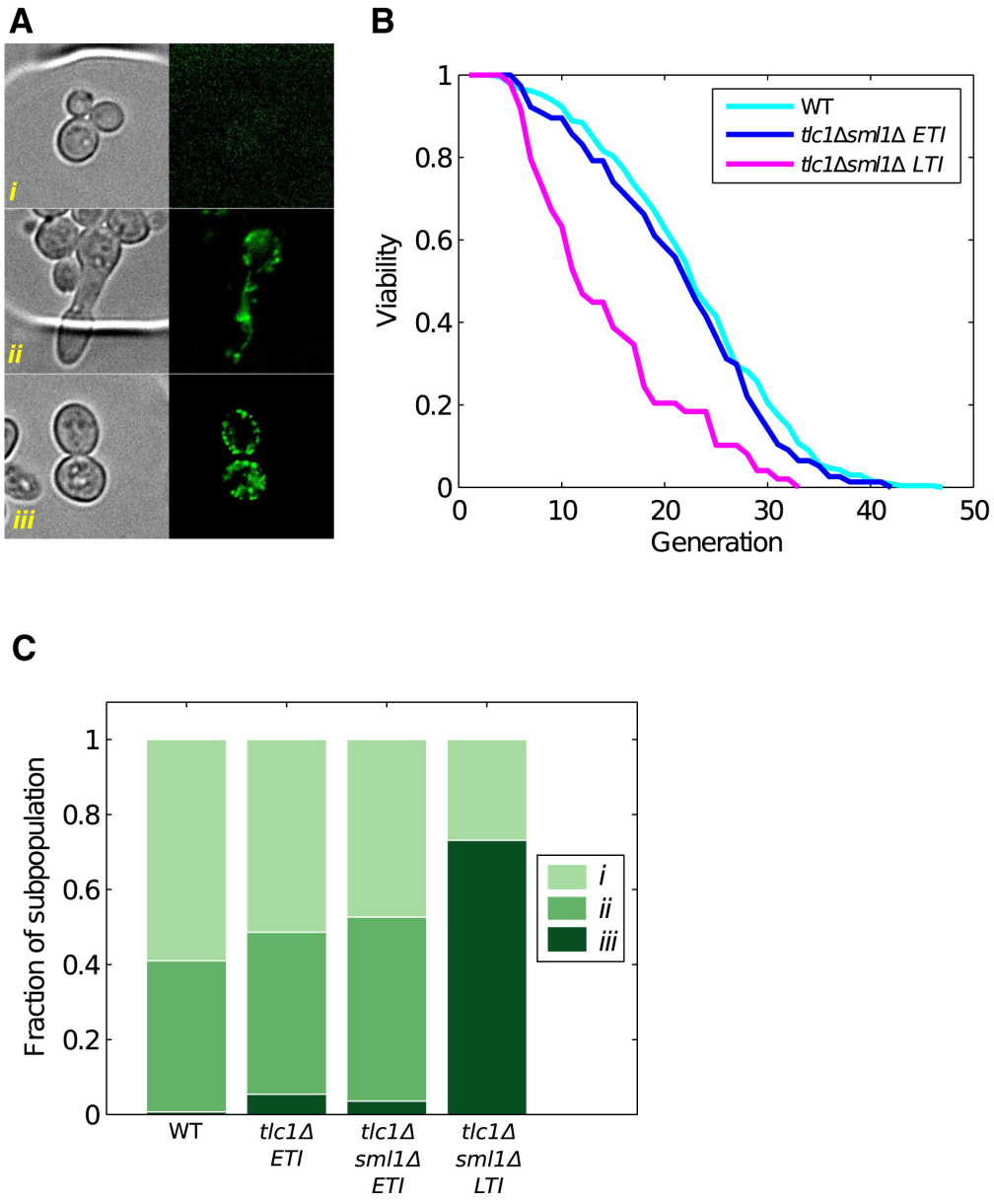
A
i
ii
iii
B
Viability
Generation
WT
tlc1Δsml1Δ ETI
tlc1Δsml1Δ LTI
C
Fraction of subpopulation
WT
tlc1Δ ETI
tlc1Δ sml1Δ ETI
tlc1Δ sml1Δ LTI
i
ii
iii

Figure 2-9

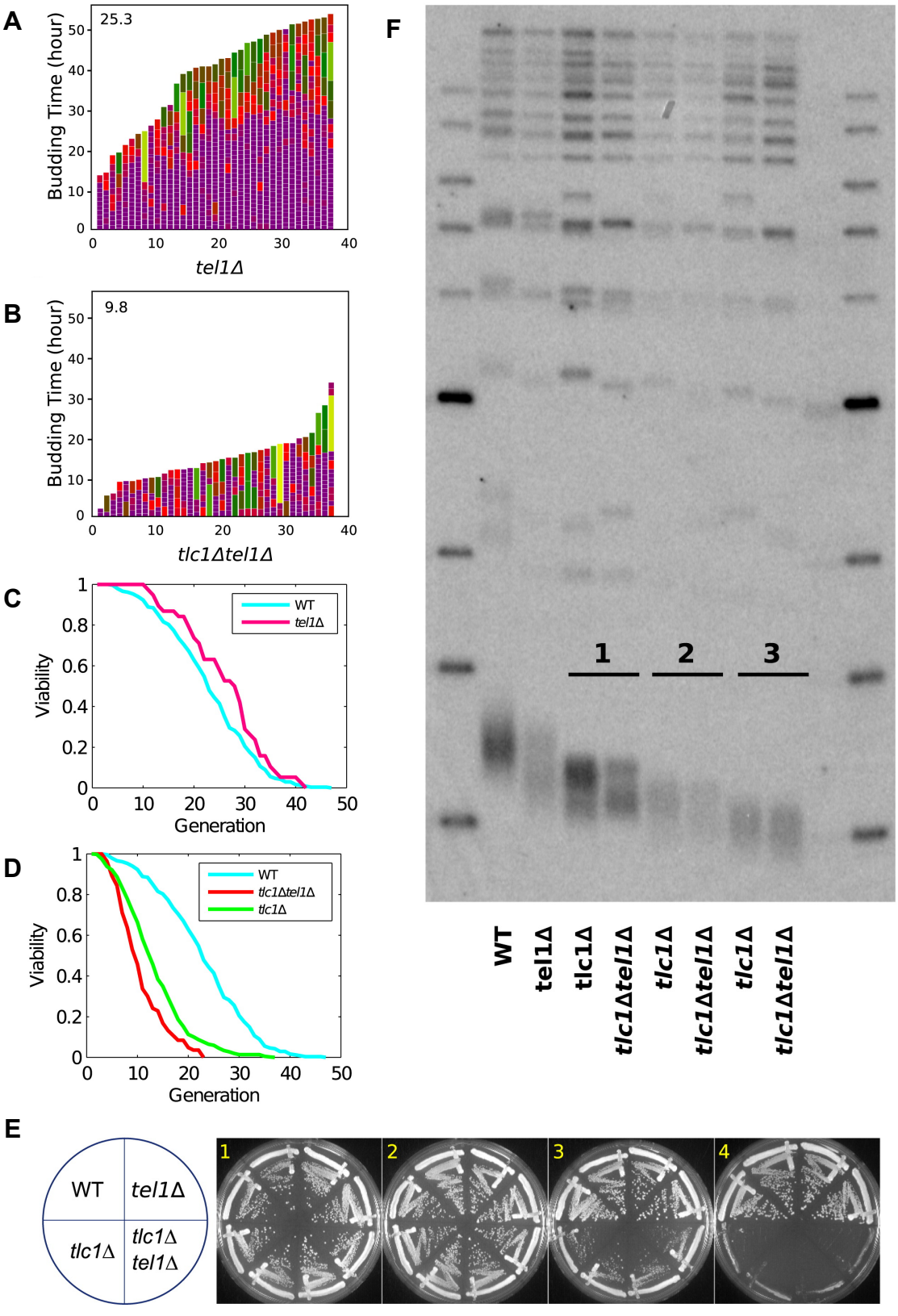
A
25.3
Budding Time (hour)
tel1Δ
B
9.8
Budding Time (hour)
tlc1Δtel1Δ
C
WT
tel1Δ
Viability
Generation
D
WT
tlc1Δtel1Δ
tlc1Δ
Viability
Generation
E
WT
tel1Δ
tlc1Δ
tlc1Δ tel1Δ
1
2
3
4
F
1
2
3
WT
tel1Δ
tlc1Δ
tlc1Δtel1Δ
tlc1Δ
tlc1Δtel1Δ
tlc1Δ
tlc1Δtel1Δ

Figure 2-10

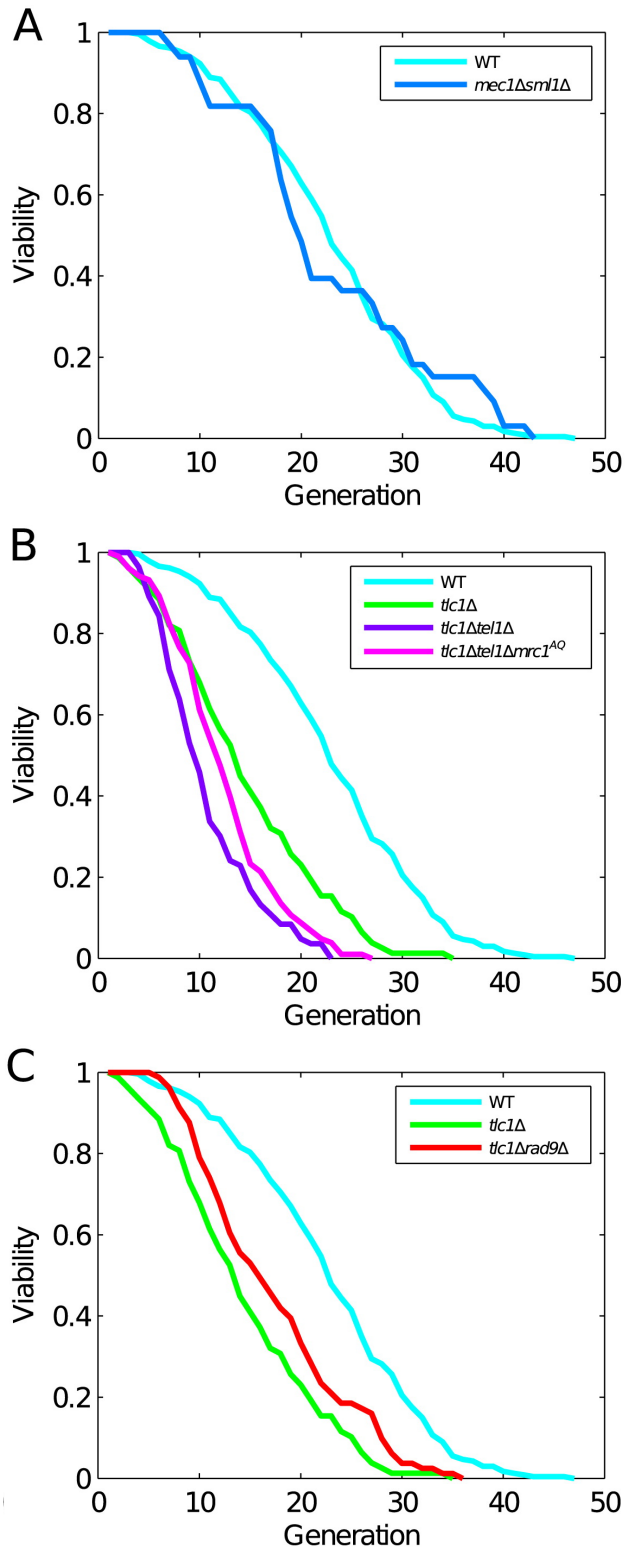
A
Viability
Generation
WT
mec1Δsml1Δ
B
Viability
Generation
WT
tlc1Δ
tlc1Δtel1Δ
tlc1Δtel1Δmrc1AQ
C
Viability
Generation
WT
tlc1Δ
tlc1Δrad9Δ

Figure 2-11

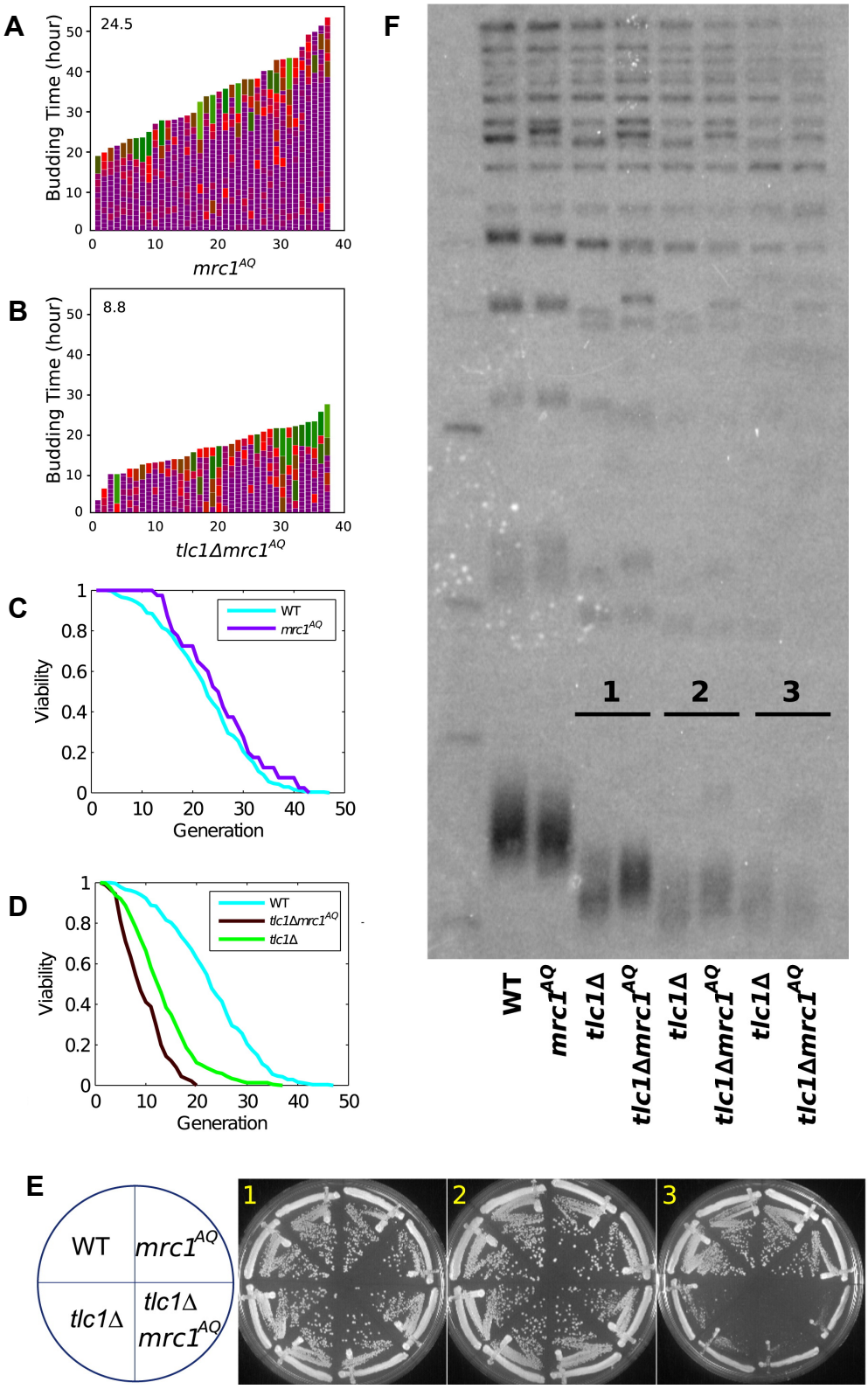
A
24.5
Budding Time (hour)
mrc1AQ
B
8.8
Budding Time (hour)
tlc1Δmrc1AQ
C
WT
mrc1AQ
Viability
Generation
D
WT
tlc1Δmrc1AQ
tlc1Δ
Viability
Generation
E
WT
mrc1AQ
tlc1Δ
tlc1Δ mrc1AQ
1
2
3
F
1
2
3
WT
mrc1AQ
tlc1Δ
tlc1Δmrc1AQ
tlc1Δ
tlc1Δmrc1AQ
tlc1Δ
tlc1Δmrc1AQ

Figure 2-12

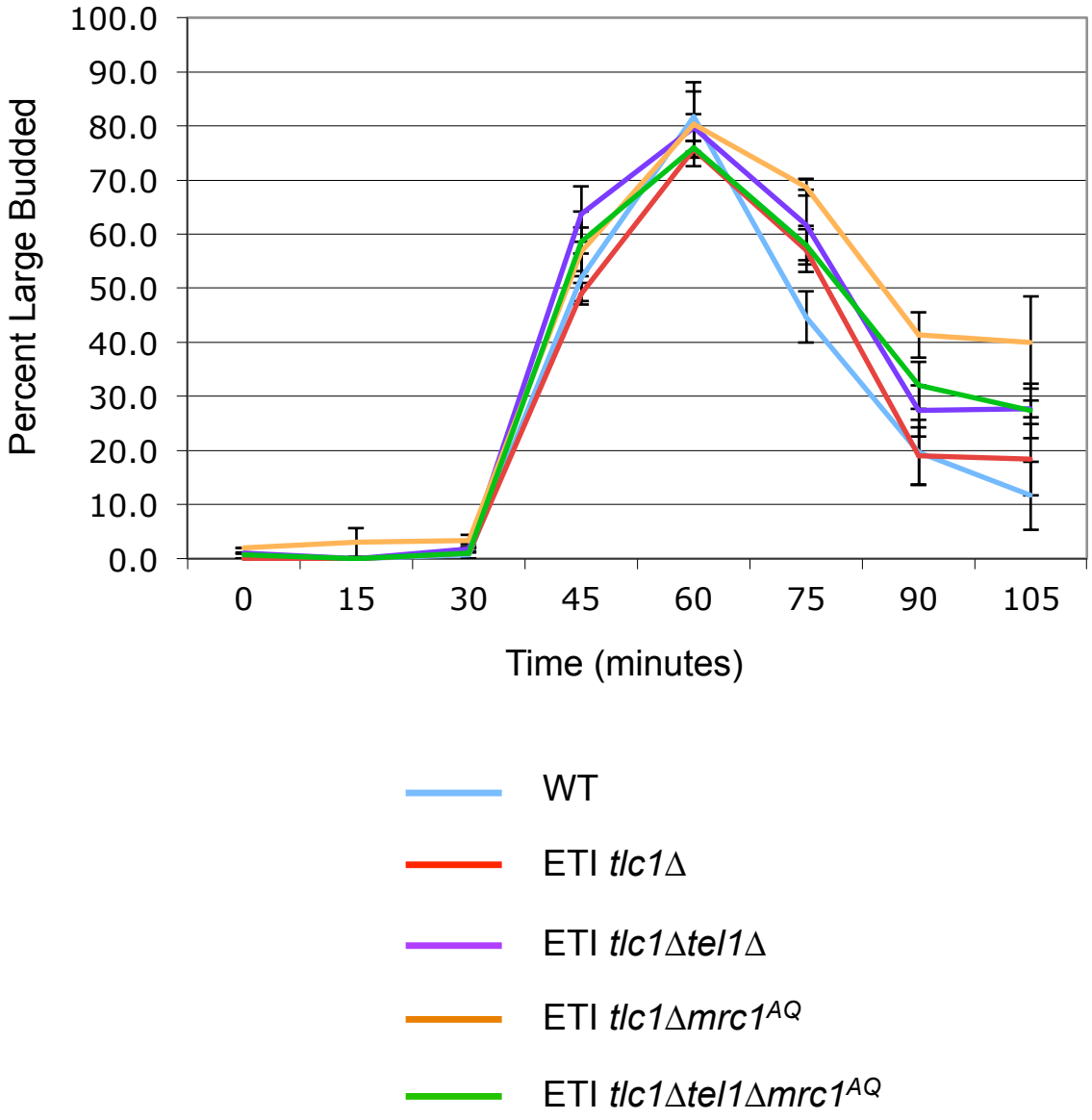
100.0
90.0
80.0
70.0
60.0
50.0
40.0
30.0
20.0
10.0
0.0
Percent Large Budded
0
15
30
45
60
75
90
105
Time (minutes)
WT
ETI tlc1Δ
ETI tlc1Δtel1Δ
ETI tlc1Δmrc1AQ
ETI tlc1Δtel1Δmrc1AQ

Figure 2-13

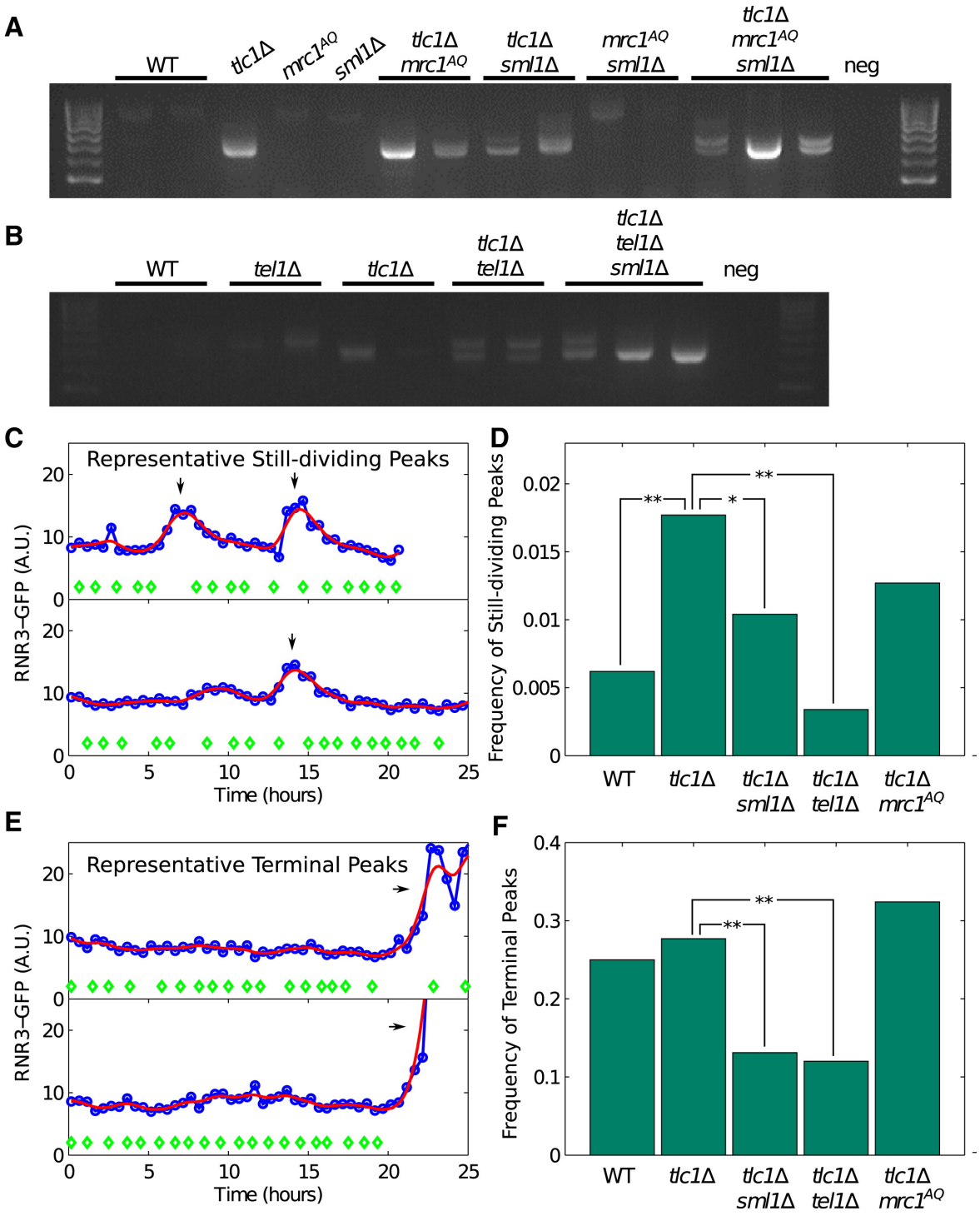
A
WT
tlc1Δ
mrc1AQ
sml1Δ
tlc1Δ mrc1AQ
tlc1Δ sml1Δ
mrc1AQ sml1Δ
tlc1Δ mrc1AQ sml1Δ
neg
B
WT
tel1Δ
tlc1Δ
tlc1Δ tel1Δ
tlc1Δ tel1Δ sml1Δ
neg
C
Representative Still-dividing Peaks
RNR3–GFP (A.U.)
Time (hours)
D
Frequency of Still-dividing Peaks
WT
tlc1Δ
tlc1Δ sml1Δ
tlc1Δ tel1Δ
tlc1Δ mrc1AQ
E
Representative Terminal Peaks
RNR3–GFP (A.U.)
Time (hours)
F
Frequency of Terminal Peaks
WT
tlc1Δ
tlc1Δ sml1Δ
tlc1Δ tel1Δ
tlc1Δ mrc1AQ

Figure 2-14

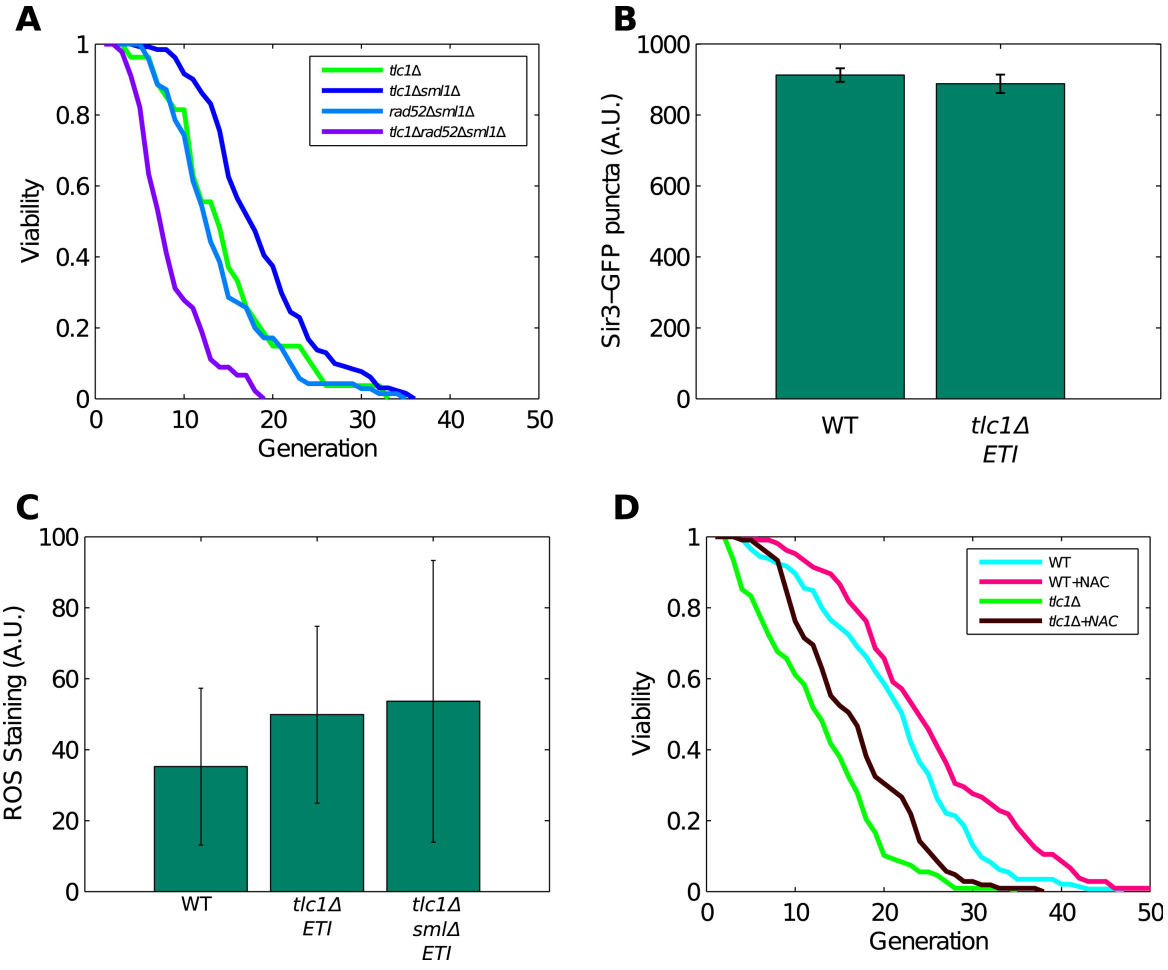
A
Viability
Generation
tlc1Δ
tlc1Δsml1Δ
rad52Δsml1Δ
tlc1Δrad52Δsml1Δ
B
Sir3–GFP puncta (A.U.)
WT
tlc1Δ ETI
C
ROS Staining (A.U.)
WT
tlc1Δ ETI
tlc1Δ smlΔ ETI
D
Viability
Generation
WT
WT+NAC
tlc1Δ
tlc1Δ+NAC

Figure 2-15

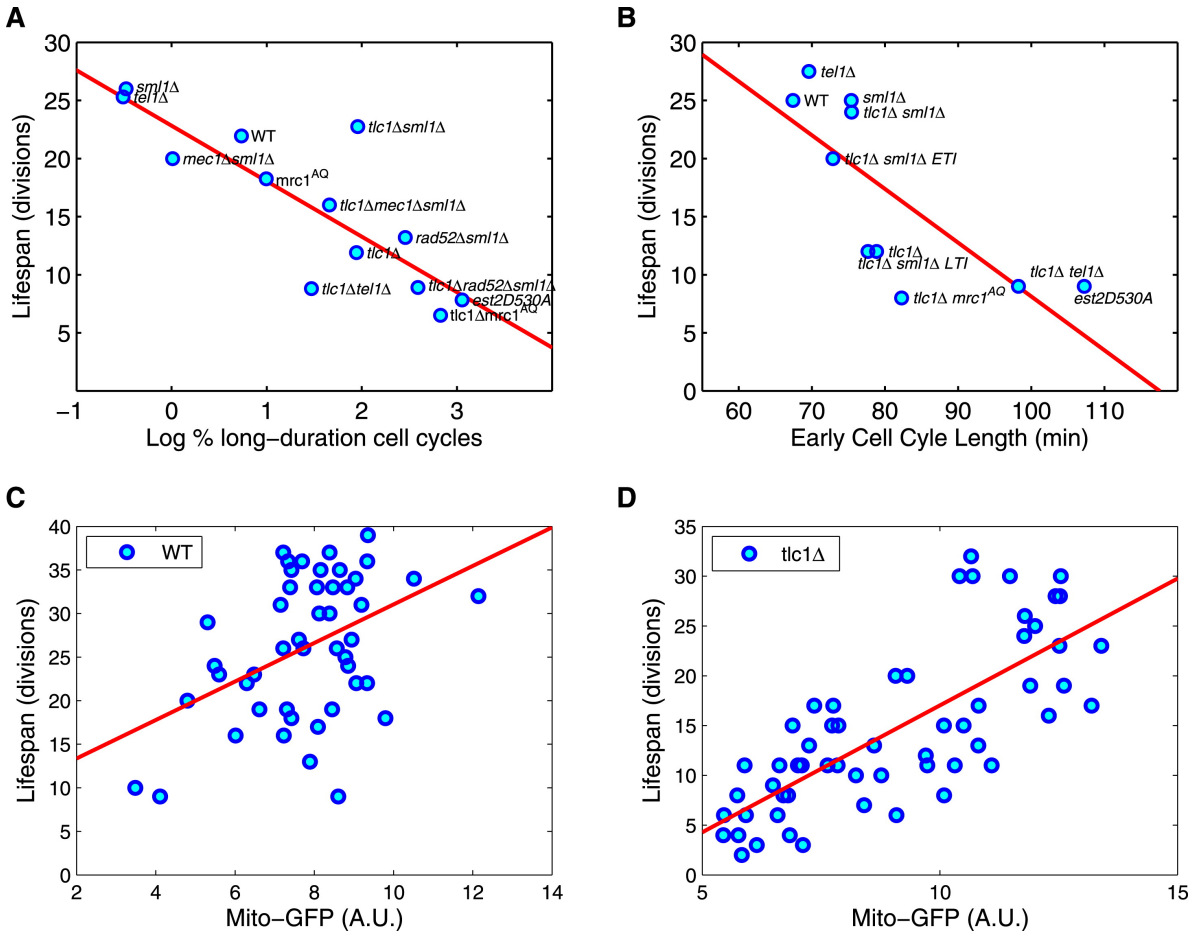
A
Lifespan (divisions)
Log % long−duration cell cycles
sml1Δ
tel1Δ
WT
tlc1Δsml1Δ
mec1Δsml1Δ
mrc1AQ
tlc1Δmec1Δsml1Δ
rad52Δsml1Δ
tlc1Δ
tlc1Δtel1Δ
tlc1Δrad52Δsml1Δ
est2D530A
tlc1ΔmrcAQ
B
Lifespan (divisions)
Early Cell Cyle Length (min)
tel1Δ
WT
sml1Δ
tlc1Δ sml1Δ
tlc1Δ sml1Δ ETI
tlc1Δ
tlc1Δ sml1Δ LTI
tlc1Δ tel1Δ
tlc1Δ mrc1AQ
est2D530A
C
WT
Lifespan (divisions)
Mito−GFP (A.U.)
D
tlc1Δ
Lifespan (divisions)
Mito−GFP (A.U.)

Figure 2-16

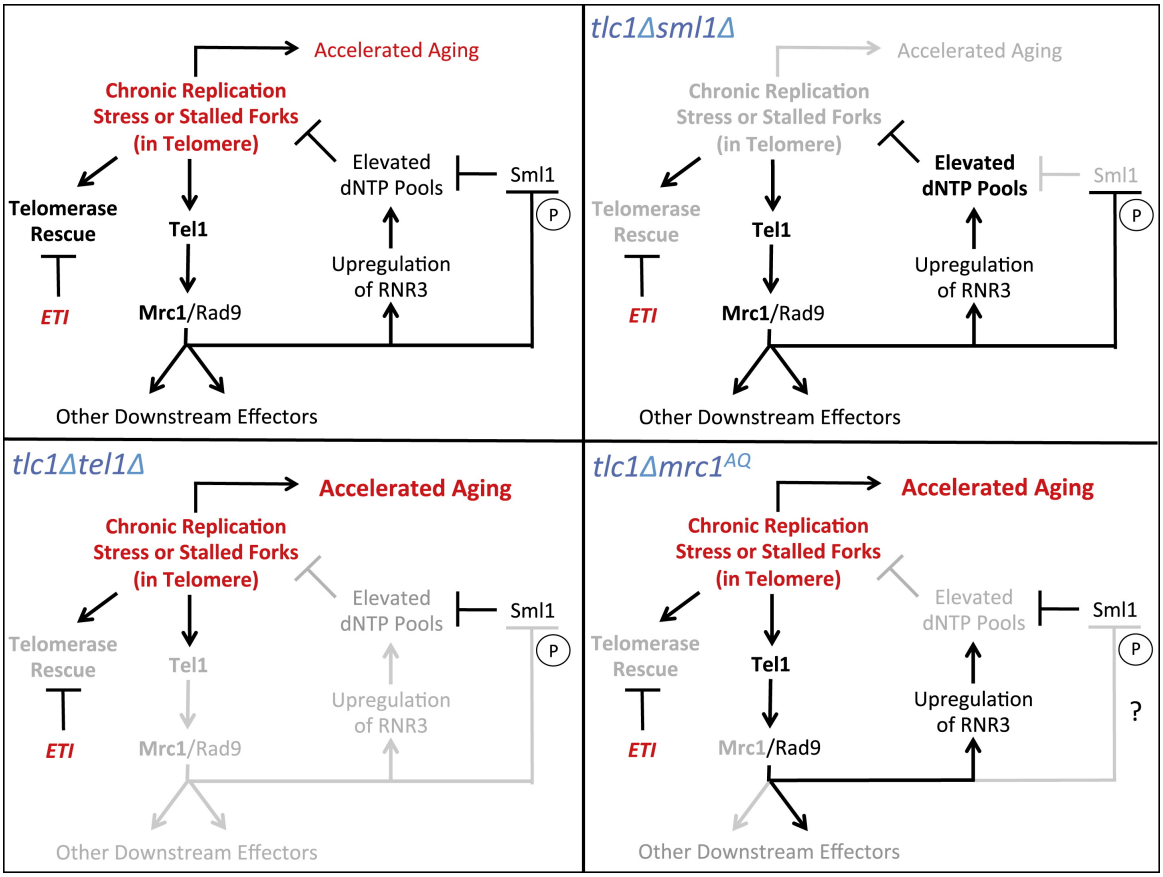
Accelerated Aging
Chronic Replication Stress or Stalled Forks (in Telomere)
Telomerase Rescue
Tel1
Elevated dNTP Pools
Sml1
P
ETI
Mrc1/Rad9
Upregulation of RNR3
Other Downstream Effectors
tlc1Δsml1Δ
Accelerated Aging
Chronic Replication Stress or Stalled Forks (in Telomere)
Elevated dNTP Pools
Sml1
Telomerase Rescue
Tel1
P
Upregulation of RNR3
ETI
Mrc1/Rad9
Other Downstream Effectors
tlc1Δtel1Δ
Accelerated Aging
Chronic Replication Stress or Stalled Forks (in Telomere)
Elevated dNTP Pools
Sml1
Telomerase Rescue
Tel1
P
Upregulation of RNR3
ETI
Mrc1/Rad9
Other Downstream Effectors
tlc1Δmrc1AQ
Accelerated Aging
Chronic Replication Stress or Stalled Forks (in Telomere)
Elevated dNTP Pools
Sml1
Telomerase Rescue
Tel1
P
Upregulation of RNR3
?
ETI
Mrc1/Rad9
Other Downstream Effectors

Table 2-2

GEO ID	Correlation	P-value	GEO annotation Title
GSM185608	0.343	1.12E-162	YER164W deletion (CHD1)
GSM971	0.338	7.35E-154	1.5mM diamide (5 min)
GSM9300	0.34	3.79E-141	By1Cy5
GSM35588	-0.34	3.79E-141	By1Cy5
GSM9302	0.32	1.11E-135	By2Cy5
GSM35590	-0.32	1.11E-135	By2Cy5
GSM105052	-0.319	3.95E-131	ylr266c deletion
GSM43068	0.309	6.56E-131	dot4-1 vs wt set2
GSM315832	0.307	4.65E-128	Yeast_mga2deletion_0.1mMH2O2_rep4

Table 2-3

GO	Description	zscore	p
GO:0035251	UDP-glucosyltransferase activity	26.14	0.00E+00
GO:0042254	ribosome biogenesis and assembly	15.825	0.00E+00
GO:0006986	response to unfolded protein	12.553	3.83E-36
GO:0016491	oxidoreductase activity	11.072	1.72E-28
GO:0006364	rRNA processing	11.1	1.26E-28

Table 2-4

Gene	Name	log2(fold change)
YBL064C	PRX1	0.88
YBR126C	TPS1	0.83
YCR021C	HSP30	2.38
YDL124W	YDL124W	0.90
YDR533C	HSP31	0.70
YGR088W	CTT1	1.39
YHR008C	SOD2	0.63
YIR037W	HYR1	0.74
YKL026C	GPX1	0.60
YKL150W	MCR1	0.60
YLL026W	HSP104	1.49
YOR120W	GCY1	1.19

Chapter 3: Early Telomerase Inactivated Cells Depend on a Functional DNA Damage Response for Full Viability

Kyle Jay

Elizabeth Blackburn

Results

ETI Cells Require a Functional DNA Damage Response for Normal Viability

As discussed in Chapter 2, mutations in one half of the DNA Damage Response (DDR) (Mrc1, Tel1) exacerbated the cell cycle and accelerated mother cell aging phenotypes observed in ETI cells, while mutations in the other half of the pathway (Mec1, Rad9) had little to no effect. Therefore I inactivated both halves of the DDR, completely eliminating the cell's ability to respond to DNA damage, to determine if this would increase the severity of ETI phenotypes. Because DDR signaling in *Saccaromyces cerevisae* is initiated at the level of the PIKK Kinases Mec1 and Tel1, eliminating these proteins is the most thorough way to eliminate DDR function (Melo and Toczyski, 2002). Mutant *mec1*Δ*, tel1*Δ*, and mec1*Δ*tel1*Δ strains were created, which also contained a *sml1*Δ mutation whenever *mec1*Δ was present in order to suppress lethality induced by deletion of Mec1 (Zhao et al., 1998). The bulk viability and colony growth of these strains was compared with and without telomerase activity via the addition of a *tlc1*Δ ETI mutation. The mec1Δsml1Δ and tel1Δ strains individually grew very well in bulk and

showed no colony formation phenotypes when an ETI mutation was introduced (Figure 3-1A). In addition, while the combined *mec1*Δ*tel1*Δ*sml1*Δ strain was already somewhat sick, the addition of the ETI *tlc1*Δ mutation surprisingly had no effect on the bulk growth of the strain (Figure 3-1B). Therefore, the *mec1*Δ*tel1*Δ*sml1*Δ mutation, and loss of upstream PIKK kinase functionality, is not detrimental to ETI strains.

To test this further, I inactivated the downstream tier of the DDR response, the semi-redundant adaptor proteins Mrc1 and Rad9. Without Mrc1 and Rad9 function, the upstream PIKK kinases are unable to phosphorylate their downstream targets, effectively negating the DDR (Alcasabas et al., 2001; Melo and Toczyski, 2002; Vialard et al., 1998). For these experiments, I again used the $mrc1^{AQ}$ allele, which retains its function as a component of the replication fork, but has lost all possible PIKK phosphorylation sites (Osborn and Elledge, 2003). Surprisingly, despite the lack of phenotype in the absence of active PIKK kinases, ETI cells also lacking Mrc1 and Rad9 function ($mrc1^{AQ}$*rad9*Δ) showed a drastic drop in viability and colony growth at the bulk population level for all three ETI mutations tested (Figure 3-2, 3-3). Therefore, in combination with inactivated DDR adaptor proteins, ETI strains exhibit a synthetic sick phenotype.

SML1 Deletion Alleviates the Requirement for the DNA Damage Response in ETI cells

This discrepancy between the ETI phenotype resulting from deletion of the PIKK kinases compared to that resulting from the inactivation of the DDR adaptor proteins

was found to be due to the presence or absence of the Sml1 protein. Sml1 is an inhibitor of Ribonucleotide Reductase (RNR), and deletion of Sml1 is known to elevate nucleotide pools, facilitate DNA replication, and provide resistance to certain forms of DNA damage (Chabes et al., 2003; Zhao et al., 1998). While necessary for viability in the *mec1*Δ*tel1*Δ mutant, the *sml1*Δ mutation is not required for viability in an *mrc1*^{AQ}*rad9*Δ background. Surprisingly, when the *sml1*Δ mutation was added to *ETI mrc1*^{AQ}*rad9*Δ strains, the colony formation defects were completely rescued, and these cells grew similarly to WT (Figure 3-2, 3-3). Therefore, the *sml1*Δ mutation obviates the need for a fully functional DDR in ETI cells.

The *mrc1*^{AQ}*rad9*-induced Synthetic Sickness with ETI is specific to Mrc1 activity

The Mrc1 protein not only facilitates signaling from the upstream PIKK kinases, but also travels as part of the replication fork in complex with two other proteins, Tof1 and Csm3, which are required for Mrc1 association with the fork (Bando et al., 2009). In order to determine if the *mrc1*^{AQ}*rad9*Δ-induced synthetic sickness was specific to Mrc1 activity, I also performed an experiment in which Tof1 was deleted in place of mutating Mrc1. In the *tof1*Δ*rad9*Δ and ETI *tlc1*Δ*tof1*Δ*rad9*Δ strains, there appeared to be no additional effect of the ETI mutation (Figure 3-4). Therefore, loss of association of Mrc1 with the replication fork is not sufficient to induce synthetic sickness in combination with ETI and Rad9 deletion mutations. Mrc1 signaling activity must be eliminated to fully disable the DDR and induce the synthetic phenotype seen in ETI *tlc1*Δ*mrc1*^{AQ}*rad9*Δ cells.

Mutation of Mrc1 and Rad9 does not Induce Synthetic Sickness in Combination with a Hypomorphic TLC1 Allele

In order to determine if a complete loss of telomerase activity was necessary to induce the synthetic phenotype with the *mrc1^{AQ}rad9*Δ mutations, these experiments were repeated using a hypomorphic TLC1 allele, *tlc1-11*. This TLC1 allele encodes a telomerase template RNA with a mutation that causes reduced RNA stability, and results in telomeres which are stable in length but have a shorter length of 210bp compared to 350bp in isogenic WT strains (Lin et al., 2004). However, when combined with the *mrc1^{AQ}rad9*Δ mutations, no synthetic phenotype was observed (Figure 3-5). Therefore, a hypomorphic telomerase and short-but-stable telomeres are not sufficient to induce the synthetic phenotype with *mrc1^{AQ}rad9*Δ; full loss of telomerase activity is required.

Phenotype Rescue by Sml1 Deletion is due to Relief of RNR Inhibition and Increase in dNTP Pools

The primary known function of Sml1 is the elevation of dNTPs in the cell via inhibition of the RNR enzyme complex (Chabes et al., 1999). Therefore, it was assumed that the rescue of the *ETI mrc1^{AQ}rad9*Δ synthetic phenotype was due to this increased concentration of dNTPs. However, I questioned whether the alleviation of the *ETI mrc1^{AQ}rad9*Δ synthetic sick phenotype might have been due to another unknown function of Sml1. To examine this possibility, I created *ETI mrc1^{AQ}rad9*Δ strains that overexpressed RNR1, the RNR subunit to which Sml1 specifically binds and inhibits (Chabes et al., 1999). By overexpressing RNR1, I was able to rescue the *ETI*

mrc1^{AQ}*rad9*Δ synthetic phenotype to approximately the same extent as in a *sml1*Δ mutant (Figure 3-6). This further supports the claim that the rescue via Sml1 mutation was due to the relief of inhibition on RNR1 and the consequent increase in dNTP levels.

ETI Strains are Not Sensitive to Reduced Levels of dNTPs

Because it was determined that the rescue induced by Sml1 deletion was due to an increase in the cellular dNTP pools and because the DDR is also important for elevating dNTP pools during S-phase or in response to DNA damage (Andreson et al., 2010; Hoch et al., 2013), another possible explanation for the observed phenotypes is that ETI cells are especially sensitive to reduced dNTP concentrations. In order to test this hypothesis, I tested ETI strains for reduced bulk population viability under various conditions that reduce cellular dNTP concentrations. First, ETI cells were treated with various concentrations of hydroxyurea (HU), a drug that inhibits RNR1, similar to the action of the Sml1 protein (Saban and Bujak, 2009). Despite using a wide range of drug concentrations (1mM – 100mM), no deleterious effect was observed in drug-treated ETI strains (Figure 3-7 and data not shown). Second, I stabilized the Sml1 protein by deleting the gene encoding Dun1, the DDR protein responsible for the phosphorylation and subsequent degradation of Sml1 in response to DDR pathway activation (Andreson et al., 2010). Likewise, I combined ETI mutations with the *sml1 4SA* mutant, which lacks the Dun1 phosphorylation sites and is insensitive to Dun1-mediated degradation (Andreson et al., 2010). These two mutations result in a hyper-stabilized Sml1 protein that cannot be degraded in response to DDR signaling. However, combining ETI mutations with the hyper-stabilized Sml1 mutants produced no noticeable changes in

the bulk growth and colony formation phenotypes (Figure 3-8, 3-9). Lastly, I produced ETI cells with *SML1* under the inducible galactose promoter. When grown on galactose, these cells will greatly overexpress Sml1, which should increase inhibition on the RNR enzyme complex. However, ETI strains with overexpressed Sml1 displayed no changes in their growth and colony formation (Figure 3-10). These experiments greatly support the conclusion that bulk growth of ETI single mutants is not sensitive to reduced levels of dNTPs. Therefore, the synthetic sickness induced in ETI cells by Mrc1 and Rad9 deletion cannot be accounted for by the reduction in dNTP pools that results from a defective DDR pathway, but is most likely due to the inability to respond to DNA damage.

Recombination is Not Required for the Synthetic ETI *mrc1^{AQ}rad9*Δ Phenotype or for the Rescue via Sml1 Deletion

Recombination has been known to play a role in the survival of cells lacking telomerase. In the absence of telomerase activity, cells may use alternative telomere lengthening mechanisms involving recombination in order to become “survivor” cells and evade the permanent cell cycle arrest that occurs during senescence (Lundblad and Blackburn, 1993). I sought to determine if recombination might be playing a role in the aforementioned ETI phenotypes, as increased dNTP pools have been shown to repress hyper-recombination in yeast (Fasullo et al., 2010). Therefore, I attempted to replicate the ETI *mrc1^{AQ}rad9*Δ synthetic sickness in recombination deficient cells. In order to prevent recombination in these strains, I deleted Rad52, which is known to prevent the development of survivor cells in the absence of telomerase (Lundblad and Blackburn,

1993). However, deletion of Rad52 seemed to have very little effect on the synthetic sick phenotype in ETI *mrc1^{AQ}rad9*Δ or on the rescue via Sml1 deletion (Figure 3-11). Therefore, I concluded that recombination does not play a substantial role in the manifestation of these phenotypes.

Synthetic ETI Phenotype with Mrc1 and Rad9 Mutation and the Rescue via Sml1 Deletion are not due to Changes in Telomere Length

The simplest explanation for these phenotypes is that telomeres are drastically shortened in ETI *mrc1^{AQ}rad9*Δ strains and lengthened by the *sml1*Δ mutation, such that the phenotypes observed are simply resulting from premature senescence. To determine if this was the case, I isolated genomic DNA from the relevant strain genotypes and measured telomere length by performing a southern blot with a telomeric repeat DNA probe. While the *tlc1*Δ*mrc1^{AQ}rad9*Δ triple mutants did have a shorter telomere length than *tlc1*Δ single mutants, this seemed to be additive with the slightly reduced telomere length seem in *mrc1^{AQ}rad9*Δ double mutants relative to WT (Figure 3-12). Also, the telomere length of first-passage (ETI) *tlc1*Δ*mrc1^{AQ}rad9*Δ cells was no shorter than that of second-passage *tlc1*Δ single mutants (Figure 3-12), which grow similarly to WT and do not typically show visible signs of senescence until the third or fourth passage on solid media (Figure 3-13). Lastly, the *tlc1*Δ*mrc1^{AQ}rad9*Δ*sml1*Δ "rescued" mutants showed only very modest telomere length increases at either the first or second passage relative to *tlc1*Δ*mrc1^{AQ}rad9*Δ mutants (Figure 3-12), despite greatly improved growth and colony formation phenotypes (Figure 3-2, 3-3). However, while these southern blots provide a good representation of bulk telomere length, a shorter

bulk distribution of telomere length predicts there will be a higher occurrence of critically short telomeres. Therefore, this result does not rule out the possibility of a single critically short telomere, as will be addressed in the following section. However, it does not appear that these mild bulk telomere length reductions or increases are the causative factors for the *ETI mrc1^{AQ}rad9*Δ synthetic sickness or the *sml1*Δ rescue, respectively.

Decapped and Fusogenic Telomeres May Play a Role in the ETI *mrc1^{AQ}rad9*Δ Synthetic Sickness and *sml1*Δ Rescue

Telomere deprotection occurs when telomeres become too short to maintain their protective cap of bound proteins. Once this occurs, telomeres may fuse to other exposed DNA ends, potentially resulting in broken chromosomes and genomic instability (O'Sullivan and Karlseder, 2010). To determine whether the phenotypes studied here were the result of decapped/fusogenic telomeres, I used a previously published telomere capture assay (Chan and Blackburn, 2003). In these experiments, a double-strand break is induced in the left arm of chromosome 7 via HO expression and an integrated HO cut site (Diede and Gottschling, 1999). The cut chromosome acts as a trap for deprotected telomeres as they are likely to fuse with it. The resulting fusion between chromosome 7 and any deprotected telomere ends can be detected via PCR using primers which hybridize to the subtelomere and to sequences proximal to the HO cut site (Chan and Blackburn, 2003). Surprisingly, the results showed that in strains with a full or partially-functional DDR, addition of the *sml1*Δ mutation either had no effect (e.g. WT, *mrc1^{AQ}*) or increased (e.g. *tlc1*Δ, *tlc1*Δ*rad9*) the amount of detected

deprotected telomeres (Figure 3-14). However, in strains completely lacking a functional DDR (e.g. *mrc1^{AQ}rad9*Δ, *tlc1*Δ*mrc1^{AQ}rad9*Δ), addition of the *sml1*Δ mutation noticeably decreased the amount of deprotected telomeres detected by the PCR assay (Figure 3-13). The originally published assay showed that these induced fusions occurred by Non-Homologous End Joining (NHEJ) and were dependent on the DNA ligase, Dnl4 (Chan and Blackburn, 2003). However, deletion of Dnl4 was unable to rescue the ETI *tlc1*Δ*mrc1^{AQ}rad9*Δ sickness as did Sml1 deletion (data not shown). This suggests that, while the *sml1*Δ mutation may play some role in reducing the number of exposed DNA ends in strains lacking a functional DDR, protection from telomere deprotection and telomere fusions is not the sole mechanism through which *sml1*Δ rescues the ETI *tlc1*Δ*mrc1^{AQ}rad9*Δ synthetic sick phenotype.

Discussion

Here I have presented phenotypes in cells lacking telomerase which manifest far earlier than previously predicted. These cells were studied *E*arly after *T*elomerase *I*nactivation (ETI) when they were still growing comparably to WT and far from entering telomere shortness-induced senescence that occurs *L*ate after *T*elomerase *I*nactivation (LTI) (Abdallah et al., 2009; d' Adda di Fagagna et al., 2003). It was discovered that these ETI cells have a dependence on a functional DNA Damage Response (DDR) for full viability and that this requirement can be alleviated by deletion of Sml1 (Figure 3-2, 3-3). In ETI cells lacking functional DDR adaptor proteins (*mrc1^{AQ}rad9*Δ), a synthetic sickness was observed that was not caused by accelerated telomere shortening (Figure 3-12) or due to an inherent sensitivity of ETI cells to reduced dNTP levels (Figure 3-7, 3-

8, 3-9, 3-10). This requirement was specific to Mrc1 activity as it was not replicated by mutation of Tof1, a partner protein which is required for Mrc1 localization to the replication fork (Figure 3-4) (Bando et al., 2009). ETI cells were found to be viable in the absence of functional upstream PIKK sensor kinases (*mec1*Δ*tel1*Δ*sml1*Δ) (Figure 3-1), but the necessity of including the rescuing *sml1*Δ mutation in *mec1*Δ strains hinders my ability to determine if Mec1 activity plays a role in the survival of ETI cells. Lastly, only a complete loss of telomerase activity (*tlc1*Δ, *est2D530A*, or *est2*Δ) was sufficient to induce the synthetic phenotype with the *mrc1*^{AQ}*rad9*Δ mutations, as it could not be replicated using a hypomorphic TLC1 allele, *tlc1-11* (Figure 3-5). This implies that in the complete absence of a functional DDR, even this reduced amount of telomerase activity is able to prevent this synthetic phenotype.

Likewise, the rescue of the synthetic phenotype by *sml1*Δ was not caused by telomere lengthening (Figure 3-12), was not dependent on recombination (Figure 3-11), nor could it be attributed to a novel function of Sml1 other than its inhibitory effect on RNR1 (Figure 3-6). The rescue may be partially due to *sml1*Δ reducing the occurrence of deprotected telomeres in cells lacking a functional DDR (Figure 3-14), but the presence of other contributing factors seems certain. Because the rescue of the synthetic *ETI* *mrc1*^{AQ}*rad9*Δ phenotype was attributed to the elevated dNTP levels resulting from *sml1*Δ, this supports a role of DNA replication stress in this phenotype. Accordingly, all of the data presented here is consistent with the model presented in Chapter 2 to explain the cell-cycle abnormalities and accelerated mother cell aging that also occur in ETI cells (see Chapter 2, Figure 2-16). It is known that telomeric sequences are

extremely difficult regions to replicate due to their repetitive, G-rich sequences and tightly bound protein components (Drosopoulos et al., 2012; Miller et al., 2006; Sfeir et al., 2009). In this model, telomerase DNA extension activity acts as an alternative bypass mechanism to stalled or backtracked forks in the telomere. Future experiments would focus on determining how telomerase assists these stalled forks, possibly through extension of the single-stranded G-rich leading strand revealed by fork backtracking. Without a functional DDR to stabilize struggling replication forks, the telomerase bypass mechanism becomes substantially more important to ensure proper replication of the telomere. In the absence of Sml1, increased dNTP pools facilitate smoother replication through the telomere, preventing fork stalling as well as fork collapse, which could result in deprotected/fusogenic chromosome ends.

The results presented here suggest that telomerase is required for reasons beyond countering the slow loss of sequence that occurs as a result of DNA replication. A loss of telomerase function, even when telomeres are long enough to support growth, burdens cells with certain genetic dependencies, indicative of a reduced ability to resolve telomeric DNA replication stress. This suggestion of a more continuous need for telomerase to alleviate replication problems in the telomere will change our understanding of telomerase function and telomere maintenance.

References

Abdallah, P., Luciano, P., Runge, K.W., Lisby, M., Géli, V., Gilson, E., and Teixeira, M.T. (2009). A two-step model for senescence triggered by a single critically short telomere. Nat. Cell Biol. *11*, 988–993.

D' Adda di Fagagna, F., Reaper, P.M., Clay-Farrace, L., Fiegler, H., Carr, P., Von Zglinicki, T., Saretzki, G., Carter, N.P., and Jackson, S.P. (2003). A DNA damage checkpoint response in telomere-initiated senescence. Nature *426*, 194–198.

Alcasabas, A.A., Osborn, A.J., Bachant, J., Hu, F., Werler, P.J., Bousset, K., Furuya, K., Diffley, J.F., Carr, A.M., and Elledge, S.J. (2001). Mrc1 transduces signals of DNA replication stress to activate Rad53. Nat. Cell Biol. *3*, 958–965.

Andreson, B.L., Gupta, A., Georgieva, B.P., and Rothstein, R. (2010). The ribonucleotide reductase inhibitor, Sml1, is sequentially phosphorylated, ubiquitylated and degraded in response to DNA damage. Nucleic Acids Res. *38*, 6490–6501.

Bando, M., Katou, Y., Komata, M., Tanaka, H., Itoh, T., Sutani, T., and Shirahige, K. (2009). Csm3, Tof1, and Mrc1 form a heterotrimeric mediator complex that associates with DNA replication forks. J. Biol. Chem. *284*, 34355–34365.

Chabes, A., Domkin, V., and Thelander, L. (1999). Yeast Sml1, a protein inhibitor of ribonucleotide reductase. J. Biol. Chem. *274*, 36679–36683.

Chabes, A., Georgieva, B., Domkin, V., Zhao, X., Rothstein, R., and Thelander, L. (2003). Survival of DNA damage in yeast directly depends on increased dNTP levels allowed by relaxed feedback inhibition of ribonucleotide reductase. Cell *112*, 391–401.

Chan, S.W.-L., and Blackburn, E.H. (2003). Telomerase and ATM/Tel1p protect telomeres from nonhomologous end joining. Mol. Cell *11*, 1379–1387.

Diede, S.J., and Gottschling, D.E. (1999). Telomerase-mediated telomere addition in vivo requires DNA primase and DNA polymerases alpha and delta. Cell *99*, 723–733.

Drosopoulos, W.C., Kosiyatrakul, S.T., Yan, Z., Calderano, S.G., and Schildkraut, C.L. (2012). Human telomeres replicate using chromosome-specific, rather than universal, replication programs. J. Cell Biol. *197*, 253–266.

Fasullo, M., Tsaponina, O., Sun, M., and Chabes, A. (2010). Elevated dNTP levels suppress hyper-recombination in Saccharomyces cerevisiae S-phase checkpoint mutants. Nucleic Acids Res. *38*, 1195–1203.

Hoch, N.C., Chen, E.S.-W., Buckland, R., Wang, S.-C., Fazio, A., Hammet, A., Pellicioli, A., Chabes, A., Tsai, M.-D., and Heierhorst, J. (2013). Molecular basis of the essential s phase function of the rad53 checkpoint kinase. Mol. Cell. Biol. *33*, 3202–3213.

Lin, J., Ly, H., Hussain, A., Abraham, M., Pearl, S., Tzfati, Y., Parslow, T.G., and Blackburn, E.H. (2004). A universal telomerase RNA core structure includes structured motifs required for binding the telomerase reverse transcriptase protein. Proc. Natl. Acad. Sci. U. S. A. *101*, 14713–14718.

Lundblad, V., and Blackburn, E.H. (1993). An alternative pathway for yeast telomere maintenance rescues est1- senescence. Cell *73*, 347–360.

Melo, J., and Toczyski, D. (2002). A unified view of the DNA-damage checkpoint. Curr. Opin. Cell Biol. *14*, 237–245.

Miller, K.M., Rog, O., and Cooper, J.P. (2006). Semi-conservative DNA replication through telomeres requires Taz1. Nature *440*, 824–828.

Osborn, A.J., and Elledge, S.J. (2003). Mrc1 is a replication fork component whose phosphorylation in response to DNA replication stress activates Rad53. Genes Dev. *17*, 1755–1767.

O'Sullivan, R.J., and Karlseder, J. (2010). Telomeres: protecting chromosomes against genome instability. Nat. Rev. Mol. Cell Biol. *11*, 171–181.

Saban, N., and Bujak, M. (2009). Hydroxyurea and hydroxamic acid derivatives as antitumor drugs. Cancer Chemother. Pharmacol. *64*, 213–221.

Sfeir, A., Kosiyatrakul, S.T., Hockemeyer, D., MacRae, S.L., Karlseder, J., Schildkraut, C.L., and de Lange, T. (2009). Mammalian Telomeres Resemble Fragile Sites and Require TRF1 for Efficient Replication. Cell *138*, 90–103.

Vialard, J.E., Gilbert, C.S., Green, C.M., and Lowndes, N.F. (1998). The budding yeast Rad9 checkpoint protein is subjected to Mec1/Tel1-dependent hyperphosphorylation and interacts with Rad53 after DNA damage. EMBO J. *17*, 5679–5688.

Zhao, X., Muller, E.G., and Rothstein, R. (1998). A suppressor of two essential checkpoint genes identifies a novel protein that negatively affects dNTP pools. Mol. Cell *2*, 329–340.

Figure Legends

Figure 3-1. ETI Cells Do Not Display Growth Defects in the Absence of Mec1 and Tel1 PIKK Kinases

(A) *sml1*Δ, *tel1*Δ, and *mec1*Δ*sml1*Δ mutations had no effect on bulk colony growth phenotypes of ETI *tlc1*Δ strains (compare left and right halves). (B) ETI *tlc1*Δ mutation caused no additional growth defects in *mec1*Δ*tel1*Δ*sml1*Δ strains (compare left and right halves). All streaks shown are first passage cells taken directly from sporulation of diploid strains heterozygous for all mutations.

Figure 3-2. ETI Mutants Show a Dependence on the DNA Damage Response that can be Alleviated by Sml1 Deletion

Three different ETI mutants, (A) *tlc1*Δ, (B) *est2D530A*, and (C) *est2*Δ, show a loss of viability in strains lacking a functional DNA damage response due to Mrc1 and Rad9 mutation. Deletion of the RNR inhibitor, Sml1, alleviates this requirement (compare left and right halves). All streaks shown are first passage cells taken directly from sporulation of diploid strains heterozygous for all mutations.

Figure 3-3. Semi-Quantitative Serial Dilutions Show ETI *mrc1^{AQ}rad9*Δ Synthetic Phenotype and Rescue via Sml1 Deletion

ETI *mrc1^{AQ}rad9*Δ Synthetic Phenotype, as in 3-2, shown via semi-quantitave serial dilutions. ETI cells show reduced colony formation and colony size in the absence of functional Mrc1 and Rad9 proteins. Colony size and growth phenotypes are restored with deletion of Sml1.

Figure 3-4. ETI *mrc1^{AQ}rad9*Δ Synthetic Phenotype is Specific for Mrc1 Activity

Deletion of the Mrc1 partner protein, Tof1, does not mimic the ETI synthetic phenotype. Serial dilutions of strains of the indicated genotypes showed no worsening of the colony growth phenotypes between *tof1*Δ*rad9*Δ and ETI *tlc1*Δ*tof1*Δ*rad9*Δ strains. Two biological replicates shown.

Figure 3-5. Hypomorphic Telomerase Does Not Show Synthetic Phenotype with *mrc1^{AQ}rad9*Δ Mutation

(A) Streaks and (B) serial dilutions attempting to replicate the ETI *mrc1^{AQ}rad9*Δ synthetic phenotype using a hypomorphic *TLC1* allele, *tlc1-11*. The *tlc1-11* mutation did not cause noticeable changes in colony growth formation of *mrc1^{AQ}rad9*Δ mutants. In order to ensure shortened telomere length, all *tlc1-11* haploid strains were obtained by sporulation of a homozygous *tlc1-11/tlc1-11* diploid, which was heterozygous for all other mutations. Strains marked with an asterisk (*) were obtained from a different diploid strain heterozygous for *tlc1*Δ in addition to the mutations shown.

Figure 3-6. RNR1 Overexpression Can Also Rescue ETI *mrc1^{AQ}rad9*Δ Synthetic Phenotype

Like *sml1*Δ, RNR1 overexpression (*RNR1**) was able to rescue the colony formation defects of ETI *mrc1^{AQ}rad9*Δ for all three ETI mutations tested, (A) *tlc1*Δ, (B) *est2D530A*, (C) *est2*Δ (compare left and right halves). All streaks shown are first passage cells taken directly from sporulation of diploid strains heterozygous for all mutations.

Figure 3-7. ETI Strains are Not Sensitive to HU Treatment

Cells were serially diluted onto rich media plates containing hydroxyurea (HU) at the indicated concentrations. Despite a strong effect on control *mec1*Δ*sml1*Δ strains, no significant sensitivity to the drug was observed in ETI cells. Higher dosages of the drug (25mM and 100mM) showed similar results (data not shown). All ETI haploid strains were isolated directly from sporulation of a diploid heterozygous for the ETI mutation indicated.

Figure 3-8. ETI Strains are Not Sensitive to Dun1 Deletion

Dun1, the kinase responsible for phosphorylation and degradation of Sml1 was deleted in ETI cells. The *dun1*Δ mutation had no discernable effect on bulk colony growth phenotypes of ETI cells. Two biological replicates shown. All streaks shown are first passage cells taken directly from sporulation of diploid strains heterozygous for all mutations.

Figure 3-9. Introduction of a Hyper-stabilized Sml1 Allele had No Significant Effect on ETI Mutants

Introduction of the hyper-stabilized, non-degradable *sml1 4SA* mutation had no significant effect on any of the three ETI strains tested, (A) *tlc1*Δ, (B) *est2D530A*, and (C) *est2*Δ (compare top and bottom halves). All streaks shown are first passage cells taken directly from sporulation of diploid strains heterozygous for all mutations.

Figure 3-10. Overexpression of Sml1 had No Effect on Colony Growth Phenotypes of ETI Mutants

Overexpression of Sml1 via a galactose-inducible promotor had no significant effect on any of the three ETI strains tested, (A) *tlc1*Δ, (B) *est2D530A*, and (C) *est2*Δ, relative to ETI alone. All streaks shown are first passage cells taken directly from sporulation of diploid strains heterozygous for all mutations. Plates were incubated for: 2 days (Dextrose) or 3 days (Galactose).

Figure 3-11. Recombination is Not Required for ETI *mrc1^{AQ}rad9*Δ Synthetic Phenotype Nor its Rescue via Sml1 Deletion

Elimination of recombination, via Rad52 deletion, did not eliminate the ETI *mrc1^{AQ}rad9*Δ synthetic phenotype, nor prevent its rescue via Sml1 deletion (compare left and right halves). All streaks shown are first passage cells taken directly from sporulation of diploid strains heterozygous for all mutations.

Figure 3-12. ETI *mrc1^{AQ}rad9*Δ Synthetic Phenotype and *sm1*Δ Rescue Cannot be Explained by Changing Telomere Lengths or Accelerated Senescence

Telomere lengths were measured using a southern blot and a telomeric DNA probe. The lowermost species represents the DNA fragment containing the terminal telomeric repeats. Telomere lengths for both first (1) and second (2) passages after sporulation of a diploid heterozygous are represented for all genotypes.

Figure 3-13. ETI Strains Reach Senescence after Three to Four passages on Solid Media

WT and *tlc1*Δ (A) or *est2D530A* (B) ETI strains were passaged on solid media until the cell population reached LTI senescence. Each passage represents approximately 20 divisions. The rate of senescence onset can vary between isolates but typically occurs after three to four passages.

Figure 3-14. Rescue via Sml1 Deletion may be Partially due to Reduction in Deprotected Telomeres in Strains Lacking a Functional DNA Damage Response

PCR assay to detect deprotected telomeres that fuse to an induced double strand break (HO cut). Intensity of bands represents approximate amounts of captured deprotected telomeres. No DNA bands were visible in experiments when either primer was excluded from the PCR reaction. Sml1 deletion had no effect or increased amount of detected deprotected telomeres in strains with a fully- or partially-functional DDR and reduced the amount of detected deprotected telomeres in strains completely lacking a DDR (*mrc1*^{AQ}*rad9*Δ).

Figure 3-1

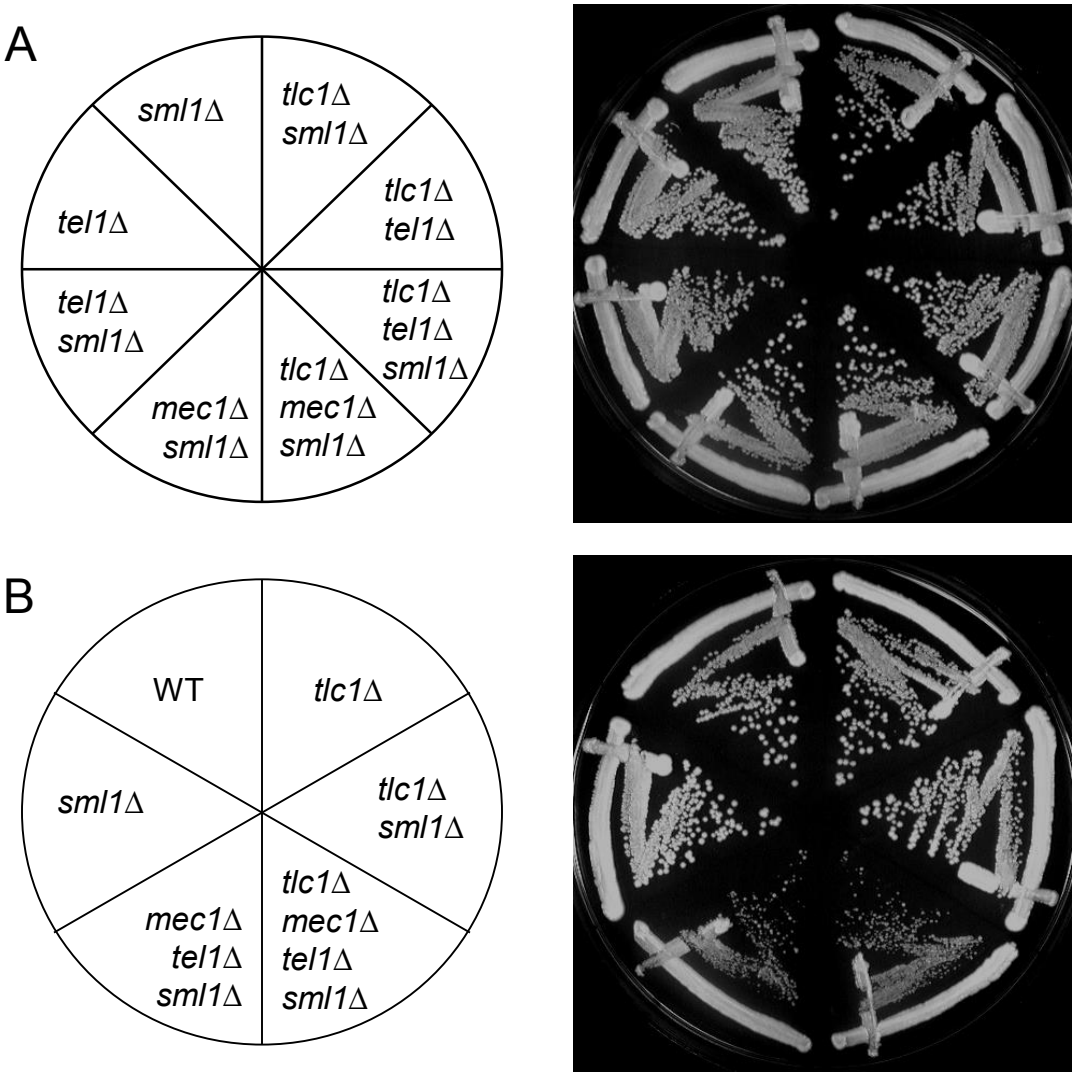
A
sml1Δ
tlc1Δ sml1Δ
tlc1Δ tel1Δ
tel1Δ
tel1Δ sml1Δ
tlc1Δ tel1Δ sml1Δ
mec1Δ sml1Δ
tlc1Δ mec1Δ sml1Δ
B
WT
tlc1Δ
sml1Δ
tlc1Δ sml1Δ
mec1Δ tel1Δ sml1Δ
tlc1Δ mec1Δ tel1Δ sml1Δ

Figure 3-2

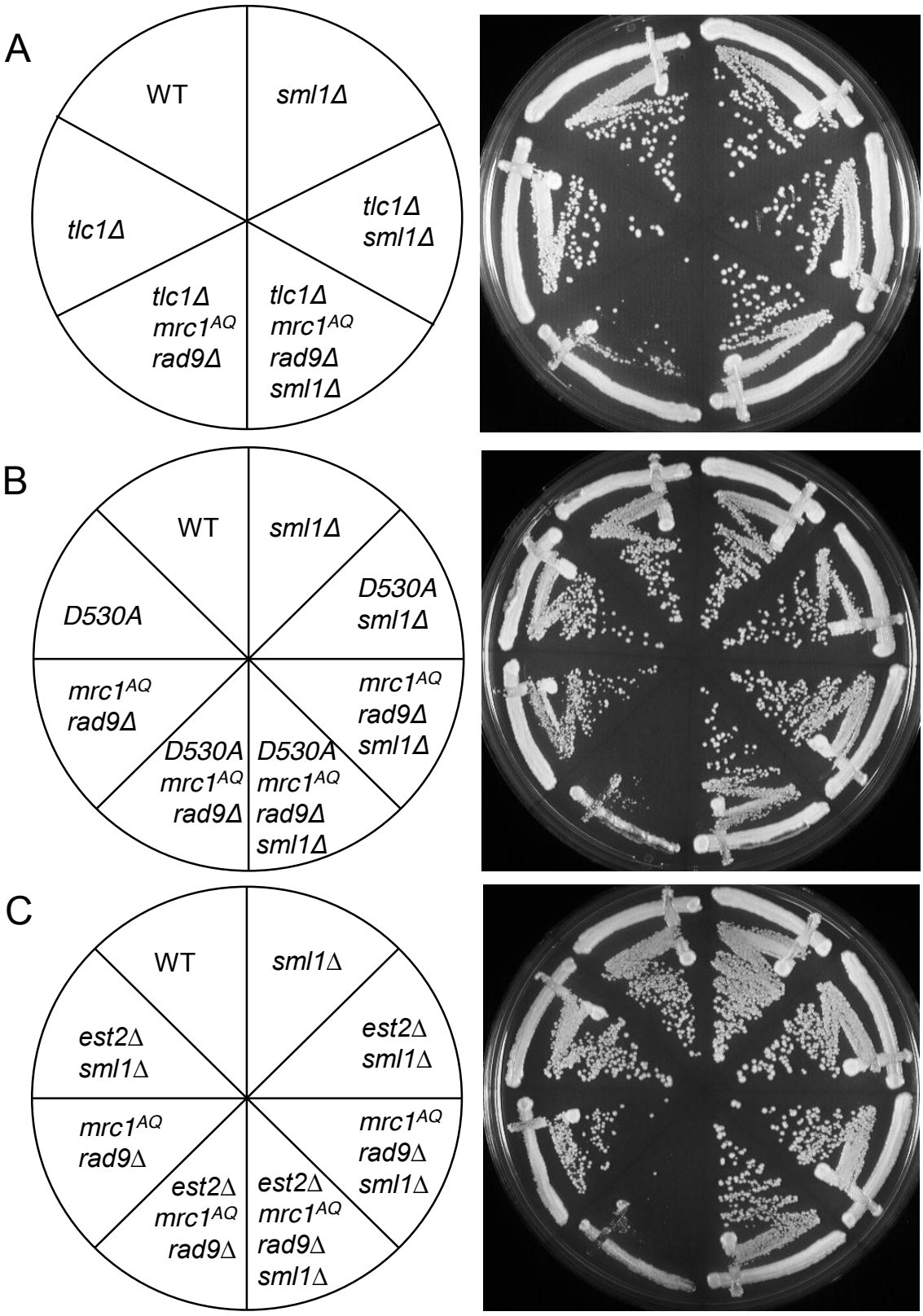
A
WT
sml1Δ
tlc1Δ
sml1Δ
tlc1Δ
tlc1Δ
mrc1AQ
rad9Δ
tlc1Δ
mrc1AQ
rad9Δ
sml1Δ
B
WT
sml1Δ
D530A
D530A
sml1Δ
mrc1AQ
rad9Δ
mrc1AQ
rad9Δ
sml1Δ
D530A
mrc1AQ
rad9Δ
D530A
mrc1AQ
rad9Δ
sml1Δ
C
WT
sml1Δ
est2Δ
sml1Δ
est2Δ
sml1Δ
mrc1AQ
rad9Δ
mrc1AQ
rad9Δ
sml1Δ
est2Δ
mrc1AQ
rad9Δ
est2Δ
mrc1AQ
rad9Δ
sml1Δ

Figure 3-3

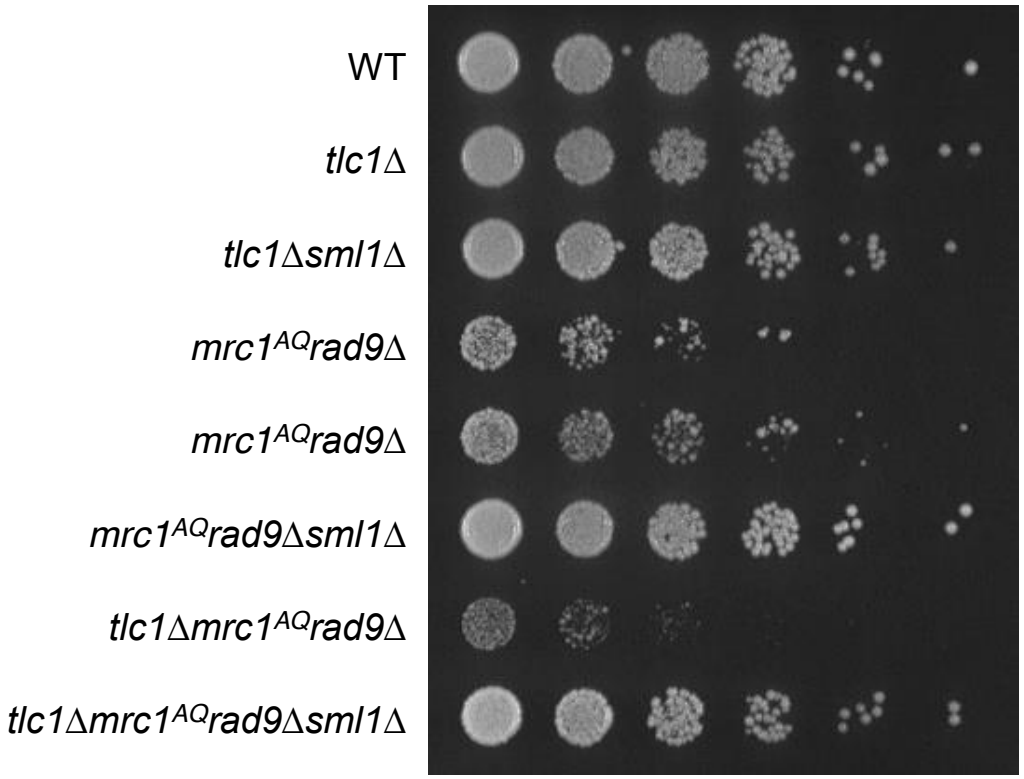
WT
tlc1Δ
tlc1Δsml1Δ
mrc1AQrad9Δ
mrc1AQrad9Δ
mrc1AQrad9Δsml1Δ
tlc1Δmrc1AQrad9Δ
tlc1Δmrc1AQrad9Δsml1Δ

Figure 3-4

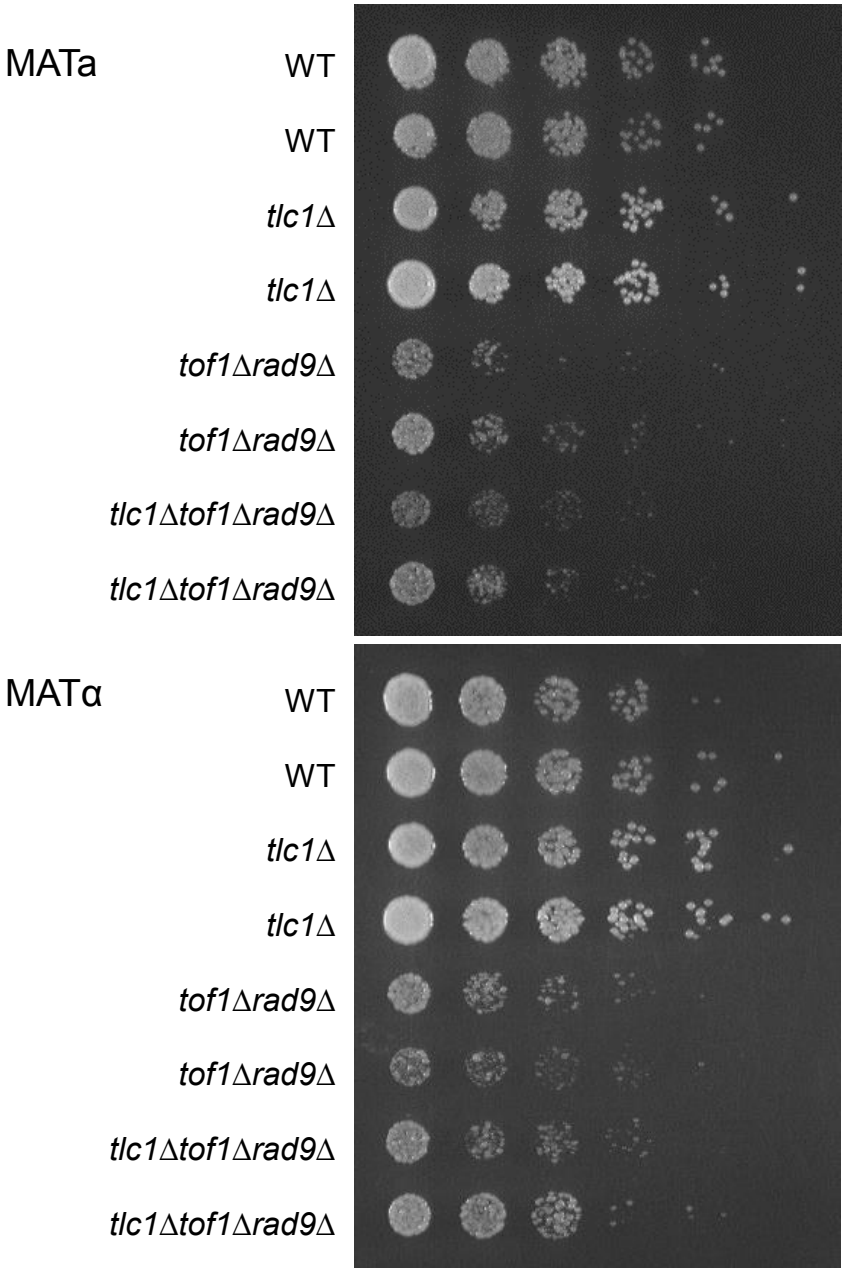
MATa
WT
WT
tlc1Δ
tlc1Δ
tof1Δrad9Δ
tof1Δrad9Δ
tlc1Δtof1Δrad9Δ
tlc1Δtof1Δrad9Δ
MATα
WT
WT
tlc1Δ
tlc1Δ
tof1Δrad9Δ
tof1Δrad9Δ
tlc1Δtof1Δrad9Δ
tlc1Δtof1Δrad9Δ

Figure 3-5

A

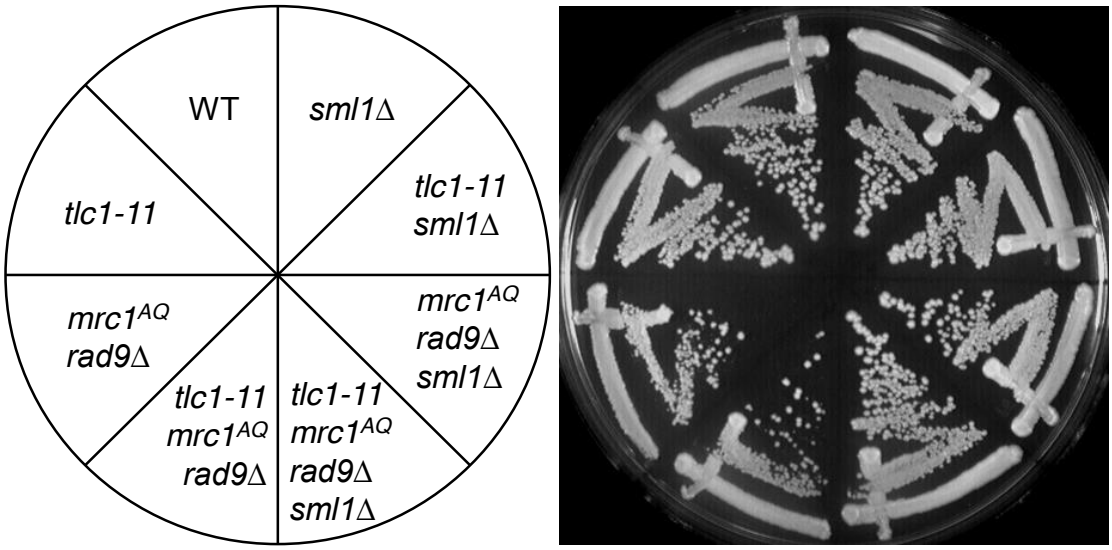
WT
sml1Δ
tlc1-11
tlc1-11 sml1Δ
mrc1AQ rad9Δ
mrc1AQ rad9Δ sml1Δ
tlc1-11 mrc1AQ rad9Δ
tlc1-11 mrc1AQ rad9Δ sml1Δ

B

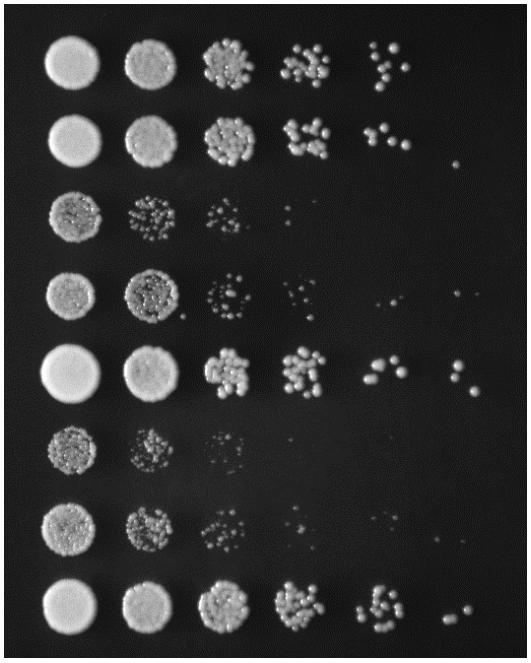
WT*
tlc1-11
mrc1AQrad9Δ*
mrc1AQrad9Δ*
mrc1AQrad9Δsml1Δ*
tlc1-11 mrc1AQrad9Δ
tlc1-11 mrc1AQrad9Δ
tlc1-11 mrc1AQrad9Δsml1Δ

Figure 3-6

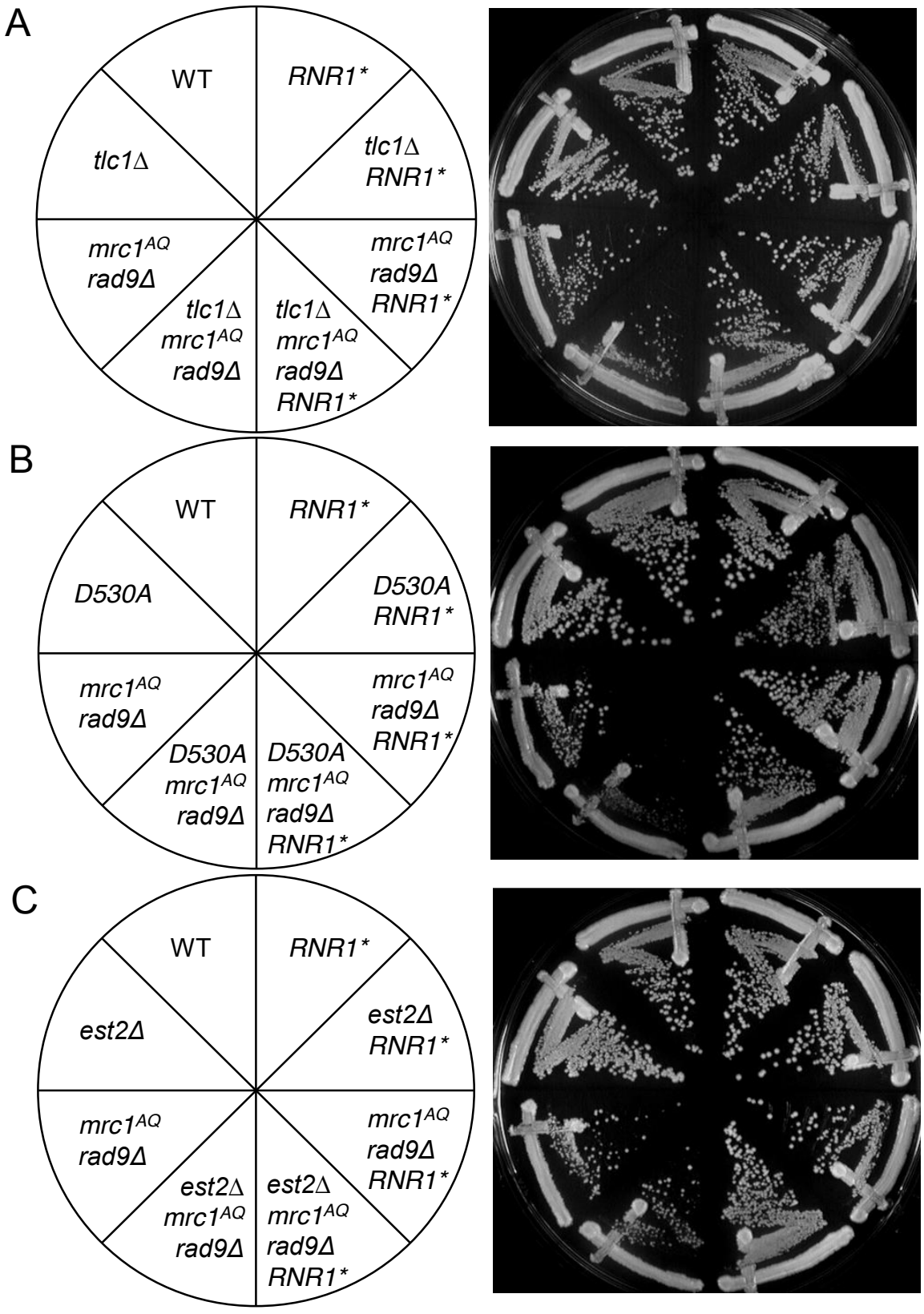
A
WT
RNR1*
tlc1Δ
tlc1Δ RNR1*
mrc1AQ rad9Δ
mrc1AQ rad9Δ RNR1*
tlc1Δ mrc1AQ rad9Δ
tlc1Δ mrc1AQ rad9Δ RNR1*
B
WT
RNR1*
D530A
D530A RNR1*
mrc1AQ rad9Δ
mrc1AQ rad9Δ RNR1*
D530A mrc1AQ rad9Δ
D530A mrc1AQ rad9Δ RNR1*
C
WT
RNR1*
est2Δ
est2Δ RNR1*
mrc1AQ rad9Δ
mrc1AQ rad9Δ RNR1*
est2Δ mrc1AQ rad9Δ
est2Δ mrc1AQ rad9Δ RNR1*

Figure 3-7

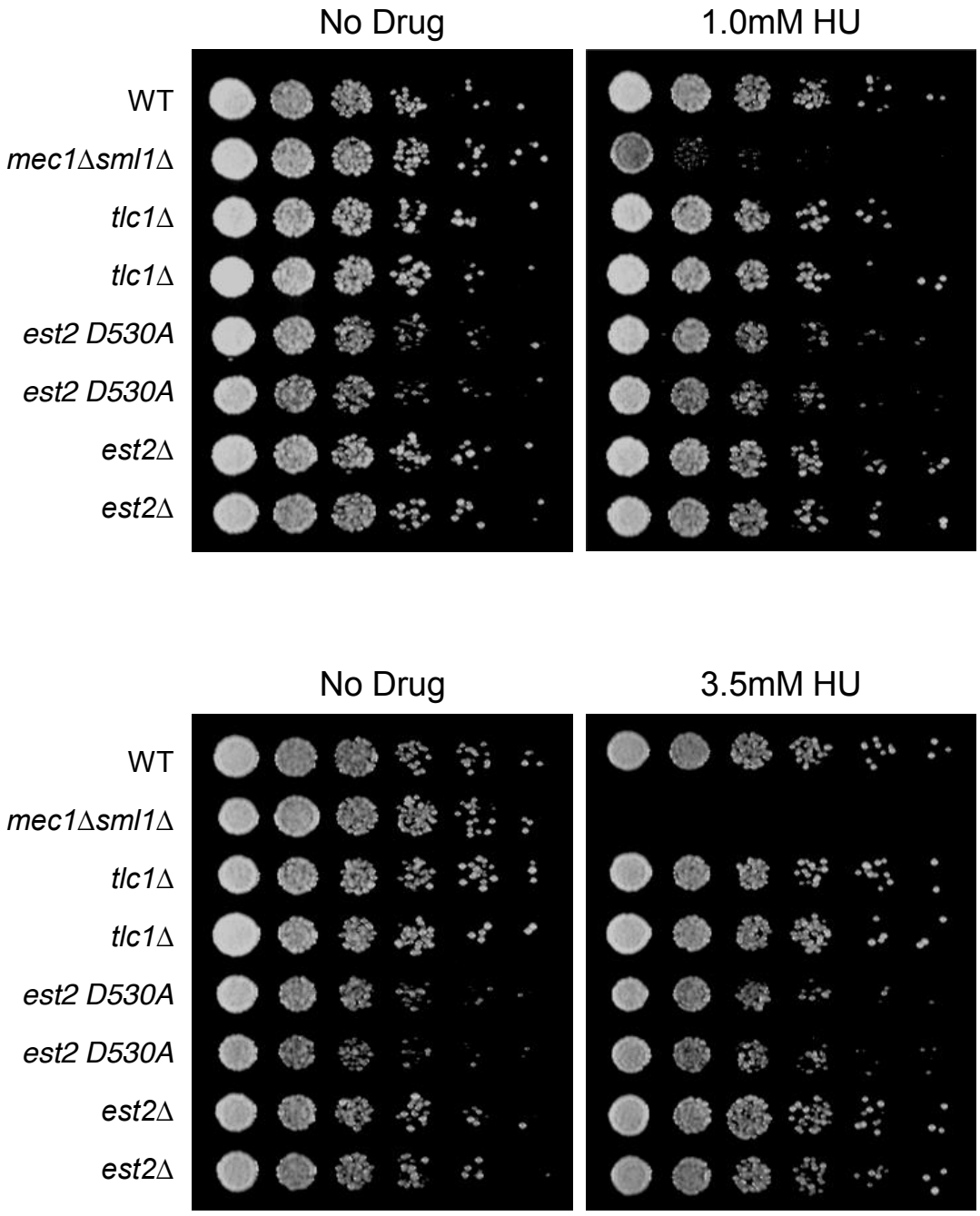
No Drug
1.0mM HU
WT
mec1Δsml1Δ
tlc1Δ
tlc1Δ
est2 D530A
est2 D530A
est2Δ
est2Δ
No Drug
3.5mM HU
WT
mec1Δsml1Δ
tlc1Δ
tlc1Δ
est2 D530A
est2 D530A
est2Δ
est2Δ

Figure 3-8

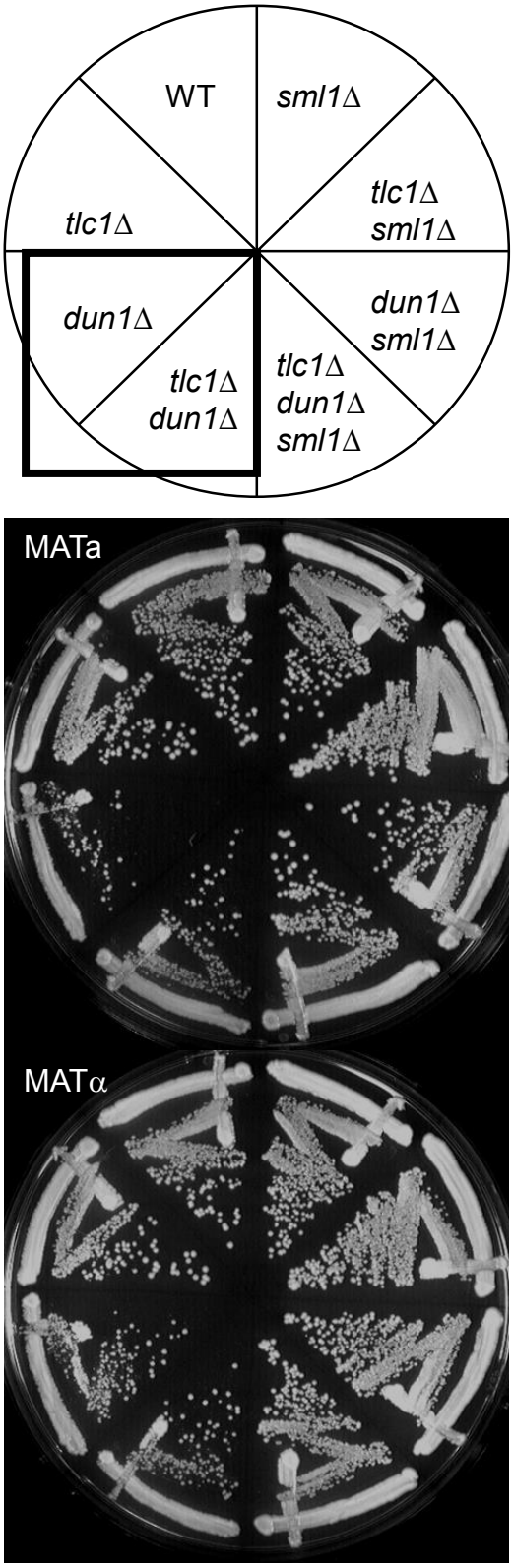
WT
sml1Δ
tlc1Δ sml1Δ
tlc1Δ
dun1Δ
dun1Δ sml1Δ
tlc1Δ dun1Δ
tlc1Δ dun1Δ sml1Δ
MATa
MATα

Figure 3-9

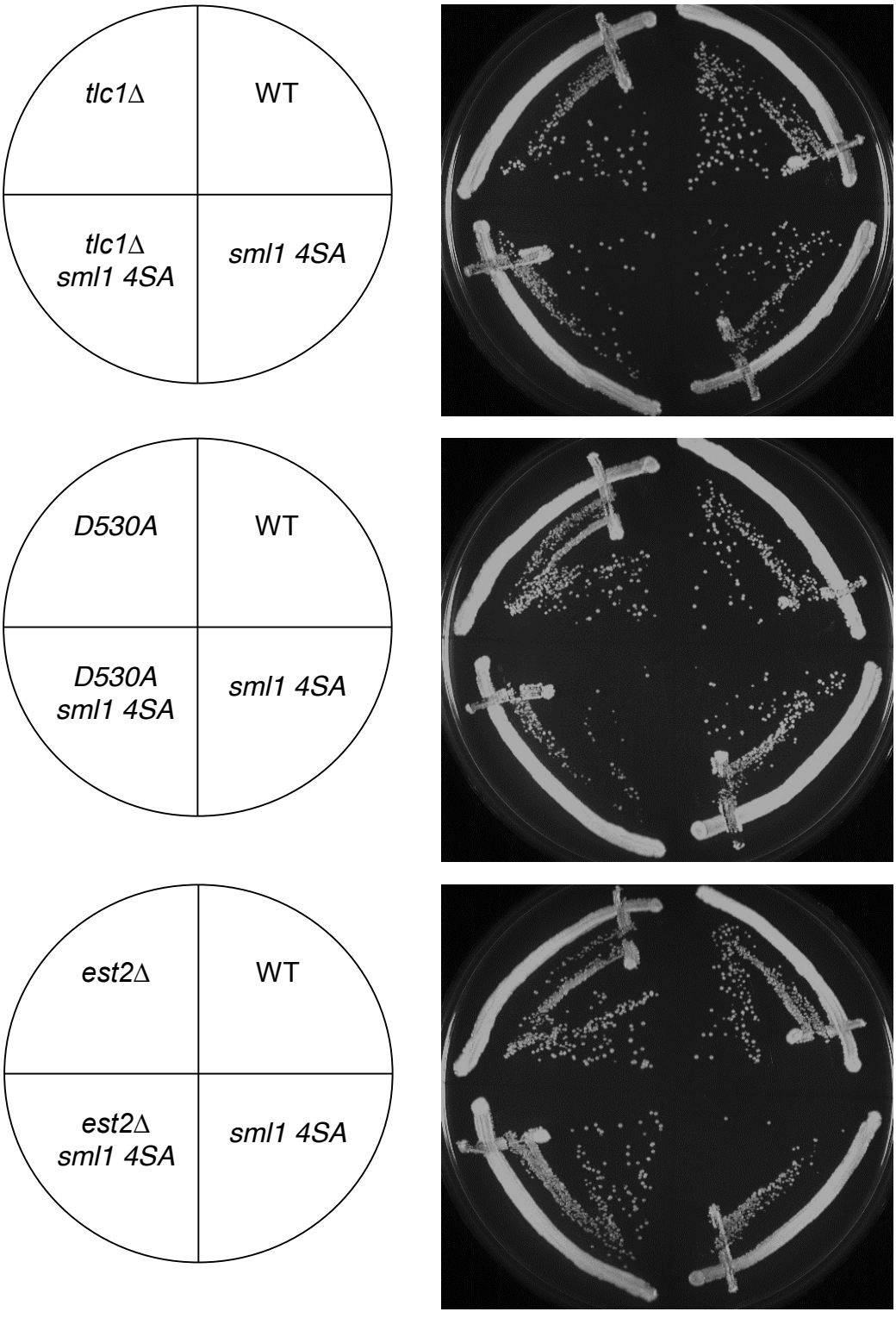
tlc1Δ
WT
tlc1Δ sml1 4SA
sml1 4SA
D530A
WT
D530A sml1 4SA
sml1 4SA
est2Δ
WT
est2Δ sml1 4SA
sml1 4SA

Figure 3-10

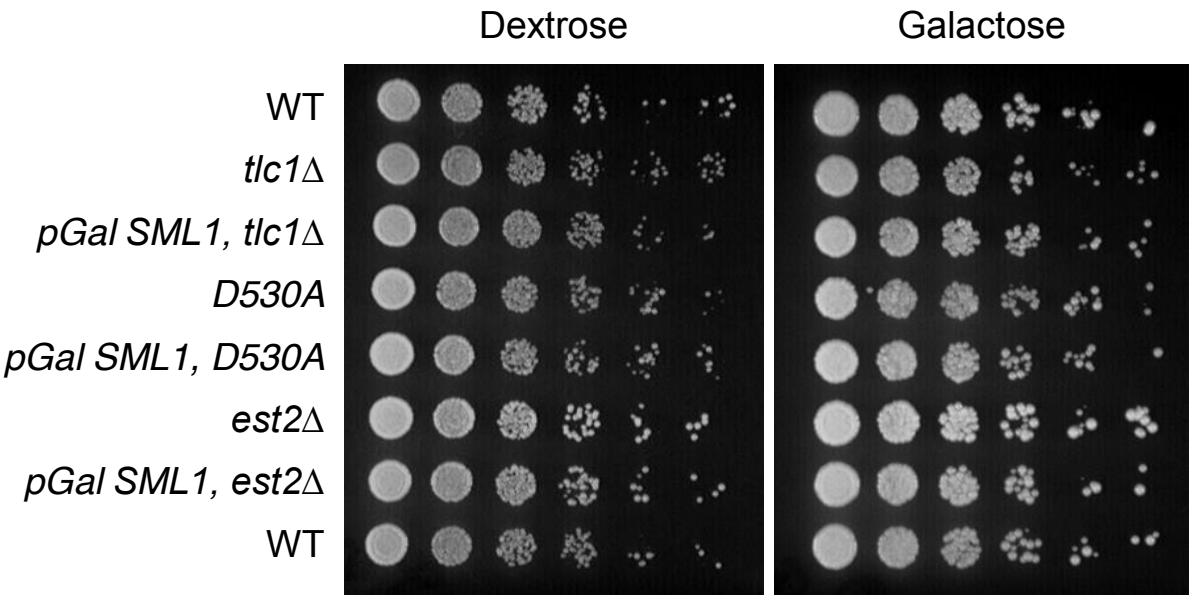
Dextrose
Galactose
WT
tlc1Δ
pGal SML1, tlc1Δ
D530A
pGal SML1, D530A
est2Δ
pGal SML1, est2Δ
WT

Figure 3-11

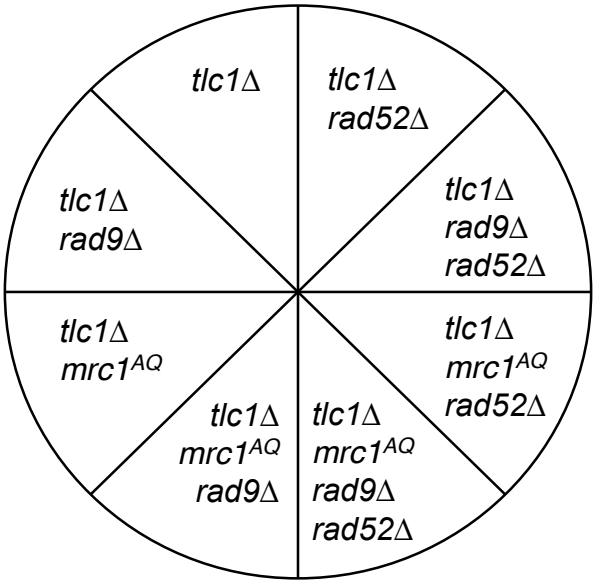
tlc1Δ
tlc1Δ rad52Δ
tlc1Δ rad9Δ rad52Δ
tlc1Δ mrc1AQ rad52Δ
tlc1Δ mrc1AQ rad9Δ rad52Δ
tlc1Δ mrc1AQ rad9Δ
tlc1Δ mrc1AQ
tlc1Δ rad9Δ

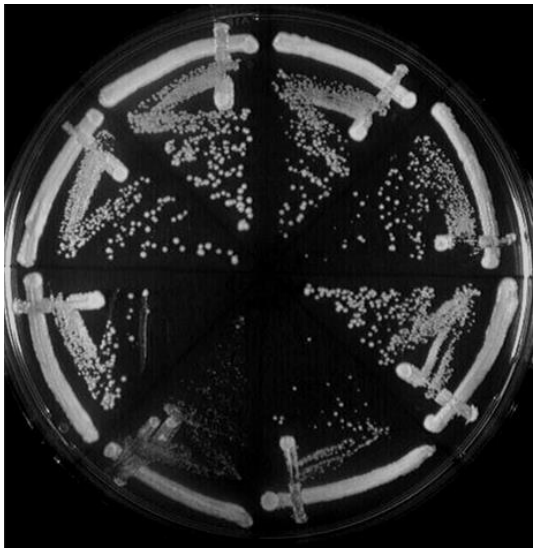

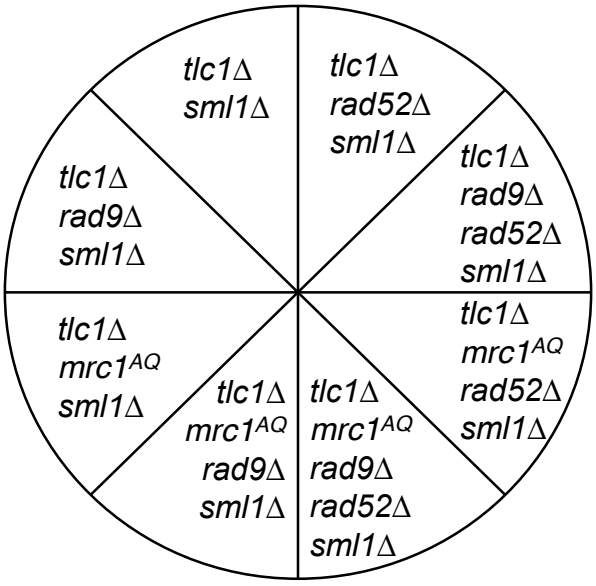
tlc1Δ sml1Δ
tlc1Δ rad52Δ sml1Δ
tlc1Δ rad9Δ rad52Δ sml1Δ
tlc1Δ mrc1AQ rad52Δ sml1Δ
tlc1Δ mrc1AQ rad9Δ rad52Δ sml1Δ
tlc1Δ mrc1AQ rad9Δ sml1Δ
tlc1Δ mrc1AQ sml1Δ
tlc1Δ rad9Δ sml1Δ

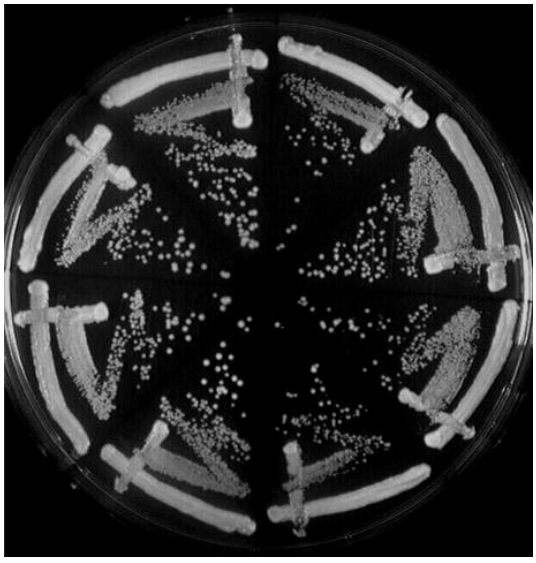

Figure 3-12

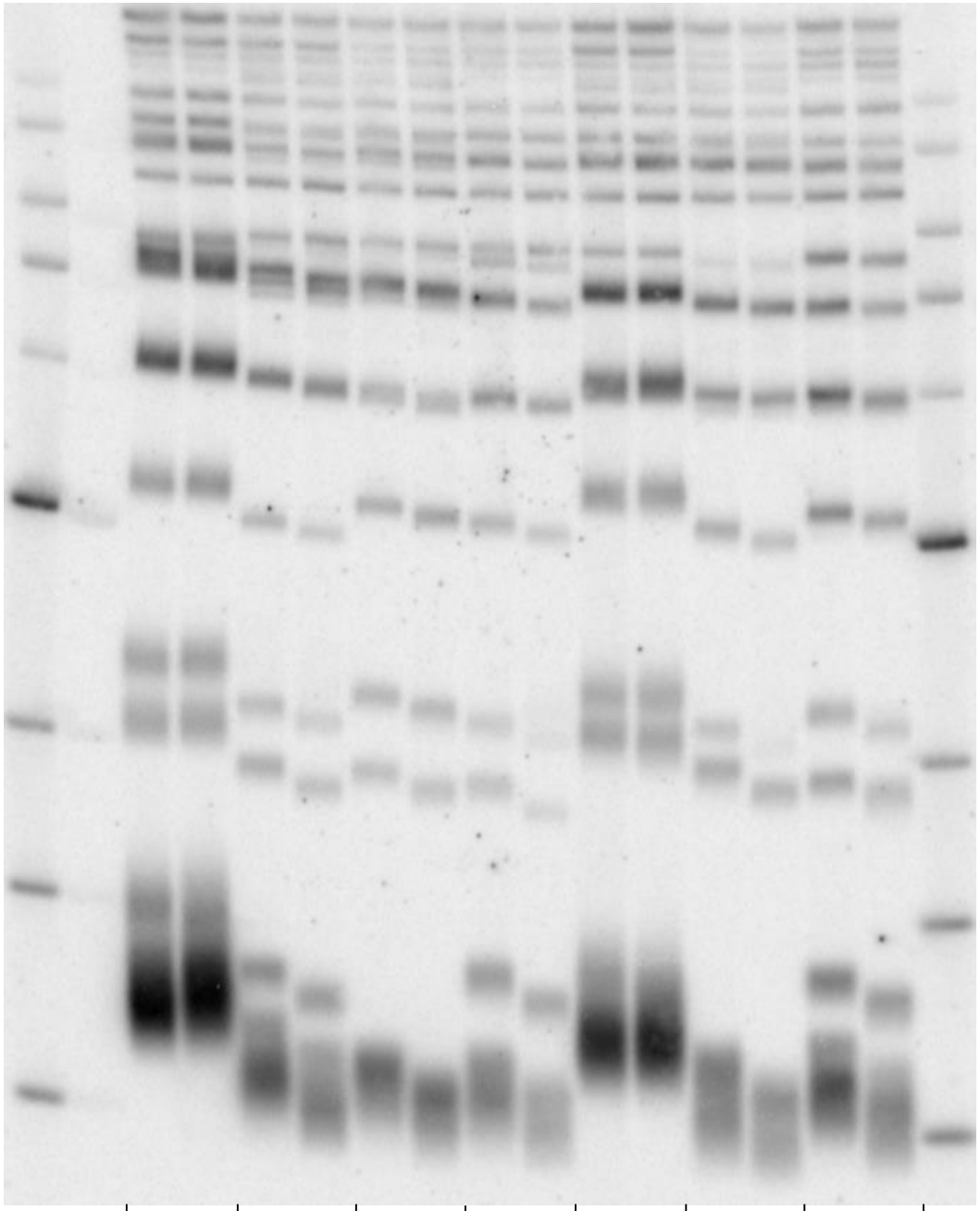
Passage
1 2
WT
1 2
tlc1Δ
1 2
tlc1Δ rad9Δ
1 2
tlc1Δ mrc1AQ
1 2
mrc1AQ rad9Δ
1 2
tlc1Δ mrc1AQ rad9Δ
1 2
tlc1Δ mrc1AQ rad9Δ sml1Δ

Figure 3-13

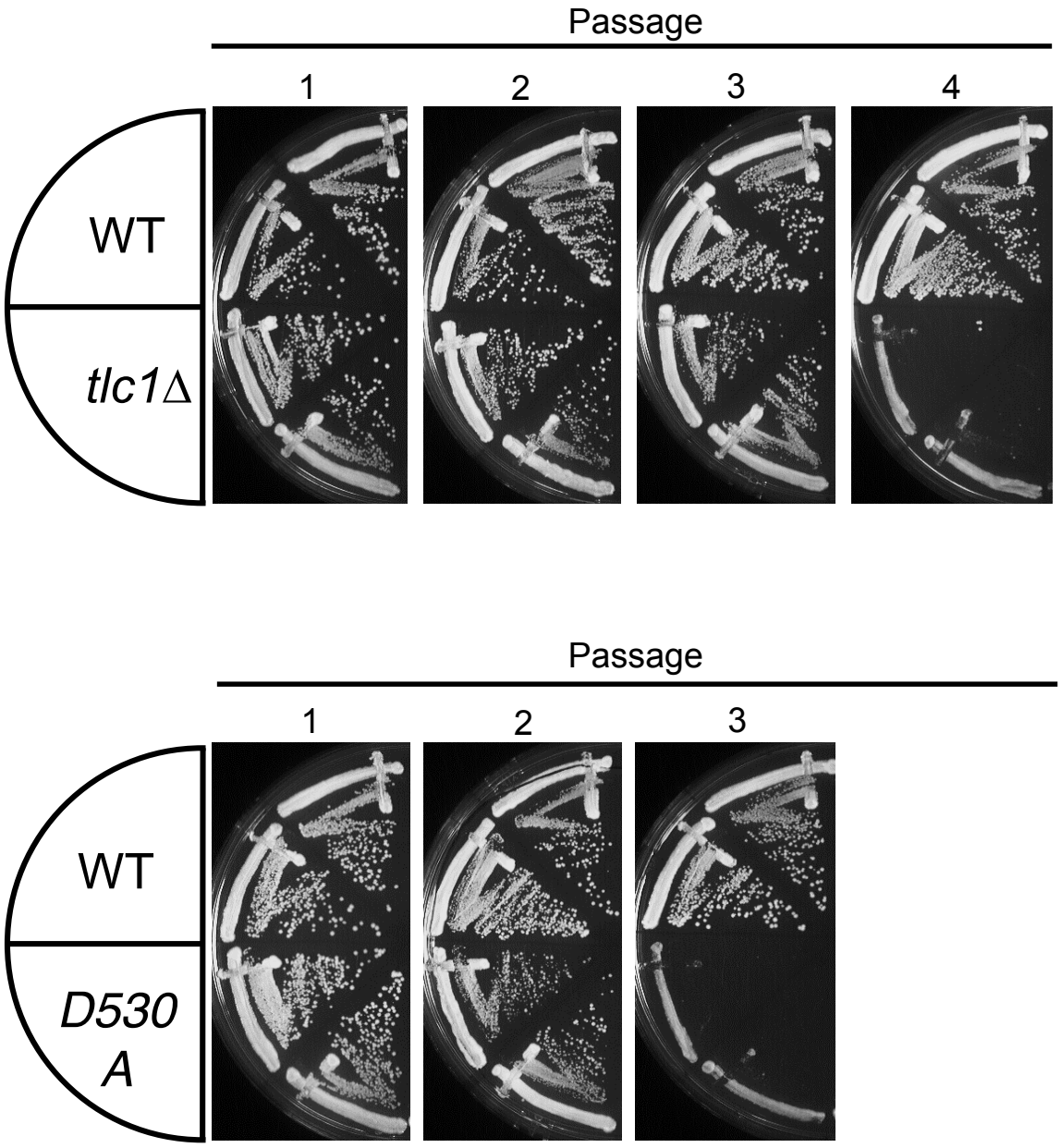

Figure 3-14

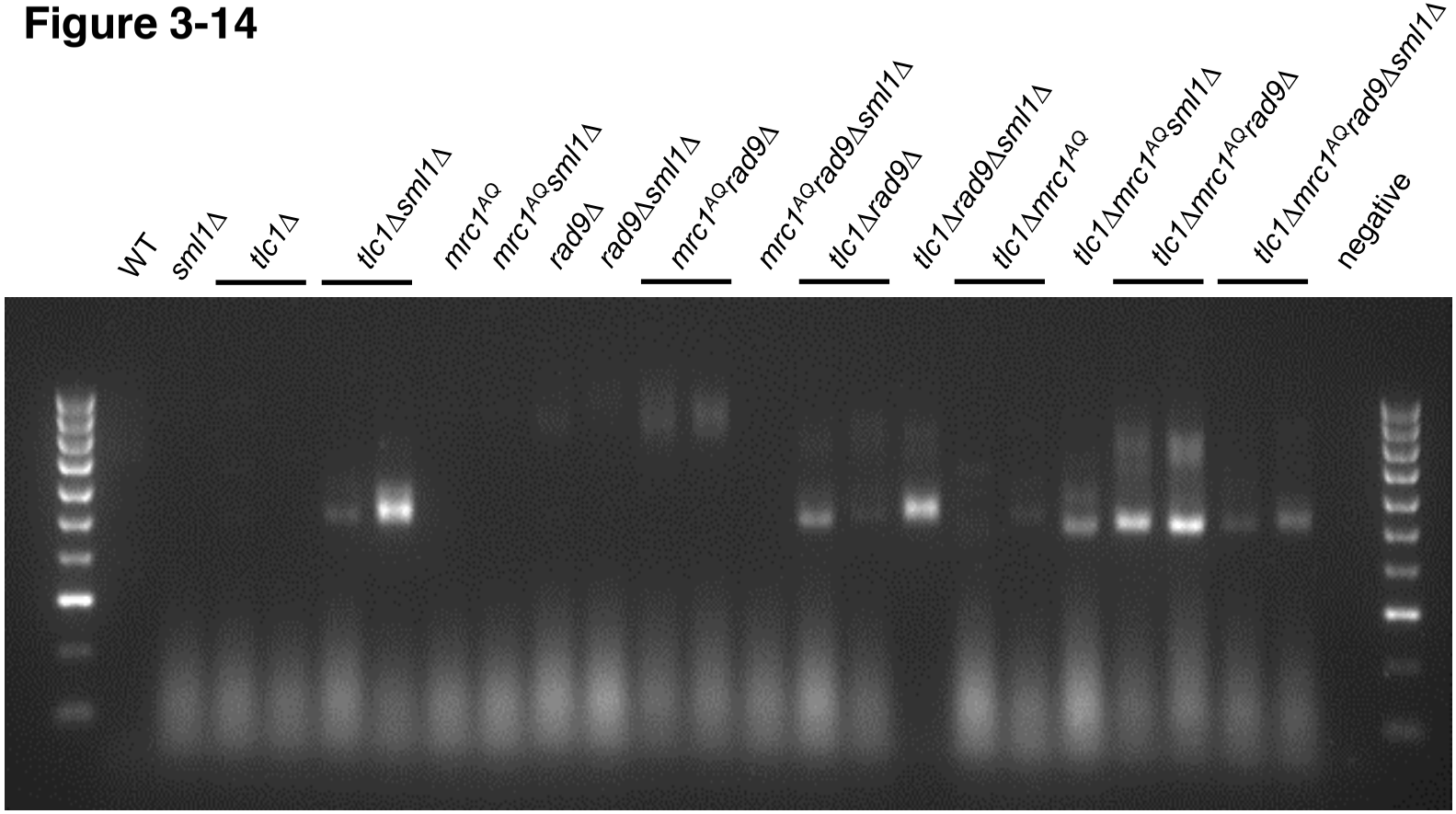
WT
sml1Δ
tlc1Δ
tlc1Δsml1Δ
mrc1AQ
mrc1AQsml1Δ
rad9Δ
rad9Δsml1Δ
mrc1AQrad9Δ
mrc1AQrad9Δsml1Δ
tlc1Δrad9Δ
tlc1Δrad9Δsml1Δ
tlc1Δmrc1AQ
tlc1Δmrc1AQsml1Δ
tlc1Δmrc1AQrad9Δ
tlc1Δmrc1AQrad9Δsml1Δ
negative

Chapter 4: Early Telomerase Inactivated Cells are Sensitive to Rapamycin and TOR Downregulation

Kyle Jay

Elizabeth Blackburn

Results

ETI Cells are Sensitive to Rapamycin Treatment

Given that the previously discussed phenotypes in *E*arly *T*elomerase *I*nactivated (ETI) cells were exacerbated by, or dependent on, mutation of the Mrc1 PIKK phosphorylation sites, it seemed reasonable to examine the potential effects of all PIKK kinases in *S. cerevisiae*. Aside from the Mec1 and Tel1 PIKK kinases (see chapter 3), yeast also possess TOR PIKK Kinases. These *T*arget *O*f *R*apamycin proteins, TOR1 and TOR2, play diverse roles in cellular regulation. TOR complex 1 (TORC1), which can contain either TOR1 or TOR2, has roles in cell metabolism, growth, and starvation responses, while TORC2, which can contain only TOR2, has a role in maintaining actin organization and cell wall integrity (Kupiec and Weisman, 2012; Loewith et al., 2002). The drug rapamycin forms a complex with the protein FKBP12, which then binds to and inhibits TORC1, but not TORC2 (Koltin et al., 1991; Loewith et al., 2002).

In order to determine if ETI cells relied on TORC1 function for viability, I treated ETI cells with rapamycin. Due to the role of TORC1 in cellular metabolism, rapamycin treatment produces effects reminiscent of starvation or caloric restriction, and individual yeast cells take several days longer to produce colonies. Rapamycin sensitivity, in the form of reduced colony formation relative to WT, was observed in ETI cells lacking either the telomerase RNA component (*tlc1*Δ) as well as in ETI cells lacking either of two telomerase accessory components, Est1 and Est3 (Figure 4-1), which are required for telomerase extension in vivo (Lingner et al., 1997). Therefore, ETI cells show reduced viability in the absence of a functional TORC1.

Rapamycin Sensitivity of Telomerase Deficient Strains Increases as Cells Approach Senescence

I repeated the rapamycin sensitivity assay using six independent ETI *tlc1*Δ isolates that had not been passaged to ensure a full, equilibrated telomere length before counter-selection of a TLC1-containing plasmid. I was surprised to find that these six ETI isolates displayed highly varying degrees of the rapamycin sensitivity observed previously (Figure 4-1, Figure 4-2A). I speculated that this may be due to heterogeneous telomere lengths among the otherwise isogenic isolates. Therefore, I passaged the six isolates on solid media and repeated the colony formation assay. I found that isolates that demonstrated sensitivity to Rapamycin on passage 1, were nearly fully senescent after passage 2 (Figure 4-2B). Likewise, isolates that did not display significant sensitivity in passage 1, showed sensitivity after a second passage (Figure 4-2B). This result implies that the sensitivity of cells lacking telomerase to

rapamycin treatment increases as cells approach senescence (as ETI cells become LTI cells), and may reflect an inverse correlation with telomere length.

ETI Cells are Sensitive to Downregulation of Both Tor1 and Tor2

In order to further discriminate the requirement of ETI cells for TOR signaling, I choose to individually downregulate TOR1 and TOR2 via a repressible galactose promoter (pGal). During growth on dextrose, the pGal:TOR promoter will drastically lower the levels of TOR1 or TOR2 protein, while overexpressing them during growth on galactose. Despite TOR2 being an essential gene, the pGal promoter was found to be leaky enough to allow growth in a pGal:TOR2 strain on dextrose media. Both TOR complexes are essential, but the TOR1 protein is not essential as either TOR1 or TOR2 can be included in TORC1 (Loewith et al., 2002). Various ETI mutations that were tested all showed a mild, reproducible sensitivity to downregulation of TOR1 (Figure 4-3) and TOR2 (Figure 4-4). In addition, when the TOR1/2 proteins were overexpressed in pGal:TOR1/2 strains grown on galactose, I observed a protection from rapamycin treatment. However, this protective effect was completely negated in the presence of ETI mutations (Figure 4-5). Therefore, both TOR1 and TOR2 proteins are required for full viability in ETI cells and ETI mutations may, to some unknown degree, hinder the action of TOR signaling pathways.

As rapamycin inhibits only TOR complex 1 and both TOR1 and TOR2 can be present in TORC1, I sought to determine whether or not TORC2 function was also important for full viability in ETI cells. In order to determine the relevant importance of the two

complexes, I used the galactose promoter system to regulate expression of several complex specific components. Kog1 is an exclusive component of TORC1, Avo3 is an exclusive component of TORC2, and Lst8 is a component of both complexes. Unfortunately, unlike the case of TOR2, the gal regulation of these essential genes resulted in inviable strains when grown on dextrose (Figure 4-6). Therefore I was unable to explicitly determine a role for TORC2 in ETI cell viability, and it cannot be excluded that the sensitivity resulting from TOR2 downregulation was completely due to its role in TORC1.

Unlike Previous ETI Phenotypes, Rapamycin Sensitivity was Not Rescued by Sml1 Deletion

Nearly all previously discussed ETI phenotypes were alleviated by Sml1 deletion and were hypothesized to be the result of telomeric DNA replication stress. Therefore, I questioned whether or not the ETI sensitivity to rapamycin would also be suppressed by Sml1 deletion. I treated both ETI and ETI *sml1*Δ strains with rapacmyicn and compared their colony formation phenotype. I found that the addition of the *sml1*Δ mutation had no visible effect on the rapamycin sensitivity phenotype (Figure 4-7).

Discussion

The data presented here show that ETI cells display a mild but reproducible sensitivity to TOR inhibition by either chemical or genetic means: rapamycin treatment (Figure 4-1) and TOR downregulation (Figure 4-3, 4-4), respectively. This sensitivity progressively increased as cells lacking telomerase were passaged (Figure 4-2), implying the

possibility of a telomere length-dependence, unlike what has been seen for other ETI phenotypes. In addition, the lack of an effect of the *sml1*Δ mutation on these TOR phenotypes (Figure 4-7) implies that it is caused by a different mechanism than the previously reported ETI phenotypes (Chapters 2 and 3).

As the sensitivity to rapamycin seemed to be progressive, it is also possible that the phenotype is based on an accumulation of DNA damage as cells approach senescence. This is consistent with work which has shown TOR signaling is required for viability of yeast in response to genotoxic stress and DNA damaging agents (Shen et al., 2007). However, I do not favor this hypothesis as the deletion of Sml1 has also been shown to be protective against DNA damage (Chabes et al., 2003), and the *sml1*Δ mutation had no visible effect on the rapamycin sensitivity of ETI cells. TORC1 inhibition by rapamycin has also been shown to reduce telomere length by lowering the levels of the heterodimeric Ku protein (Ungar et al., 2011). The *Ku*Δ mutations result in a short and stable telomere phenotype (Porter et al., 1996) and have been shown to be synthetically lethal with telomerase mutations (Nugent et al., 1998). It would be of value to determine in future experiments whether or not over-expression of Ku protein can suppress the ETI sensitivity to TOR downregulation. If this Ku overexpression restored telomere lengths to near WT levels and ETI cells were still sensitive to TOR downregulation under these conditions, this would imply a telomere length-independent need for TOR signaling in ETI cells.

Taken together, these results suggest that what we observe as rapamycin sensitivity may be accelerated senescence resulting from the simultaneous shortening of telomeres by rapamycin and by the lack of telomerase. To determine this, future experiments would need to more closely examine the telomere lengths of ETI cells grown in the presence of rapamycin or with reduced levels of TOR proteins. However, this simple explanation based on telomere length does not seem to explain why overexpression of TOR proteins was protective against rapamycin in WT cells but not in ETI cells. More analysis of the effects of TOR overexpression and repression via the galactose promoter on telomere length would also be enlightening in this case. Though the exact nature of this interaction remains unknown, it is exciting that novel connections are being discovered between telomere length maintenance pathways and the cell's metabolic regulation through TOR signaling.

References

Chabes, A., Georgieva, B., Domkin, V., Zhao, X., Rothstein, R., and Thelander, L. (2003). Survival of DNA damage in yeast directly depends on increased dNTP levels allowed by relaxed feedback inhibition of ribonucleotide reductase. Cell *112*, 391–401.

Koltin, Y., Faucette, L., Bergsma, D.J., Levy, M.A., Cafferkey, R., Koser, P.L., Johnson, R.K., and Livi, G.P. (1991). Rapamycin sensitivity in Saccharomyces cerevisiae is mediated by a peptidyl-prolyl cis-trans isomerase related to human FK506-binding protein. Mol. Cell. Biol. *11*, 1718–1723.

Kupiec, M., and Weisman, R. (2012). TOR links starvation responses to telomere length maintenance. Cell Cycle Georget. Tex *11*, 2268–2271.

Lingner, J., Cech, T.R., Hughes, T.R., and Lundblad, V. (1997). Three Ever Shorter Telomere (EST) genes are dispensable for in vitro yeast telomerase activity. Proc. Natl. Acad. Sci. U. S. A. *94*, 11190–11195.

Loewith, R., Jacinto, E., Wullschleger, S., Lorberg, A., Crespo, J.L., Bonenfant, D., Oppliger, W., Jenoe, P., and Hall, M.N. (2002). Two TOR complexes, only one of which is rapamycin sensitive, have distinct roles in cell growth control. Mol. Cell *10*, 457–468.

Nugent, C.I., Bosco, G., Ross, L.O., Evans, S.K., Salinger, A.P., Moore, J.K., Haber, J.E., and Lundblad, V. (1998). Telomere maintenance is dependent on activities required for end repair of double-strand breaks. Curr. Biol. CB *8*, 657–660.

Porter, S.E., Greenwell, P.W., Ritchie, K.B., and Petes, T.D. (1996). The DNA-binding protein Hdf1p (a putative Ku homologue) is required for maintaining normal telomere length in Saccharomyces cerevisiae. Nucleic Acids Res. *24*, 582–585.

Shen, C., Lancaster, C.S., Shi, B., Guo, H., Thimmaiah, P., and Bjornsti, M.-A. (2007). TOR signaling is a determinant of cell survival in response to DNA damage. Mol. Cell. Biol. *27*, 7007–7017.

Ungar, L., Harari, Y., Toren, A., and Kupiec, M. (2011). Tor complex 1 controls telomere length by affecting the level of Ku. Curr. Biol. CB *21*, 2115–2120.

Figure Legends

Figure 4-1. ETI Cells are Sensitive to Rapamycin Treatment

Serial dilutions of WT and various ETI strains (*tlc1*Δ, *est1*Δ, *est3*Δ) were plated on dextrose solid media with or without rapamycin. ETI cells displayed sensitivity to the drug relative to WT. Plates were incubated at 30°C: No Drug plate (2 days), Rap plate (5 days). ETI cells obtained from counter-selection of covering plasmids from haploid mutant cells.

Figure 4-2. ETI Sensitivity to Rapamycin Treatment is Progressive

Six independent ETI *tlc1*Δ isolates were serially diluted and plated on solid dextrose media with or without rapamycin. Sensitivity to rapamycin increased from passage 1 to passage 2, and rapamycin sensitivity during passage 1 predicted viability in passage 2. Plates were incubated at 30°C: No Drug plates (2 days), Rapamycin plates (6 days). ETI cells obtained from counter-selection of covering plasmids from haploid mutant cells.

Figure 4-3. ETI Cells are Sensitive to Genetic Repression of TOR1

ETI cells (*tlc1*Δ, *est2D530A*) with or without the TOR1 gene under a galactose promoter were serially diluted and plated on galactose (overexpression) or dextrose (repression). ETI cells showed a mild but reproducible sensitivity to TOR1 repression compared to ETI mutation or TOR1 repression alone. Plates were incubated at 30°C: Galactose

plates (3 days), Dextrose plates (2 days). Strains were obtained from sporulation of diploids heterozygous for relevant mutations.

Figure 4-4. ETI Cells are Sensitive to Genetic Repression of TOR2

As in Figure 4-3, but TOR2 was placed under galactose promoter control in place of TOR1. ETI cells (*tlc1*∆, *est2D530A*, *est2*∆) showed sensitivity to genetic repression of TOR2. Plates were incubated at 30°C: Galactose plates (2-3 days), Dextrose plates (2 days). Strains were obtained from sporulation of diploids heterozygous for relevant mutations.

Figure 4-5. ETI Mutations Negate Resistance to Rapamycin Provided by TOR1/2 Overexpression

ETI cells (*tlc1*∆, *est2D530A*) with or without TOR1/2 under galactose promoter control were plated onto rapamycin plates containing either galactose or dextrose. Overexpression of TOR1/2 on galactose media provided a protective effect against rapamycin. This effect was negated by the addition of ETI mutations. Plates were incubated at 30°C: Galactose + Rap plates (5,7 days), Dextrose + Rap plates (5 days). Strains were obtained from sporulation of diploids heterozygous for relevant mutations.

Figure 4-6. Strains Become Inviable When Kog1, Avo3, or Lst8 are Placed Under Galactose Promoter Control

Essential genes Kog1, Avo3, and Lst8 were put under the galactose promoter to discriminate between TORC1 and TORC2. However, unlike essential gene TOR2,

genetic repression of these three genes produced inviable strains regardless of whether or not they were combined with ETI (*tlc1*Δ) mutations. Plates were incubated at 30°C: No Drug plate (2 days), Rap plate (5 days). Strains were obtained from sporulation of diploids heterozygous for relevant mutations.

Figure 4-7. Deletion of Sml1 had No Effect on ETI Rapamycin Sensitivity

ETI cells (*tlc1*Δ, *est2D530A*) with or without the *sml1*Δ mutation were serially diluted and plated onto solid dextrose media with or without rapamycin. Addition of the *sml1*Δ mutation had no effect on the ETI sensitivity to rapamycin. Plates were incubated at 30°C: No Drug plate (2 days), Rap plate (5 days). Strains were obtained from sporulation of diploids heterozygous for relevant mutations.

Figure 4-1

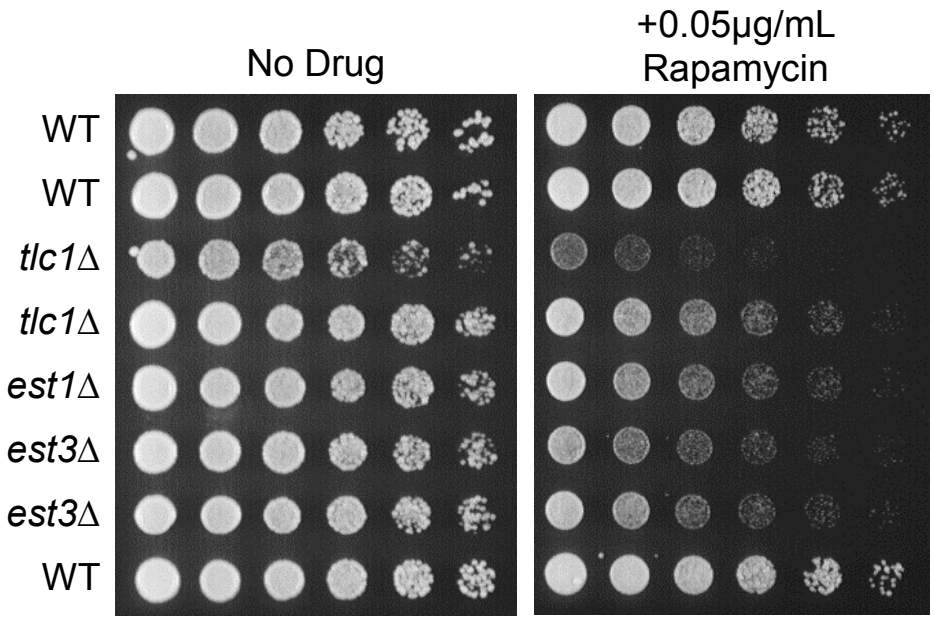
No Drug
+0.05µg/mL
Rapamycin
WT
WT
tlc1Δ
tlc1Δ
est1Δ
est3Δ
est3Δ
WT

Figure 4-2

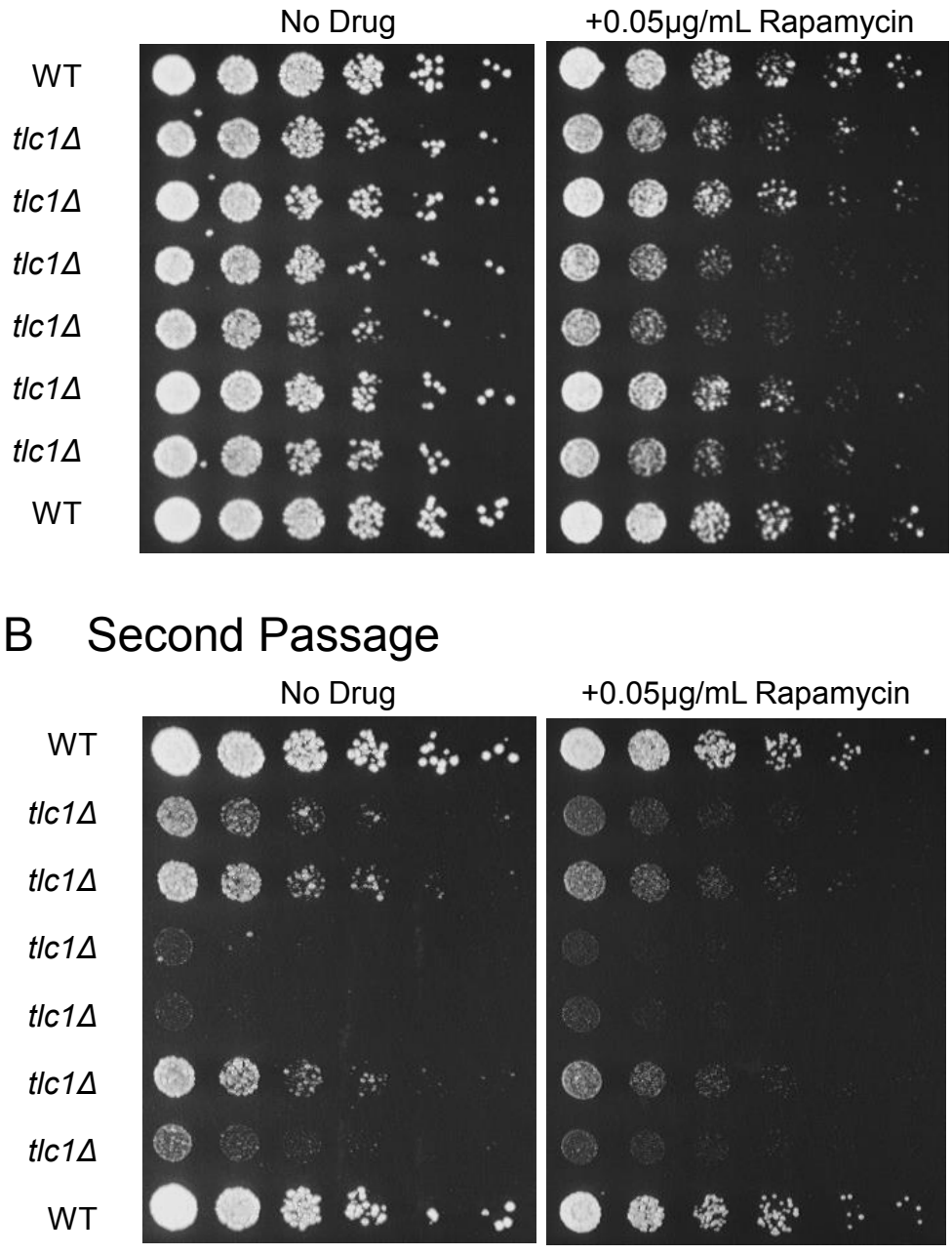
A First Passage
No Drug
+0.05µg/mL Rapamycin
WT
tlc1Δ
tlc1Δ
tlc1Δ
tlc1Δ
tlc1Δ
tlc1Δ
WT
B Second Passage
No Drug
+0.05µg/mL Rapamycin
WT
tlc1Δ
tlc1Δ
tlc1Δ
tlc1Δ
tlc1Δ
tlc1Δ
WT

Figure 4-3

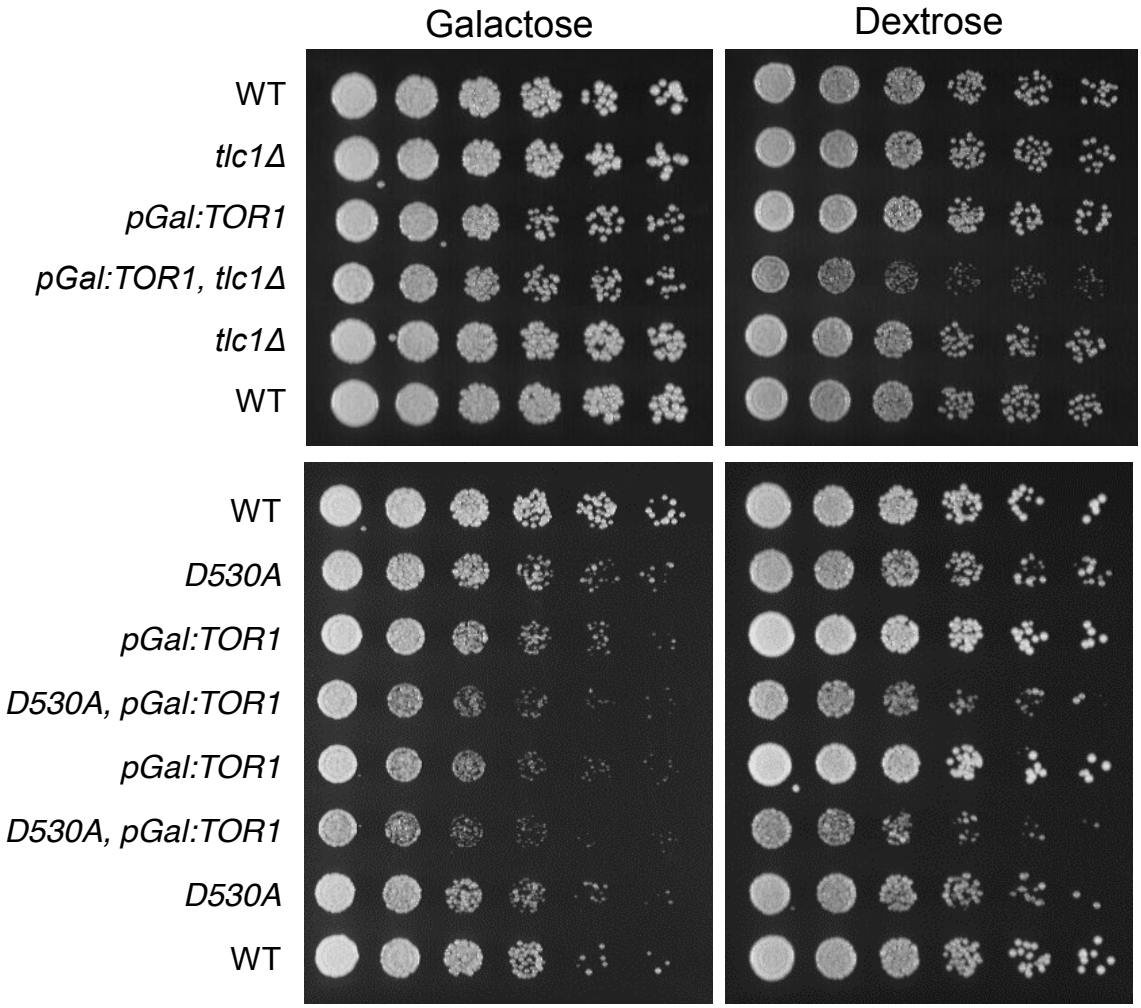
Galactose
Dextrose
WT
tlc1Δ
pGal:TOR1
pGal:TOR1, tlc1Δ
tlc1Δ
WT
WT
D530A
pGal:TOR1
D530A, pGal:TOR1
pGal:TOR1
D530A, pGal:TOR1
D530A
WT

Figure 4-4

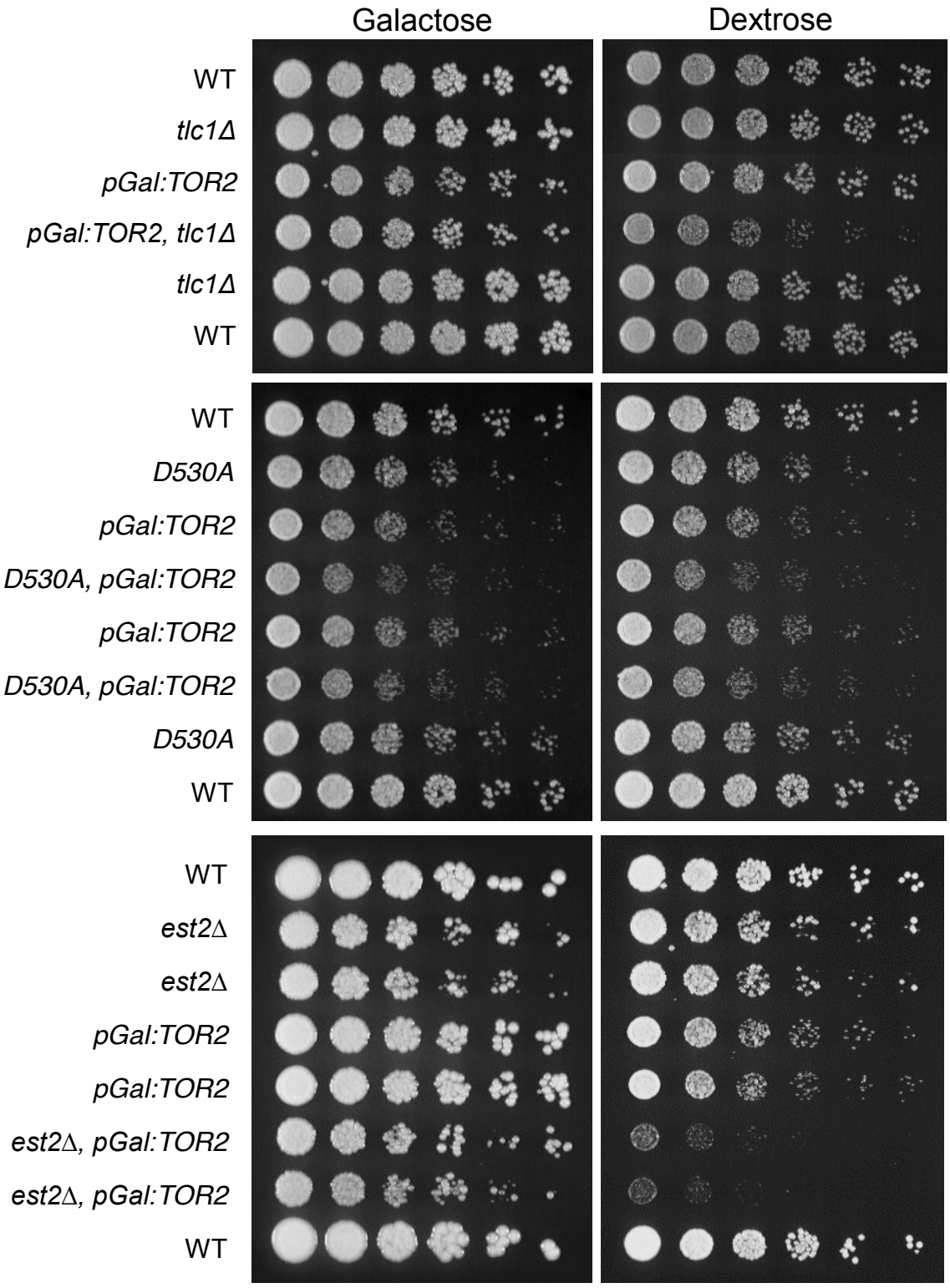
Galactose
Dextrose
WT
tlc1Δ
pGal:TOR2
pGal:TOR2, tlc1Δ
tlc1Δ
WT
WT
D530A
pGal:TOR2
D530A, pGal:TOR2
pGal:TOR2
D530A, pGal:TOR2
D530A
WT
WT
est2Δ
est2Δ
pGal:TOR2
pGal:TOR2
est2Δ, pGal:TOR2
est2Δ, pGal:TOR2
WT

Figure 4-5

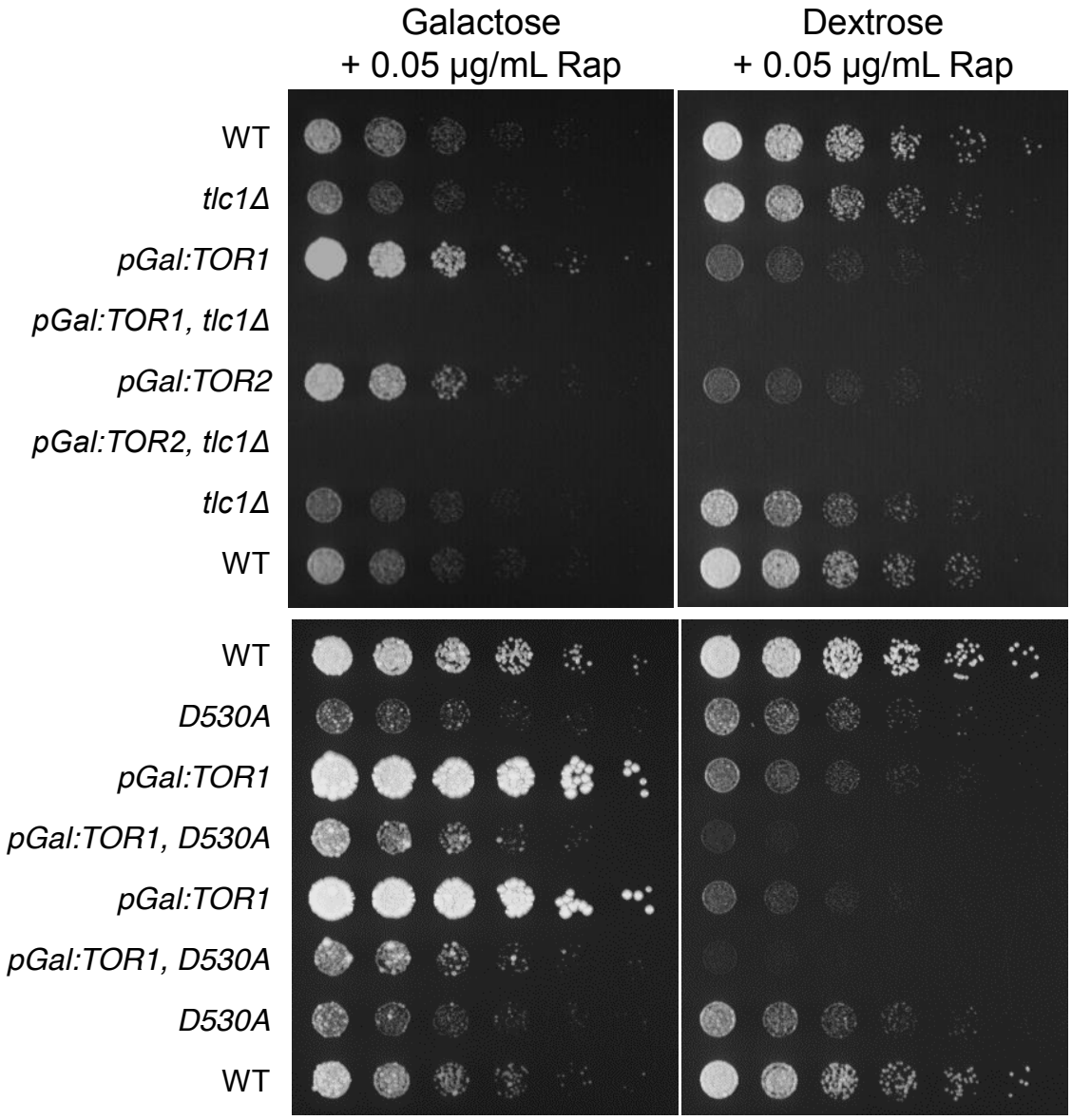
Galactose
+ 0.05 µg/mL Rap
Dextrose
+ 0.05 µg/mL Rap
WT
tlc1Δ
pGal:TOR1
pGal:TOR1, tlc1Δ
pGal:TOR2
pGal:TOR2, tlc1Δ
tlc1Δ
WT
WT
D530A
pGal:TOR1
pGal:TOR1, D530A
pGal:TOR1
pGal:TOR1, D530A
D530A
WT

Figure 4-6

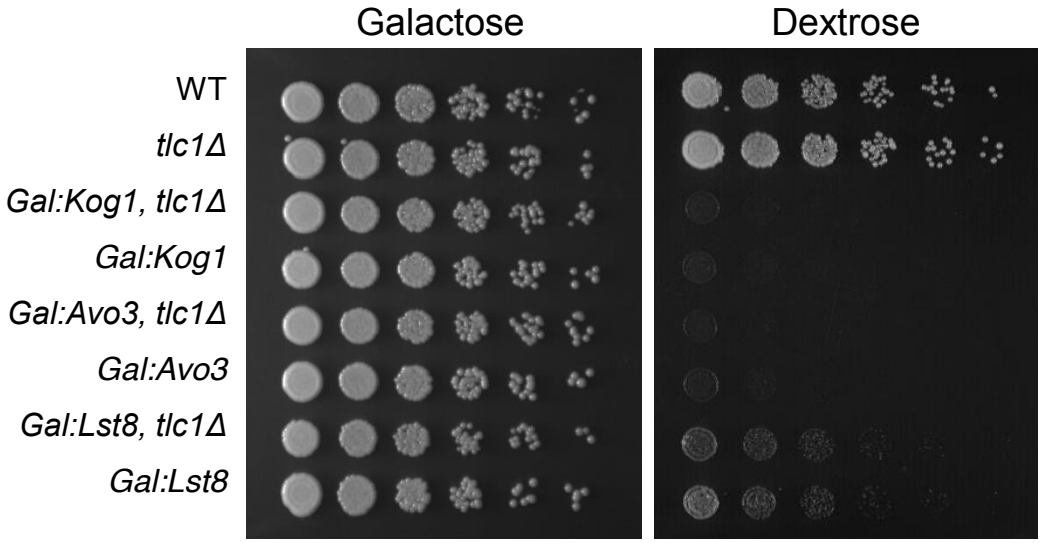
Galactose
Dextrose
WT
tlc1Δ
Gal:Kog1, tlc1Δ
Gal:Kog1
Gal:Avo3, tlc1Δ
Gal:Avo3
Gal:Lst8, tlc1Δ
Gal:Lst8

Figure 4-7

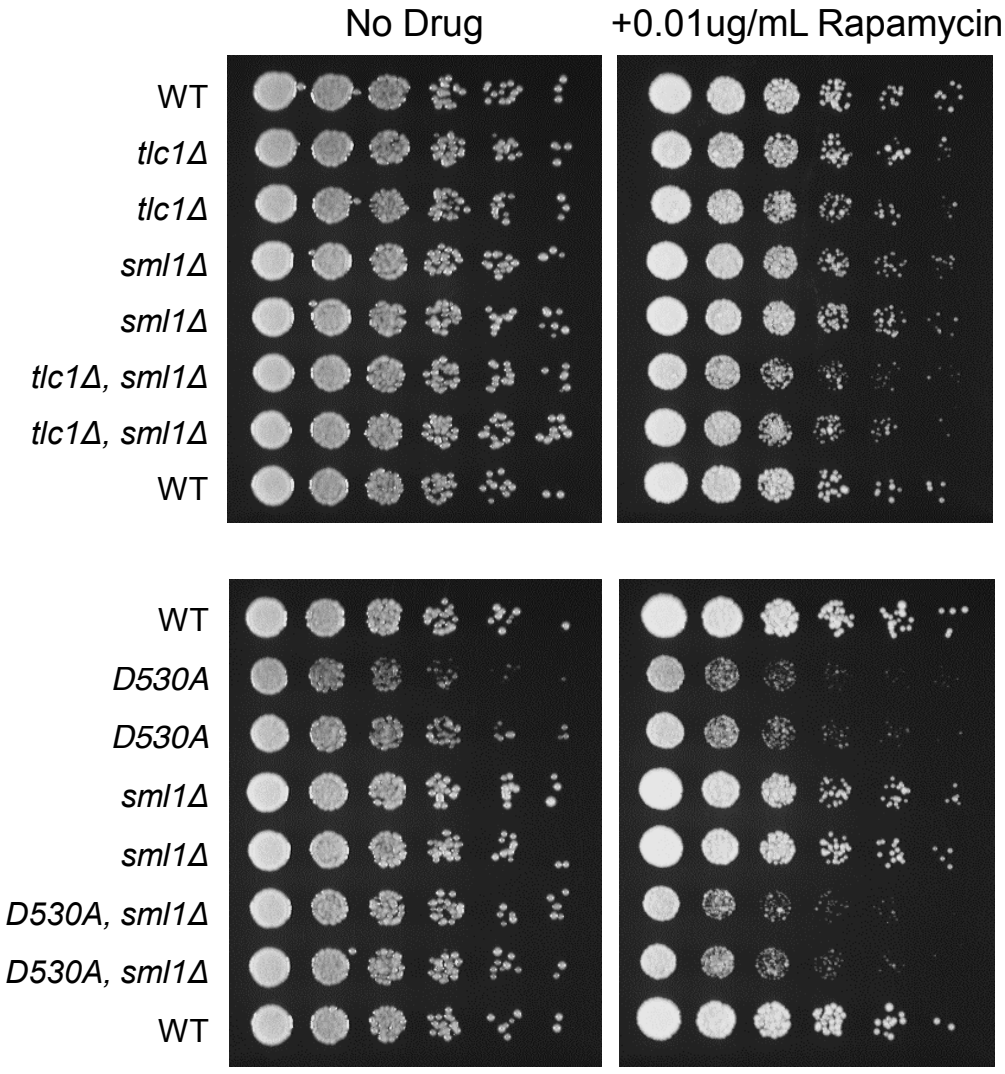
No Drug
+0.01ug/mL Rapamycin
WT
tlc1Δ
tlc1Δ
sml1Δ
sml1Δ
tlc1Δ, sml1Δ
tlc1Δ, sml1Δ
WT
WT
D530A
D530A
sml1Δ
sml1Δ
D530A, sml1Δ
D530A, sml1Δ
WT

Materials and Methods

Yeast Strain Construction

All strains used in this thesis are listed in Appendix 1. Plasmid and oligo sequences are available upon request. Strain background was W303 or S288C (and isogenic with BY4736, Chan and Blackburn, 2003) as indicated. Diploids were isolated on selective media with subsequent sporulation on TSPO plates (W303), by double auxotrophy selection, or by visual isolation of zygotes after 5 hours of mating and liquid sporulation (S288C). Complete disruption of ORFs was carried out by using PCR-mediated gene disruption (Rose, M. D. et al., 1990). Disruption cassettes for *NAT* or *HYGMX4* are as described (Sambrook J and Russel D. W., 2001). Galactose promoter regulation was performed using PCR-mediated insertion of the promoter upstream of the desired coding sequence as described (Longtine et al., 1998). RNR1 overexpression was accomplished by PCR-mediated insertion of the pTEF promoter upstream of the RNR1 coding sequence. Overexpression was verified via quantitative RT PCR. Altered telomerase genes were covered with pRS CEN/ARS plasmids containing either the wild type *TLC1* or *EST2* with endogenous promoters and terminators, and sequence verified.

All *mrc1*^{AQ} strains in the 3,000 series were made by first deleting MRC1, and then pRS403-*mrc1*^{AQ} was digested with BspEI and integrated into the *mrc1*Δ strain at the endogenous *MRC1* promoter. The *MRC1* gene including 600 and

400bp of upstream and downstream regions, respectively, was PCR amplified and cloned into pRS403 using SalI and BamHI cloning sites to yield pEHB3201. pEHB3201 was used to construct pEHB3202, a plasmid bearing the *mrc1*^{AQ} allele (Osborn and Elledge, 2003), cloned into pRS403. SQ and TQ motifs on the N terminus of the gene were mutated to AQ by assembly of an ~900bp gene fragment from oligonucleotides and cloning of the fragment into pEHB3201 digested with SacI and EcoRI. SQ and TQ motifs in the central and C-terminal portions of the gene were mutated to AQ using an overlap extension PCR strategy (Sambrook J and Russel D. W., 2001). All *mrc1*^{AQ} strains in the 30,000 series were made by cloning the *mrc1*^{AQ}-containing SalI-BamHI fragment of pRS403-*mrc1*^{AQ} into pRS406. pRS406-*mrc1*^{AQ} was digested with BspEI and integrated into WT strain 3056. 5-FOA selection was used to select for loop-outs, and strains in which *MRC1* was fully replaced by *mrc1* ^{AQ} were identified by PCR analysis.

Growth of Mutants for Monitoring Early Loss of Telomerase

Early Telomerase Inactivated (ETI) are defined as cells without telomerase for approximately 25-30 generations and were produced by two methods: sporulation of diploid heterozygote strains (*tlc1*Δ/*TLC1, est2D530A*/*EST2*), or by loss of a covering plasmid in a haploid telomerase-deficient background strain struck on solid media. Diploid strains were passaged 3-5 times (depending on genotype) to equilibrate telomere lengths before sporulation. Fully grown spore colonies (2 days of growth at 30˚C) contain cells that have been without

telomerase for approximately 20 generations. Cells derived from these original spore colonies, or telomerase-negative colonies after plasmid loss, were passaged (10-20 additional generations via patching, streaking, or growth in liquid culture) and are referred to as "passage 1” cells.

Because populations of cells lacking telomerase action on telomeres will eventually undergo senescence after 50-80 cell divisions, when the telomeres have become critically shortened, we performed most of our analyses at 25-30 generations after genetic removal of active telomerase when telomeres were still relatively long, well before senescence of the bulk cell population. We confirmed that these ETI cells grew healthily by the following criteria: cell and colony morphologies were wild type, 95% of the cells entered a budding cycle following release from an alpha-factor arrest and continued growing through at least the next full cell cycle, and there was no detectable Rad53 or Mrc1 phosphorylation, which normally only become detectable later after telomerase loss, at the onset of senescence of the cell population

Bulk Population Budding and Chromosome Segregation Assays

For bulk budding and chromosome segregation time courses, yeast cultures were grown at 30°C with shaking at 225rpm. All synchronized cell cycle experiments were carried out by arresting cells in 1mg/mL of alpha-factor (PAN Facility, Stanford) for 4 hours (W303) or in 5mg/mL for 2.5 hours (S288C). After arrest, cells were washed twice with 50mL of pre-warmed YPD (30°C), and

released into 25mL of pre-warmed YPD plus 1.5μg/mL nocodazole (Sigma). For chromosome segregation assays, 1mL samples were collected every 15 minutes and held on ice until the end of a time course. To fix cells, harvested samples were pelleted and resuspended in 100mL of 4% paraformaldehyde, 3.4% sucrose at room temperature for 15 minutes. For cell cycle profiling, samples were taken every 15 minutes and cells were immediately fixed by adding 0.3mL of culture to 0.7mL of 100% ethanol. Cells were washed once in 1mL of 0.1M potassium phosphate, 1.2M sorbitol buffer and resuspended in the same buffer. Cells were sonicated before microscopy. Only cells that responded to alpha-factor were scored for budding morphology, spindle length, or chromosome segregation.

For chromosome segregation and spindle-elongation assays, the W303 background was used. Chromosome IV was marked as described previously (Lin et al., 2004) 12kb from the centromere with 256 tandem repeats of the lactose repressor operator sequence. $CuSO_4$ was added to a final concentration of 0.25mM to induce expression of green fluorescent protein (GFP)-LacI fusion. Spindle measurement was made through visualization of GFP-Tub1 or with tubulin antibody. Indirect immunofluorescence was carried out as described previously (Rose, M. D. et al., 1990). 4-6-Diamidino-2-phenylindole was obtained from Molecular Probes (Eugene, OR) and used at 1mg/mL final concentration. Rat anti-tubulin antibodies were obtained from Accurate Chemical & Scientific

(Westbury, NY) and used at a 1:1000 dilution. In all microscopy experiments, at least three sets of 100 cells for each time point were counted.

Microfluidics Technique Analyses of Mother Cells

Mother cells were continuously monitored for two days by repeated microscopic imaging (Xie et al., 2012; Zhang et al., 2012). The microfluidic device contains a set of microposts (side length in the range 40~100μm, depth of the chamber in the range 3.8~4.2μm) that clamp mother cells in place while the newly formed daughter cells are washed away by hydrodynamically-controlled flow of the surrounding liquid medium. Using such a device, both cell cycle/budding kinetics and morphological and other characteristics of cell death/budding cessation of mother cells can be simultaneously monitored in multiple individual cells, using time-lapse microscopy at high temporal resolution. Since these cells are taken from logarithmically growing cell populations, nearly all cells are newborn or very young mother cells, which are ~2 generations old on average, as described in (Zhang et al., 2012), at the onset of each time course analysis. Thus, the lifespan of wild type cells determined by our method is slightly shorter than that obtained by traditional micro-dissection (22.1 vs. 25). The cell cycle durations analyzed in the work exclude the first cycles observed after the cells are placed in the microfluidics device, because some of these mother cells will be part-way through a budding cycle at the start of the monitoring period. Also excluded from the analyses are the terminal two mother cell budding cycles (those just before the mother cells cease budding permanently), because even in wild type strains,

these last two cycles are typically of long duration and highly heterogeneous. Analyses of the duration times of just these last two heterogeneous cycles showed no significant differences in duration between different genotypes (data not shown).

Southern Blotting Analysis of Telomere Length

Genomic DNA was prepared from cells collected from the densest portion of serial streaks on solid media after the indicated number of passages. Genomic DNA was then digested with XhoI and run on 0.8% agarose gels alongside NEB 1kb DNA ladder. DNA was transferred from the gels to Hybond N+ membranes and probed with γ^{32}P end-labeled WT telomeric repeat oligonucleotide (TGTGGTGTGTGGGTGTGGTGT) as described previously (Rose, M. D. et al., 1990; Sambrook J and Russel D. W., 2001). Membranes were exposed using Amersham Biosciences storage phosphor screens and visualized using a Typhoon 9400 variable mode imager.

Mitochondrial and SIR3 Quantification

The original mito-tagged (mt)GFP on the plasmid pVT100U was obtained from Jodi Nunnari at UC Davis (Meeusen et al., 2004). The mtGFP uses amino acids 1-69 of subunit 9 of F0 ATPase as a transportation signal at the 5' end of GFP. The plasmid was digested with SpeI/XhoI and mtGFP was inserted into the pFA6a vector under the Tef2 promoter. It was then integrated into the genomic *HIS* locus with a *NAT* selection marker. Cells containing mtGFP were placed on

a microfluidics chip as described above. Images were taken every 2 hours to reduce blue light toxicity to the cells, and mtGFP intensity was measured relative to WT to determine volume of mitochondria. Bright field images were also taken every ten minutes. We then used the mtGFP intensity to estimate the relative volume of mitochondria in the focal plane. For Sir3-GFP foci, eleven images were taken for the Z stack, projected to a single image using the maximum value of the column, and the fluorescence intensity of the foci was measured using customized software Cellseg 5.4.

NAC Treatment and ROS Staining

N-Acetyl-L-Cysteine was bought from SIGMA-ALDRICH. Cells were incubated in YPD before loading to the chip and then YPD, with or without 20mM NAC, was pumped in (by syringe pumps from Longerpump Inc.) for the lifespan tracking. For ROS staining, a 10mM stock solution of 2',7'-dichlorfluorescein-diacetate (DCFH-DA) was made in DMSO. Cells were grown to OD600 ~0.5, washed twice with PBS, and then were incubated in 10μM DCFH-DA in PBS for 15min. The fluorescence was measured by FACS, and 30,000 cells were measured for each strain. The fluorescence of non-staining cells was also measured in order to determine the background fluorescence, which was then subtracted.

Statistical Analysis

Lifespans were compared using the Wilcoxon Rank-Sum test. Significance for the variation of cell cycle length was determined by F-tests. We used Fisher's

exact test to determine the significance of frequency of RNR3 peaks in different genotypes. Cells with “long” cell cycle durations in Figure 2-4 and Figure 2-15 were identified by selecting cells that form a second, minor peak in the histogram plot of cell cycle length produced using graphpad software.

Quantification of RNR3 Peaks

All assays were performed in SD media to reduce the background fluorescence. Lifespan assays were performed with strains containing RNR3-GFP and fluorescence was measured every 30 minutes by an Andor EMCCD camera on a Nikon Ti-e time-lapse microscope. Peaks were divided into two categories: peaks that occurred before the last two cell cycles (“still-dividing”) and peaks that occurred within or after the last two cell cycles (“terminal”). RNR3 induction peak height was measured and the number of occurrences with magnitudes at least 1.3 fold over background was scored. The frequency of RNR3 peaks was calculated as peak number divided by all cell cycles for “still dividing” cells and as peak number divided by the number of mother cells for “terminal” peaks. At least two independent experiments were performed for each genotype.

PCR Assay for Deprotected Telomeres

Assay was performed as described (Chan and Blackburn, 2003) with slight modifications. Diploid strains were created that were heterozygous for all mutations, expressed an HO gene driven by a galactose-inducible promoter, and contained a modified chromosome VII-L containing an HO cut site. Colonies of

the desired genotypes were taken directly from dissection plates and grown overnight in 2.5% raffinose media. Colonies were then induced for 8 hours in 3% galactose. Cells were pelleted and genomic DNA was purified using a glass bead and phenol chloroform DNA prep. PCR reactions consisted of: 5μL Qiagen Q solution, 2.5μL Qiagen 10x PCR Buffer, 0.5μL dNTPs (10mM each), 0.125μL (100μM) of each primer (CGCGCGCGGCCGTGACATGGTTATAACTGTTAGC, GTCAGTGATTATGTATTGTGTAGTATAGTATATTGTAAG), 0.5μL of Platinum Taq, 11.25μ water, and 100ng genomic DNA in 5μL water (25μL total volume). The following cycling conditions were used: 95°C (5 min); 35 cycles of 95°C (5 sec), 52°C (30 sec), 72°C (1 min); 72°C (5 min).

Serial Streaking and Serial Dilution Assays

Serial streaks were made using cells from original dissection colonies after genotyping. They were passaged on solid YPD media and underwent two days of growth at 30˚C before imaging. Multiple individual colonies from a given streak/passage were used to create the next streak in the series. Each streak represents approximately 20 cell divisions. For serial dilution experiments, genotyped dissection colonies were grown overnight in liquid culture (5-10 divisions) and diluted to O.D. ~0.1-0.2. Cells underwent approximately 4 hours of growth at 30˚C and were placed on ice. Cells were sonicated and cell concentration was measured using a hemocytometer. $4x10^5$ cells were resuspended in 100μL of appropriate media and 5 fold serial dilutions were

plated on YEP agar medium containing either 2% dextrose or galactose, and indicated drugs (if applicable) at the specified concentrations.

References

Chan, S.W.-L., and Blackburn, E.H. (2003). Telomerase and ATM/Tel1p protect telomeres from nonhomologous end joining. Mol. Cell *11*, 1379–1387.

Lin, J., Smith, D.L., and Blackburn, E.H. (2004). Mutant Telomere Sequences Lead to Impaired Chromosome Separation and a Unique Checkpoint Response. Mol. Biol. Cell *15*, 1623–1634.

Longtine, M.S., McKenzie, A., Demarini, D.J., Shah, N.G., Wach, A., Brachat, A., Philippsen, P., and Pringle, J.R. (1998). Additional modules for versatile and economical PCR-based gene deletion and modification in Saccharomyces cerevisiae. Yeast Chichester Engl. *14*, 953–961.

Meeusen, S., McCaffery, J.M., and Nunnari, J. (2004). Mitochondrial Fusion Intermediates Revealed in Vitro. Science *305*, 1747–1752.

Osborn, A.J., and Elledge, S.J. (2003). Mrc1 is a replication fork component whose phosphorylation in response to DNA replication stress activates Rad53. Genes Dev. *17*, 1755–1767.

Rose, M. D., Winston, F., and Heiter, P (1990). Methods in Yeast Genetics (Cold Spring Harbour, New York: Cold Spring Harbour Laboratory Press).

Sambrook J, and Russel D. W. (2001). Molecular Cloning (Cold Spring Harbour, New York: Cold Spring Harbour Laboratory Press).

Xie, Z., Zhang, Y., Zou, K., Brandman, O., Luo, C., Ouyang, Q., and Li, H. (2012). Molecular phenotyping of aging in single yeast cells using a novel microfluidic device. Aging Cell.

Zhang, Y., Luo, C., Zou, K., Xie, Z., Brandman, O., Ouyang, Q., and Li, H. (2012). Single Cell Analysis of Yeast Replicative Aging Using a New Generation of Microfluidic Device. PLoS ONE *7*, e48275.

Appendix 1: Strains Used in this Thesis

The relevant genotypes were derived from fresh sporulation of a diploid strain heterozygous for the desired marker (*), or by early loss of a covering plasmid (**), in order to capture Early Telomerase Inhibition (ETI) events. Plasmids are indicated in brackets. RNR3-GFP and Sir3-GFP strains were obtained from UCSF's GFP strain collection.

Table A1-1

Strain name/ Associated Figure	Strain Background	EHB number	Relevant genotype
WT	S288C-BY4741	3055 30,113	*MATa his3Δ1, leu2Δ0, met15Δ0, ura3Δ0*
WT	S288C-BY4742	3056 30,105	*MATα his3Δ1, leu2Δ0, lys2Δ0, ura3Δ0*
tlc1Δ	S288C-BY4741	3063**	*MATa his3Δ1, leu2Δ0, met15Δ0, ura3Δ0, tlc1Δ:LEU2 [pRS316-TLC1]*
tlc1Δ	S288C-BY4741	3064**	*MATα his3Δ1, leu2Δ0, lys2Δ0, ura3Δ0, tlc1Δ:LEU2 [pRS316-TLC1]*
est2D530A	S288C-BY4741	30,116**	*MATa est2D530A [pRS315 EST2]*
est2D530A	S288C-BY4742	30,046**	*MATα est2D530A [pRS315 EST2]*
est2Δ	S288C-BY4742	30,133**	*MATα est2Δ:LEU2 [pRS316-EST2]*
est2Δ	S288C-BY4741	30,134**	*MATa est2Δ:LEU2 [pRS316-EST2]*
sml1Δ	S288C-BY4741	30,099	*MATa sml1Δ:HYG*
sml1Δ	S288C-BY4742	30,015	*MATα sml1Δ:HYG*
mec1Δsml1Δ	S288C-BY4742	30,021	*MATα mec1Δ:NAT sml1Δ:HYG*
tel1Δ	S288C-BY4741	30,187	*MATa tel1Δ:HIS3*
Figure 2-1	S288C	30,101* 30,102*	*MATa/α tlc1Δ:LEU2/TLC1, sml1Δ:HYG/SML1*
	S288C	30,318*	*MATa/α tlc1Δ:LEU2/TLC1, $mrc1^{AQ}$/MRC1*
	S288C	30,317*	*MATa/α tlc1Δ:LEU2/TLC1, tel1Δ:HIS3/TEL1*
Figure 2-2	W303	5001	*MATa ura3-1, leu2-3,112 his3-11:pCUP1-GFP12-LacI12:HIS trp1-1:lacO(256 repeats)TRP can1-100 ade2-1 bar1-1 lys2Δ*
	W303	5404*	*MATa ura3-1:TUB1-GFP:URA3*
	W303	5403*	*MATa tlc1Δ:KAN, ura3-1:TUB1-GFP:URA3*
	W303	5482*	*MATa est2-D530A, ura3-1:TUB1-GFP:URA3*

Strain name/ Associated Figure	Strain Background	EHB number	Relevant genotype
Figure 2-2	S288C-BY4741	3230**	*MATa tlc1Δ:LEU2, mrc1Δ:NAT:pRS403MRC1*
	S288C-BY4741	3228**	*MATa tlc1Δ:LEU2, mrc1Δ:NAT:pRS403 mrc1^{AQ}*
	W303	5636*	*MATa tlc1Δ:KAN, ura3-1:TUB1-GFP:URA3*
	W303	5636*	*MATa tlcΔ:KAN, mrc1Δ:NAT:pRS403 mrc1AQ, ura3-1:TUB1-GFP:URA3*
	S288C-BY4741	3140	*MATa sml1Δ:MET15*
	S288C-BY4741	3138**	*MATa sml1Δ:MET15, tlc1Δ:HIS3*
	S288C-BY4741	3141**	*MATa sml1Δ:MET15 tlc1Δ:HIS3, tel1Δ:KAN*
	S288C-BY4741	3142**	*MATa sml1Δ:MET15, tlc1Δ:HIS3, mec1Δ:KAN*
	S288C-BY4704	1184*	*MATa tel1Δ:HIS*
	S288C-BY4704	1184*	*MATa mec1Δ:LEU2, sml1Δ:KANMX4*
	S288C-BY4704	1184*	*MATa mec1Δ:LEU2 sml1Δ:KANMX4 tel1Δ:HIS*
	S288C-BY4704	1184*	*MATa tlc1Δ:TRP1*
	S288C-BY4704	1184*	*MATa tlc1Δ:TRP1 tel1Δ*
	S288C-BY4704 S288C-BY4704	1184* 1184*	*MATa tlc1Δ:TRP1 tel1Δ* *MATa tlc1Δ:TRP1 mec1Δ:LEU2 sml1Δ:KANMX4*
	S288C-BY4704	1184*	*MATa tlc1Δ:TRP1 mec1Δ:LEU2 sml1Δ:KANMX4 tel1Δ:HIS*
	S288C-BY4736	5398	*MATa ade2Δ:HISG his3Δ1 met15Δ0 trp1Δ63*
	S288C-BY4736	3152	*MATa mec1Δ:KANMX4 sml1Δ:TRP1*
	S288C-BY4736	3270	*MATa mrc1Δ:MRC1 pRS403-MRC1(at endogenous MRC1 locus)*
	S288C-BY4741	3271	*MATa mrc1Δ:NAT/MRC1 pRS403-MRC1(at endogenous MRC1 locus)*
	S288C-BY4741	3272	*MATa mrc1Δ:mrc1^{AQ}*
Figure 2-3	S288C	30,261*	*MATa/α tlc1Δ:LEU2/TLC1, cdc5AD/CDC5*
Figure 2-5	S288C	30,101* 30,102*	*MATa/α tlc1Δ:LEU2/TLC1, sml1Δ:HYG/SML1*
Figure 2-6	S288C	30,103* 30,104*	*MATa/α est2D530A/EST2, sml1Δ:HYG/SML1*
Figure 2-7	S288C-BY4742	30,015	*MATα sml1Δ:HYG*
	S288C-BY4742	30,021	*MATα mec1Δ:NAT sml1Δ:HYG*
	S288C-BY4742	30,017	*MATα mrc1^{AQ}*
	S288C-BY4742	30,043	*MATα rad9Δ:NAT*
	S288C-BY4742	30,044	*MATα mrc1^{AQ}, rad9Δ:NAT*
	S288C-BY4742	30,107	*MATα mrc1^{AQ}, rad9Δ:NAT, sml1Δ:HYG*
Figure 2-8	S288C-BY4741	zwx118	*MATa his3:mtGFP-NAT*
	S288C	30,101* 30,102*	*MATa/α tlc1Δ:LEU2/TLC1, sml1Δ:HYG/SML1*
Figure 2-9	S288C	30,317*	*MATa/α tlc1Δ:LEU2/TLC1, tel1Δ:HIS3/TEL1*
Figure 2-10	S288C-BY4742	30,021	*MATα mec1Δ:NAT sml1Δ:HYG*
	S288C	30,209*	*MATa/α tlc1Δ:LEU2/TLC1, mrc1^{AQ}/MRC1, tel1Δ:HIS3/TEL1*

Strain name/ Associated Figure	Strain Background	EHB number	Relevant genotype
Figure 2-10	S288C	30,316*	*MATa/α tlc1Δ:LEU2/TLC1, rad9Δ:NAT/RAD9*
Figure 2-11	S288C	30,318*	*MATa/α tlc1Δ:LEU2/TLC1, mrc1^{AQ}/MRC1*
	S288C-BY4742	30,017	*MATα mrc1^{AQ}*
Figure 2-12	S288C	30,209*	*MATa/α tlc1Δ:LEU2/TLC1, mrc1^{AQ}/MRC1, tel1Δ:HIS3/TEL1*
Figure 2-13	S288C	30,383*	*MATa/α tlc1Δ:HIS3/TLC1, mrc1^{AQ}/MRC1, sml1Δ:HYG/SML1, LEU2-Gal-HO/WT, VII-L:ADE2-TG-HO site-LYS2/WT, rad52ΔKan/RAD52*
	S288C	30,381* 30,382*	*MATa/α tlc1Δ:HIS3/TLC1, tel1Δ:NAT/TEL1, sml1Δ:HYG/SML1, LEU2-Gal-HO/WT, VII-L:ADE2-TG-HO site-LYS2/WT, rad52ΔKan/RAD52*
	S288C	30,101* 30,102*	*MATa/α tlc1Δ:LEU2/TLC1, sml1Δ:HYG/SML1*
	S288C	30,318*	*MATa/α tlc1Δ:LEU2/TLC1, mrc1^{AQ}/MRC1*
	S288C	30,317*	*MATa/α tlc1Δ:LEU2/TLC1, tel1Δ:HIS3/TEL1*
Figure 2-14	S288C	30,328* 30,329*	*MATa/α tlc1Δ:LEU2/TLC1, rad52Δ:KAN/RAD52, sml1Δ:HYG/SML1*
	S288C	30,101* 30,102*	*MATa/α tlc1Δ:LEU2/TLC1, sml1Δ:HYG/SML1*
Figure 3-1	S288C	30215*	*MATa/α tlc1Δ:LEU2/TLC1, mec1Δ:NAT/MEC1, tel1Δ:HIS3/TEL1, sml1Δ:HYG/SML1*
Figure 3-2	S288C	30,094* 30,010*	*MATa/α tlc1Δ:LEU2/TLC1, mrc1^{AQ}/MRC1, rad9Δ:NAT/RAD9, sml1Δ:HYG/SML1*
	S288	30,108*	*MATa/α est2D530A/EST2, mrc1^{AQ}/MRC1, rad9Δ:NAT/RAD9, sml1Δ:HYG/SML1*
	S288C	30,137* 30,138*	*MATa/α est2Δ:LEU2/EST2, mrc1^{AQ}/MRC1, rad9Δ:NAT/RAD9, sml1Δ:HYG/SML1*
Figure 3-3	S288C	30,094* 30,010*	*MATa/α tlc1Δ:LEU2/TLC1, mrc1^{AQ}/MRC1, rad9Δ:NAT/RAD9, sml1Δ:HYG/SML1*
Figure 3-4	S288C	30,003*	*MATa/α tlc1Δ:LEU2/TLC1, tof1Δ:KAN/TOF1, rad9Δ:NAT/RAD9*
Figure 3-5	S288C	30,147*	*MATa/α tlc1-11 /TLC1, mrc1^{AQ}/MRC1, rad9Δ:NAT/RAD9, sml1Δ:HYG/SML1*
Figure 3-6	S288C	30,202* 30,203*	*MATa/α tlc1Δ:LEU2/TLC1, mrc1^{AQ}/MRC1, rad9Δ:NAT/RAD9, HIS-pTef-RNR1/RNR1*
	S288C	30,204* 30,205*	*MATa/α est2D530A/EST2, mrc1^{AQ}/MRC1, rad9Δ:NAT/RAD9, HIS-pTef-RNR1/RNR1*
	S288C	30,206* 30,207*	*MATa/α est2Δ:LEU2/EST2, mrc1^{AQ}/MRC1, rad9Δ:NAT/RAD9, HIS-pTef-RNR1/RNR1*
Figure 3-7	S288C-BY4741	3055 30,113	*MATa his3Δ1, leu2Δ0, met15Δ0, ura3Δ0*
	S288C-BY4742	3056 30,105	*MATα his3Δ1, leu2Δ0, lys2Δ0, ura3Δ0*

Strain name/ Associated Figure	Strain Background	EHB number	Relevant genotype
Figure 3-7	S288C-BY4741	3063**	*MATa his3Δ1, leu2Δ0, met15Δ0, ura3Δ0, tlc1Δ:LEU2 [pRS316-TLC1]*
	S288C-BY4742	3064**	*MATα his3Δ1, leu2Δ0, lys2Δ0, ura3Δ0, tlc1Δ:LEU2 [pRS316-TLC1]*
	S288C-BY4741	30,116**	*MATa est2D530A [pRS315 EST2]*
	S288C-BY4742	30,046**	*MATα est2D530A [pRS315 EST2]*
	S288C-BY4742	30,133**	*MATα est2Δ:LEU2 [pRS316-EST2]*
	S288C-BY4741	30,134**	*MATa est2Δ:LEU2 [pRS316-EST2]*
Figure 3-8	S288C	30,255* 30,256*	*MATa/α tlc1Δ:LEU2/TLC1, dun1Δ:NAT/DUN1, sml1Δ:HYG/SML1*
Figure 3-9	S288C	30,172*	*MATa/α tlc1Δ:LEU2/TLC1, sml14SA/SML1*
	S288C	30,175*	*MATa/α est2D530A/EST2, sml14SA/SML1*
	S288C	30,176*	*MATa/α est2Δ:LEU2/EST2, sml14SA/SML1*
Figure 3-10	S288C	30,285*	*MATa/α tlc1Δ:LEU/TLC1, KAN:pGal SML1/SML1*
	S288C	30,286*	*MATa/α est2D530A/EST2, KAN:pGal SML1/SML1*
	S288C	30,287*	*MATa/α est2Δ:LEU2/EST2, KAN:pGal SML1/SML1*
Figure 3-11	S288C	30,310* 30,311	*MATa/α tlc1Δ:LEU2/TLC1, $mrc1^{AQ}$/MRC1, rad9Δ:NAT/RAD9, sml1Δ:HYG/SML1, rad52Δ:KAN/RAD52*
Figure 3-12	S288C	30,094* 30,010*	*MATa/α tlc1Δ:LEU2/TLC1, $mrc1^{AQ}$/MRC1, rad9Δ:NAT/RAD9, sml1Δ:HYG/SML1*
Figure 3-13	S288C	30,101* 30,102*	*MATa/α tlc1Δ:LEU2/TLC1, sml1Δ:HYG/SML1*
	S288C	30,103* 30,104*	*MATa/α est2D530A/EST2, sml1Δ:HYG/SML1*
Figure 3-14	S288C	30,404*	*MATa/α tlc1Δ:HIS3/TLC1, mrc1AQ/MRC1, rad9Δ:NAT/RAD9, sml1Δ:HYG/SML1, LEU2-Gal-HO/WT, VII-L:ADE2-TG-HO site-LYS2/WT, rad52Δ:Kan/RAD52*
Figure 4-1	S288C-BY4742	3056 30,105	*MATα his3Δ1, leu2Δ0, lys2Δ0, ura3Δ0*
	S288C	22,321	*MATa his3Δ1, leu2Δ0, lys2Δ0, met15Δ0, trp1Δ63, ura3Δ0, bar1Δ0*
	S288C	22,465	*MATa his3Δ1, leu2Δ0, lys2Δ0, met15Δ0, trp1Δ63, ura3Δ0, bar1Δ0*

Strain name/ Associated Figure	Strain Background	EHB number	Relevant genotype
Figure 4-1	S288C	22,650**	*MATa his3Δ1, leu2Δ0, lys2Δ0, met15Δ0, trp1Δ63, ura3Δ0, bar1Δ0, tlc1Δ:LEU2 [pRS316-TLC1]*
	S288C	22,651**	*MATa his3Δ1, leu2Δ0, lys2Δ0, met15Δ0, trp1Δ63, ura3Δ0, bar1Δ0, tlc1Δ:LEU2 [pRS316-TLC1]*
	S288C	22,647**	*MATa his3Δ1, leu2Δ0, lys2Δ0, met15Δ0, trp1Δ63, ura3Δ0, bar1Δ0, est1Δ:LEU2 [pRS316-EST1]*
	S288C	22,648**	*MATa his3Δ1, leu2Δ0, lys2Δ0, met15Δ0, trp1Δ63, ura3Δ0, bar1Δ0, est3Δ:LEU2 [pRS316-EST3]*
	S288C	22,649**	*MATa his3Δ1, leu2Δ0, lys2Δ0, met15Δ0, trp1Δ63, ura3Δ0, bar1Δ0, est3Δ:LEU2 [pRS316-EST3]*
Figure 4-2	S288C-BY4742	3056 30,105	*MATα his3Δ1, leu2Δ0, lys2Δ0, ura3Δ0*
	S288C-BY4742	30,088**	*MATα tlc1Δ:LEU2 [pRS316-TLC1]*
	S288C-BY4742	30,089**	*MATα tlc1Δ:LEU2 [pRS316-TLC1]*
	S288C-BY4742	30,090**	*MATα tlc1Δ:LEU2 [pRS316-TLC1]*
	S288C-BY4742	30,091**	*MATα tlc1Δ:LEU2 [pRS316-TLC1]*
	S288C-BY4742	30,092**	*MATα tlc1Δ:LEU2 [pRS316-TLC1]*
	S288C-BY4742	30,093**	*MATα tlc1Δ:LEU2 [pRS316-TLC1]*
Figure 4-3	S288C	30,076*	*MATa/α tlc1Δ:LEU2/TLC1, KAN:pGal:HA:TOR1/TOR1 [pRS316-TLC1]*
	S288C	30,085*	*MATa/α est2D530A/EST2, KAN:pGal:HA:TOR1/TOR1 [pRS315 EST2]*
Figure 4-4	S288C	30,077*	*MATa/α tlc1Δ:LEU2/TLC1, KAN:pGal:HA:TOR2/TOR2 [pRS316-TLC1]*
	S288C	30,086*	*MATa/α est2D530A/EST2, KAN:pGal:HA:TOR2/TOR2 [pRS315 EST2]*
	S288C	30,141*	*MATa/α est2Δ:LEU2/EST2, KAN:pGal:HA:TOR2/TOR2*
Figure 4-5	S288C	30,076*	*MATa/α tlc1Δ:LEU2/TLC1, KAN:pGal:HA:TOR1/TOR1 [pRS316-TLC1]*

Strain name/ Associated Figure	Strain Background	EHB number	Relevant genotype
Figure 4-5	S288C	30,077*	*MATa/α tlc1Δ:LEU2/TLC1, KAN:pGal:HA:TOR2/TOR2 [pRS316-TLC1]*
	S288C	30,085*	*MATa/α est2D530A/EST2, KAN:pGal:HA:TOR1/TOR1 [pRS315 EST2]*
Figure 4-6	S288C	30,054*	*MATa/α tlc1Δ:LEU2/TLC1, KAN:pGal:HA:KOG1/KOG1 [pRS316-TLC1]*
	S288C	30,055*	*MATa/α tlc1Δ:LEU2/TLC1, KAN:pGal:HA:AVO3/AVO3 [pRS316-TLC1]*
Figure 4-6	S288C	30,056*	*MATa/α tlc1Δ:LEU2/TLC1, KAN:pGal:HA:LST8/LST8 [pRS316-TLC1]*
Figure 4-7	S288C-BY4741	3055 30,113	*MATa his3Δ1, leu2Δ0, met15Δ0, ura3Δ0*
	S288C-BY4742	3056 30,105	*MATα his3Δ1, leu2Δ0, lys2Δ0, ura3Δ0*
	S288C-BY4741	3063**	*MATa his3Δ1, leu2Δ0, met15Δ0, ura3Δ0, tlc1Δ:LEU2 [pRS316-TLC1]*
	S288C-BY4742	3064**	*MATα his3Δ1, leu2Δ0, lys2Δ0, ura3Δ0, tlc1Δ:LEU2 [pRS316-TLC1]*
	S288C-BY4741	30,099	*MATa sml1Δ:HYG*
	S288C-BY4742	30,015	*MATα sml1Δ:HYG*
	S288C-BY4741	30,109**	*MATa tlc1Δ:LEU2, sml1Δ:HYG [pRS316-TLC1]*
	S288C-BY4742	30,110**	*MATα tlc1Δ:LEU2, sml1Δ:HYG [pRS316-TLC1]*
	S288C-BY4742	30,046**	*MATα est2D530A [pRS315 EST2]*
	S288C-BY4742	30,047**	*MATα est2D530A [pRS315 EST2]*
	S288C-BY4741	30,111**	*MATa est2D530A, sml1Δ:HYG [pRS315 EST2]*
	S288C-BY4742	30,112**	*MATα est2D530A, sml1Δ:HYG [pRS315 EST2]*
Figure A2-1	S288C-BY4741	3063**	*MATa his3Δ1, leu2Δ0, met15Δ0, ura3Δ0, tlc1Δ:LEU2 [pRS316-TLC1]*
	S288C-BY4741	3064**	*MATα his3Δ1, leu2Δ0, lys2Δ0, ura3Δ0, tlc1Δ:LEU2 [pRS316-TLC1]*
	S288C-BY4741	30,116**	*MATa est2D530A [pRS315 EST2]*
	S288C-BY4742	30,046**	*MATα est2D530A [pRS315 EST2]*

Strain name/ Associated Figure	Strain Background	EHB number	Relevant genotype
Figure A2-2	S288C-BY4742	30,133**	*MATα est2Δ:LEU2 [pRS316-EST2]*
	S288C-BY4741	30,134**	*MATa est2Δ:LEU2 [pRS316-EST2]*
	S288C-BY4741	30,116**	*MATa est2D530A [pRS315 EST2]*
	S288C-BY4742	30,046**	*MATα est2D530A [pRS315 EST2]*

Appendix 2: Telomere Length Comparison in Various ETI Mutants

Haploid ETI cells of the indicated genotype were passaged on solid media with a covering plasmid containing one copy of the WT telomerase component (Passage 0) or after counter selection of the covering plasmid such that the cell was completely lacking telomerase activity (Passages 1, 2, and 3). Each passage represents approximately 20 cell divisions after loss of telomerase activity. Genomic DNA was prepared from the indicated passages and telomere lengths were measured via southern blots as described in Materials and Methods. Despite similar shortening rates across all haploid ETI strains, haploid strains carrying one copy of the *est2D530A* mutation and one copy of WT Est2 were found to have slightly shorter telomeres relative to haploids carrying one copy of *tlc1*Δ or *est2*Δ and the respective covering plasmids (Figure A2-1, A2-2, Passage 0). This is presumably due to the fact that the *est2D530A* catalytically-inactive point mutant still forms a complete telomerase complex. I hypothesize that this inactive telomerase complex competes with active telomerase complexes for binding to the telomere and therefore has a slight dominant negative effect on telomere length.

Figure A2-1

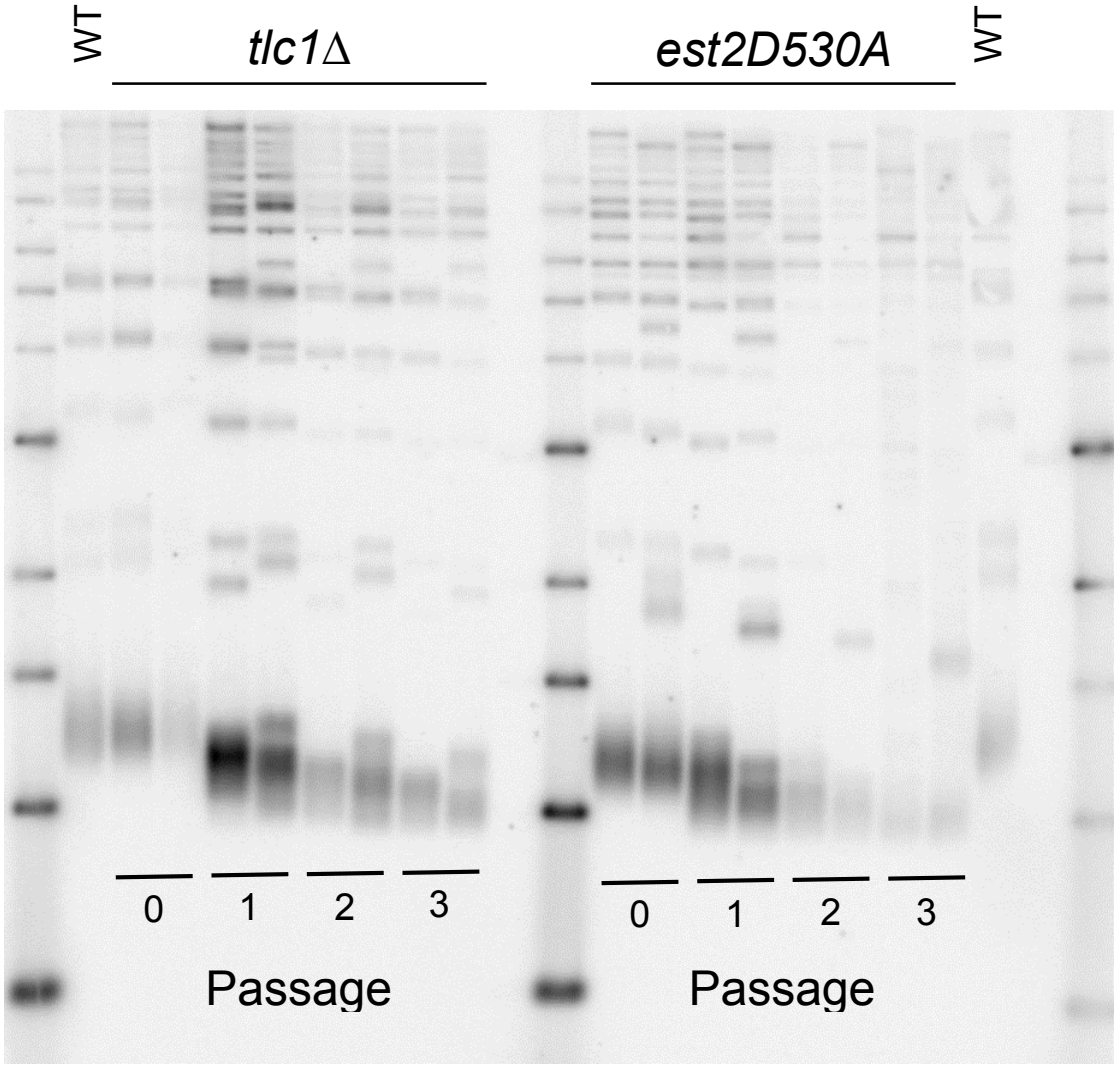

Figure A2-2

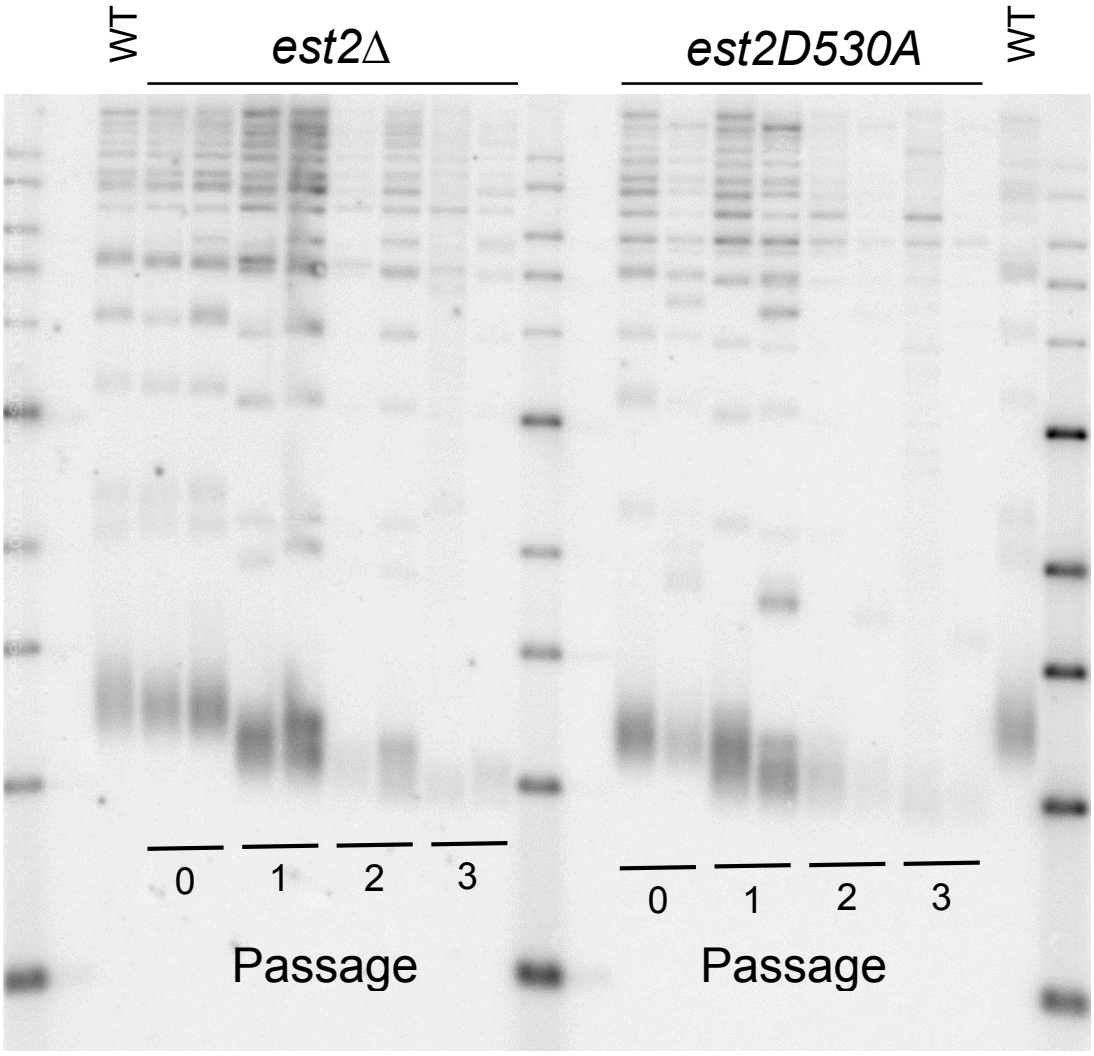

Publishing Agreement

It is the policy of the University to encourage the distribution of all theses, dissertations, and manuscripts. Copies of all UCSF theses, dissertations, and manuscripts will be routed to the library via the Graduate Division. The library will make all theses, dissertations, and manuscripts accessible to the public and will preserve these to the best of their abilities, in perpetuity.

Please sign the following statement:

I hereby grant permission to the Graduate Division of the University of California, San Francisco to release copies of my thesis, dissertation, or manuscript to the Campus Library to provide access and preservation, in whole or in part, in perpetuity.

Kyle Jay

Author Signature

5/21/15

Date